GRAVITY WAVES IN THE IONOSPHERE

BY

ROBERT MORRIS CLARK

S.B., Massachusetts Institute of Technology, 1959
M.S., University of North Dakota, 1965

THESIS

Submitted in partial fulfillment of the requirements
for the degree of Doctor of Philosophy in Electrical Engineering
in the Graduate College of the
University of Illinois at Urbana-Champaign, 1970

Urbana, Illinois

UNIVERSITY OF ILLINOIS AT URBANA-CHAMPAIGN

THE GRADUATE COLLEGE

July, 1970

I HEREBY RECOMMEND THAT THE THESIS PREPARED UNDER MY SUPERVISION BY ROBERT MORRIS CLARK

ENTITLED GRAVITY WAVES IN THE IONOSPHERE

BE ACCEPTED IN PARTIAL FULFILLMENT OF THE REQUIREMENTS FOR THE DEGREE OF DOCTOR OF PHILOSOPHY

K C Yeh
In Charge of Thesis

E. B. Jordan
Head of Department

Recommendation concurred in†

Committee on Final Examination†

† Required for doctor's degree but not for master's

D517

ACKNOWLEDGMENT

I am indebted to Dr. K. C. Yeh, without whose help, encouragement, and assistance this report would not have been possible; and to Dr. C. H. Liu, who provided much assistance and advice in my research work.

The research effort was supported by National Science Foundation grants number NSF GA 1249 and GA 13723.

TABLE OF CONTENTS

		Page
1.	INTRODUCTION	1
2.	GRAVITY WAVES IN THE ATMOSPHERE	5
	2.1 Introduction	5
	2.2 Assumptions	6
	2.3 The Linearized Equations	9
	2.4 Constraints on the Neutral Wind Model	21
	2.5 The Dispersion and Polarization Relations. . .	23
	2.6 Energy Flux	26
3.	IONIZATION DENSITY VARIATIONS IN TIME AND SPACE . .	31
	3.1 Introduction	31
	3.2 Development of the Equation of Continuity . .	32
	3.3 Boundary and Initial Conditions	34
	3.4 Ionization Production and Loss	36
	3.5 The Effect of Gravity Waves on a Computation of Ion Density	38
	3.6 Temporal Effects and Perturbed Variables . . .	39
4.	ION DRAG EFFECTS	44
	4.1 Introduction	44
	4.2 The Effect of Gas Parcel Orbits on Ion Damping	45
	4.3 The Relative Importance of Ion Drag and Thermal Conduction	47
	4.4 Comparison with Experimental Observations . .	48

Page

5. EXPERIMENTAL RESULTS AND NUMERICAL COMPUTATIONS . . 51

5.1 Introduction 51

5.2 Comparison with Experimental Observations . . 54

5.3 The Relative Importance of Perturbed Parameters 58

5.4 Phase Relationships Between Wave Parameters . 70

5.5 The Significance of Ion Drag 74

5.6 Importance of the $\dot{H}$ Term 80

6. CONCLUSION 83

LIST OF REFERENCES 88

APPENDIX 92

VITA 123

LIST OF SYMBOLS

Symbol	Description	Units
A	Amplitude of GW	$dynes^{1/2}\text{-}sec^2$
A'	$A \exp j(\omega t - k_x x - k_y y)$	"
$\hat{B}_o$	unit vector in direction of earth's magnetic field	
C	velocity of sound	cm/sec
c_1	$\frac{\omega'}{gH} - \frac{k_x^2}{\omega'-j\nu\sin^2 I} - \frac{k_y^2}{\omega'-j\nu}$	sec/cm^2
c_2	$\gamma_1 + k^2\psi$	--
c_3	$\omega'(\omega'-j\nu)/(\omega'-j\nu\sin^2 I)$	sec^{-1}
F_w	wave energy flux	dynes/cm-sec
$g, \bar{g}$	acceleration due to gravity	cm/sec^2
G_1	$\frac{K \sin I\ (T_i+T_e)}{m_i \nu_{in}}$	cm^2/sec
G_2	$\frac{g \sin I}{\nu_{in}} + \frac{K \sin I}{m_i \nu_{in}} \frac{\partial}{\partial \zeta} (T_i+T_e) -$	
	$v_{nx} \cos I - v_{nz} \sin I$	cm/sec
H	neutral gas scale height	cm
I	magnetic dip angle, measured positive upward	degrees
j	$\sqrt{-1}$	
K	Boltzmann's constant $(.13805 \cdot 10^{-5})$	erg/°K

$k, \bar{k}$	GW wave number in the horizontal direction	cm^{-1}
k_x	GW wave number in direction of magnetic North	cm^{-1}
k_y	GW wave number in direction of magnetic West	cm^{-1}
K_z	GW wave number in vertical direction, positive upward	cm^{-1}
k_1	$\frac{k_x \nu \cos I \sin I}{\omega' - j\nu \sin^2 I}$	cm^{-1}
L	ion loss term in the continuity equation	$cm^{-3}sec^{-1}$
m	mean neutral molecular mass	grams
m_i	mean ion molecular mass	grams
N	total ion number density	cm^{-3}
N	polarization relation used in Chap. 2	cm^{-3}
n	number density of a specific atmospheric constituent	cm^{-3}
p	neutral gas pressure	$dynes/cm^2$
q	ion production rate	$cm^{-3}sec^{-1}$
Q	heat input to a gas parcel	
R	polarization relation for density	$dynes^{-1/2}sec^{-2}$
$\tilde{\tilde{S}}$	viscous stress tensor	$dynes/cm^2$
S	intensity of solar ionizing radiation flux	$dynes/cm^2$
T	polarization relation for temperature	$dynes^{-1/2}sec^{-2}$
T_∞	neutral exospheric temperature	°K
t	time	sec

T_n	neutral gas temperature	°K
T_o	unperturbed neutral gas temperature	°K
T_i	ion temperature	°K
T_e	electron temperature	°K
U	polarization relation for v_{nx}	$\frac{cm}{sec^3 (dynes)^{1/2}}$
V	polarization relation for v_{ny}	"
$\bar{v}_n, v_n$	neutral gas velocity	cm/sec
v_{nx}, v_{ny}	components of $\bar{v}_n$ in x- and y-directions	cm/sec
$v_i, \bar{v}_i$	ion gas velocity cm/sec	cm/sec
v_{ph}	ω/k; phase velocity in the horizontal direction	cm/sec
W	polarization relation for vertical velocity	$\frac{cm}{sec^3 (dynes)^{1/2}}$
x	coordinate distance in direction of magnetic North	cm
y	coordinate distance in direction of magnetic West	cm
z	coordinate distance in vertical direction, where z = 0 is a point 120 km above the earth's surface	cm
α	ionization recombination coefficient	cm^3/sec
β	ionization attachment coefficient	sec^{-1}
γ	ratio of specific heats	--
γ_1	$\frac{\gamma}{\gamma-1}$	--
Γ_∞	ionization flux at upper boundary, positive flowing out of the ionosphere	$cm^{-2} sec^{-1}$

ζ	z	cm
λ	thermal conductivity coefficient	$\frac{\text{dynes}}{\text{sec-}^\circ\text{K}}$
μ	viscosity coefficient	$\frac{\text{gm}}{\text{cm-sec}}$
ν	$\nu_{in}\rho_i/\rho_o$	
ν_{in}	ion-neutral collision frequency	sec^{-1}
ξ	x sin I - z cos I	cm
ρ	neutral gas mass density	$\frac{\text{gm}}{\text{cm}^3}$
ρ_i	ion gas mass density	$\frac{\text{gm}}{\text{cm}^3}$
σ_{io}	effective ionization cross-section of atomic oxygen	$\frac{\text{cm}^2}{\text{cm}}$
ϕ	GW azimuth of propagation	degrees
χ	solar zenith angle, measured from the vertical	degrees
ψ	$\lambda_o T_o/j\omega\rho_o gH$	cm^2
ω	GW frequency	sec^{-1}
ω'	$\omega-k_x v_{nxo}-k_y v_{nyo}$	sec^{-1}
$\overline{\Omega}$	angular velocity of the earth	sec^{-1}

Note: A subscript 'o' in general means the value of the subscripted quantity in the absence of a GW. Differentiation with respect to z is denoted by a ($\dot{}$) .

1. INTRODUCTION

During the past ten years, a considerable amount of experimental and theoretical evidence has been amassed concerning the presence of travelling ionospheric disturbances (TID's) in the earth's ionosphere. The disturbances have a wavelike appearance when studied over an extended time or spatial scale, and are important in the understanding of the dynamics of the upper atmosphere.

The bulk of the collected evidence points to a cause-effect relationship between TID's and acoustic-gravity waves (GW's) propagating upward and outward from atmospheric disturbances originating below or in the ionosphere. These waves are significant because, in accordance with the law of energy conservation, the wave must grow in amplitude as it propagates upward. This exponential growth, which is inversely proportional to the square root of pressure, continues until the wave is either modified by nonlinear processes (such as turbulence) or attenuated by losses, such as conversion of the wave energy into heat energy. Indeed, the heating effect due to GW dissipation has been estimated to be as important as any other source of heating in the thermosphere (20).

While the problem of the sources of GW's is not a settled one, a clear link has been shown to exist between atmospheric nuclear and thermonuclear explosions and resulting GW's, and some auroral region phenomena such as the auroral electrojet have been linked to TID's through the gravity wave mechanism.

Other possible sources include the jet stream and tropospheric weather disturbances. These and other sources have been ably discussed in a recent symposium on acoustic-gravity waves, and the interested reader is referred to the symposium proceedings (14).

The basic mathematical theory concerning GW propagation has been set down by Eckart (8) and Hines (17), (18). Several studies have followed over the years, each attempting to explain the nature of the link between GW's and TID's. It is necessary in the course of analysis to make certain simplifying assumptions, and many of the studies to date are limited in their usefulness for explaining TID's because of the constraints imposed by these assumptions. The division of approaches to the problem may be made on the basis of what energy loss mechanisms are considered (or neglected), and whether the stress is on the dynamics of the GW or of the resulting TID.

Three sources of loss are generally agreed to exist at ionospheric heights: Thermal conducitivity, viscous damping, and ion drag. Thermal conductivity loss occurs, in a gas, due to the loss of heat from a parcel of gas which has been compressed due to the wave motion. Viscous damping may be thought of as a frictional force opposing the motion of a parcel of gas. Ion drag occurs when both a plasma and a magnetic field are present; for ions do not readily move across magnetic field lines in response to collisons with neutral

particles, and they therefore tend to slow neutral gas motion perpendicular to the field lines. Ion drag is also significant in that it introduces terms involving ionization density into the neutral gas equations set down in Section 2.1. Since the ion continuity equation discussed in Chapter 3 has a term involving neutral gas velocity, the proper approach to the problem would be to solve the neutral and ion gas equations in coupled form. The coupled equation problem is a very difficult one and it is commonly circumvented by breaking the problem up into two parts, one part leading to a solution for the neutral GW, the second leading to a solution for the TID resulting from the GW. The usual method of decoupling the equations is to assume that ion drag is negligible. Thus Volland (47) solves the first part neglecting ion drag and viscosity; Thome and Rao (42) solve both parts, neglecting thermal conduction and ion drag; Klostermeyer (29) solves the first part neglecting viscosity and thermal conductivity; and Hooke (25) solves the second part, using a constant loss of unspecified nature.

In this study, we will solve the first part of the problem (Chapter 2) taking into account ion drag and thermal conductivity, and using an approximation to include viscosity. The coupling term in the neutral equations is approximated using Hooke's results (25). We then solve the second part of the problem (Chapter 3) using the GW model of Chapter 2. A numerical solution is necessary because of the nonlinearity

of the continuity equation. The numerical approach which was used is described in the appendix. A discussion of the significance of ion drag is included in Chapter 4.

2. GRAVITY WAVES IN THE ATMOSPHERE

2.1 Introduction

In order to find out what characteristics a plane GW in the ionosphere possesses, we must derive a dispersion relation which relates the wave number to the frequency, as a function of the physical parameters of the ionosphere. It is also necessary to determine the conditions under which such a relation is valid. In order to do this, we will find a solution to the set of equations given below(32). Three loss effects are included in the equations: thermal conductivity, viscous dissipation, and ion drag.

The equation of continuity:

$$\frac{\partial \rho}{\partial t} + \bar{v}_n \cdot \nabla \rho + \rho \nabla \cdot \bar{v}_n = 0 \tag{2.1}$$

The equation of momentum conservation:

$$\rho \frac{\partial \bar{v}_n}{\partial t} + \rho (\bar{v}_n \cdot \nabla) \bar{v}_n = \rho \bar{g} - \nabla p + \nabla \cdot \tilde{\tilde{S}} - \nu_{in} \rho_i (\bar{v}_n - \bar{v}_i)$$

$$- 2\rho (\bar{\Omega} \times \bar{v}_n) \tag{2.2}$$

The energy equation:

$$\frac{\rho K}{(\gamma - 1) m} \left(\frac{\partial T_n}{\partial t} + \bar{v}_n \cdot \nabla T_n \right) = Q + \nabla \cdot (\lambda \nabla T_n) - p \nabla \cdot \bar{v}_n$$

$$+ \tilde{\tilde{S}} : \nabla \bar{v}_n + \nu_{in} \rho_i (\bar{v}_n - \bar{v}_i) \cdot (\bar{v}_n - \bar{v}_i) \tag{2.3}$$

The equation of state:

$$p = \frac{\rho K T}{m} \quad n \tag{2.4}$$

2.2 Assumptions

1. We assume a plane earth, whose rotation can be neglected. This implies that we set $\bar{\Omega} = 0$ in (2.2). The assumption is valid for waves whose scale is small compared to the earth's radius, and whose period is less than about two hours. The overwhelming majority of observed TID's have time and spatial scales which fit within this restriction.

2. The GW wave number in the horizontal direction, k, is purely real and constant with altitude. This assumption is necessary in order to satisfy the boundary conditions of a horizontally stratified atmosphere (assumption 5). The vertical wave number, K_z, is complex due to the presence of losses.

3. A plane GW of perturbation magnitude exists in the ionosphere. The wave has a single constant frequency, and is supported by an upward energy flux existing at the $z = 0$ plane of reference (taken at 120 km above the earth's surface in this study). The single-frequency assumption simplifies analysis. The perturbation assumption is based on TID observations which show large-magnitude waves to be the exception.

4. The ionization velocity $\bar{v}_i$ due to the GW is simply the component of $\bar{v}_n$ along the magnetic field line. This implies that ν_{in} is much less than the ion gyrofrequency, a relation which holds throughout the region of our interest. It is also necessary to assume that $\nu_{in} >> \omega$. This becomes a poor approximation near the upper boundary of the region to

be considered, 700 km altitude, but the GW is so weak at this altitude that no real problem exists due to the approximation. In any event, the mean free path of gas particles is comparable to one scale height at the upper boundary, so the hydrodynamic description may not be valid anyway.

The assumption that $\overline{v}_i = (\overline{v}_n \cdot \hat{B}_o)\hat{B}_o$ is not inconsistent with the expression for $\overline{v}_i$ given in equation (3.2) later. Here we are making an approximation of (3.2) where waves are present, to permit a ready solution of the problem. The use of (3.2) in this chapter would force us to solve a set of coupled equations, since the diffusion term in (3.2) contains $\nabla N/N$. The justification for this approximation is discussed by Hooke, and we examine it further in Chapter 5.

5. We assume a horizontally stratified atmosphere, with slabs of thickness Δz. Within each slab, unperturbed pressure, density, and neutral temperature have only a vertical spatial variation, which follow the models given by Jacchia (27).

This assumption seems to contradict the assumption of a neutral wind, since a gradient of some kind is necessary in order for a horizontal wind to exist. However, the gradient is so small, compared with the gradient introduced by a neutral wave structure, that it can be neglected in the perturbation equations to follow. In contrast, the wind effect on the perturbation equations cannot readily be neglected. In the zero-order equations, terms involving a horizontal gradient, as well as neutral wind terms, will be suppressed in order to avoid the problem of solving for a neutral wind.

In summary, we will ignore the question of how a neutral constant wind came into existence; we simply postulate its existence in order to discuss some aspects of its effect on the GW.

6. Losses due to viscous damping are neglected in comparison with thermal conduction losses ($\mu = 0$, or $\tilde{\tilde{S}} = [0]$ in equations (2.2) and (2.3)). The effect of this assumption is to eliminate from consideration two types of waves, called the ordinary and extraordinary viscosity waves by Volland (46). This assumption is necessary in order to reduce the GW dispersion relation to manageable dimensions. An equation which included all wave types would be of eighth order in K_z; by setting $\mu = 0$, we reduce it to a fourth order equation.

For justification of this assumption, we note that viscosity and thermal conduction affect GW's in much the same way, but the effect of thermal conductivity is greater (23), (34). Also, Volland has shown that, below 500 km altitude, viscosity waves are almost completely uncoupled from the remaining two wave types--GW's and thermal conduction waves (46). We will compensate for the neglected viscous effect by increasing the value of λ by 9/5 in computations.

7. The layer thickness, Δz, will be chosen to be sufficiently small so that the magnitude of a perturbation is essentially constant in the layer. This requires that Δz be no more than 1/10 th of a vertical wavelength (44), (46).

2.3 The Linearized Equations

In the presence of a GW, the field variables are perturbed; the perturbation in the horizontal plane and in time will be of the form

$$A' = A \exp j(\omega t - k_x x - k_y y)$$

where A is the amplitude of the GW. The field variables may be written as

$$\rho = \rho_o(z)[1+A'R(z)]$$

$$p = P_o(z)[1+A'P(z)]$$

$$T_n = T_o(z)[1+A'T(z)]$$

$$\bar{v}_n = [v_{nxo}(z)+A'U(z)]\hat{x} + [v_{nyo}(z)+A'V(z)]\hat{y} + W(z)A'\hat{z}$$

We should note here that the field variables shown above, as well as many variables to be discussed further on, are given in complex form. This is a notational convenience; in all cases, the variable actually is taken as the real part of the complex expression. For example, the actual density is

$$\rho = \rho_o[1 + \text{Real } (A'R)]$$

Using assumption (4) we can write the ionization velocity as

$$\bar{v}_i = (\bar{v}_n \cdot \hat{B}_o)\hat{B}_o$$

$$= [(v_{nxo}+A'U)\cos I + WA'\sin I](\hat{x}\cos I + \hat{z}\sin I)$$

so that

$$\bar{v} - \bar{v}_i = \hat{x}[(v_{nxo} + A'U)\sin^2 I - WA'\cos I \sin I] + \hat{y}(v_{nyo} + A'V)$$

$$+ \hat{z}[WA'\cos^2 I - (v_{nxo} + A'U)\cos I \sin I]$$

Normally, no consideration is given to possible perturbations in loss coefficients such as λ and ν_{in}; yet such perturbations do exist, and we will consider them below.

The ion-neutral collision frequency, ν_{in}, is usually neglected in analysis of GW effects on the ionosphere, under the assumption that $\nu << \omega$, where

$$\nu = \frac{\nu_{in}\rho_i}{\rho_o}$$

This is a poor assumption to make for GW's with periods of one hour or greater; at or above the F-layer peak, ν is typically of the same order of magnitude as $\omega(\sim.001\ \text{sec}^{-1})$, and may even be greater than ω. We will retain this ion drag effect imposed by ν_{in}, and later will make a comparison of its importance with that of other loss processes.

The magnitude of ν_{in} is directly proportional to the neutral number density, and is weakly dependent on temperature also (30):

$$\nu_{in} \propto \rho T_n^{0.4}$$

A reasonable approximation to the perturbed ν_{in} is therefore the expression

$$\nu_{in} \simeq \nu_{ino}(z)(1+A'R)$$

It follows that

$$\nu \simeq \nu_o T_n^{0.4} \rho_i (1+A'R)$$

where ν_o is a constant. In this expression, ρ_i is <u>not</u> treated as a perturbed quantity, and indeed its form is not known precisely at this point. If we had a model of ρ_i, we could conclude our work forthwith, since such a model is the goal of this paper. The appearance of ρ_i at this point introduces a coupling term involving the solution of the continuity equation for ions which is discussed in Chapter 3. The coupling is weak, however, and is taken into account when ν is computed in the numerical solution. We can do this by using the model of ρ_i computed at one fixed time in computing the value of ν in the next computation cycle. Since the time increment involved is small (1/20 of a wave period), the error in ν so computed is quite small. For our purposes in this chapter, it is sufficient to think of ρ_i as being the ambient electron density.

The coefficient of thermal conductivity, λ , is given as (16):

$$\lambda = \frac{\sum_i c_i n_i}{\sum_i n_i} \sqrt{T_n}$$

where the c_i's are constants, and n_i is the number density of the i^{th} constituent. It follows from the binomial theorem that

$$\lambda \propto [T_o(1+A'T)]^{1/2} \simeq \sqrt{T_o}(1+\tfrac{1}{2}A'T)$$

so that, for $|A'T| << 1$,

$$\lambda(z) = \lambda_o(z)(1+ \tfrac{1}{2} A'T)$$

We can neglect perturbations in the factor $\frac{\sum_i c_i n_i}{\sum_i n_i}$ because for the region under consideration, the three predominant atomic and molecular species (N_2, O_2 and O) have the same value of c_i, which is 180 ergs $\cos^{-1}\sec^{-1}{}^\circ K^{-1/2}$ (16). The factor above therefore reduces to this constant to a high degree of approximation.

If we were including the effects of viscosity, the viscous damping coefficient would also be perturbed. Since $\mu \propto (T_n)^{.71}$, it would have the form

$$\mu(z) \simeq \mu_o(z)(1+ .71A'T)$$

However, we will apply assumption (6) and assume that $\mu = 0$ from here on.

We are now in a position to rewrite equations (2.1) through (2.4), using the expressions for perturbed field variables and coefficients which have been developed. This leads us to two sets of equations: a zero-order set containing only unperturbed variables; and a set which contains only perturbed terms of the first order, all higher order terms having been suppressed. The zero order equations (simplifying by the use of assumption (5)) are (differentiation with respect to z is denoted by a ($\dot{}$)):

$$\rho_o g + \dot{p}_o = 0 \qquad (2.5)$$

$$p_o = \rho_o K T_o / m \tag{2.6}$$

$$0 = Q + \dot{\lambda}_o \dot{T}_o + \lambda_o \ddot{T}_o \tag{2.7}$$

Next define a neutral gas scale height

$$H(z) = KT_o/mg$$

then we may use (2.5) and (2.6) to obtain

$$p_o = \rho_o g H = -\dot{p}_o H$$

or

$$p_o(z) = p_o(z_o) \exp\left[- \int_{z_o}^{z} \frac{d\zeta}{H(\zeta)} \right]$$

clearly,

$$\frac{\dot{p}_o}{p_o} = - \frac{1}{H}$$

but

$$\frac{\dot{\rho}_o}{\rho_o} = \frac{1}{\rho_o} \frac{\partial}{\partial z} \left(\frac{p_o}{gH} \right) = - \frac{1}{H} - \frac{\dot{H}}{H} \tag{2.8}$$

the $\dot{H}/H$ term is zero in an isothermal atmosphere; but near the bottom of the F layer, where temperature increases rapidly with altitude, $\dot{H}$ may be of order unity, and cannot be neglected.

The relation between temperature and scale height is

$$T_o = mgH/K$$

therefore,

$$\frac{\dot{T}_o}{T_o} = \frac{\dot{H}}{H}$$

since $\lambda_o \propto T_o^{1/2}$, it follows at once that

$$\frac{\dot{\lambda}_o}{\lambda_o} = \frac{1}{2} \frac{\dot{T}_o}{T_o}$$

using assumptions (1), (5), and (6), we can now write the perturbed equations corresponding to equations (2.1) through (2.4). Let us represent the Doppler-shifted frequency by

$$\omega' = \omega - k_x v_{nxo} - k_y v_{nyo}$$

Then we get

$$j\omega' R\rho_o + W\dot{\rho}_o + \rho_o(-jk_x U - jk_y V + \dot{W}) = 0 \tag{2.9}$$

$$j\omega' U\rho_o + \rho_o \dot{v}_{nxo} W = jk_x p_o P - \nu_{ino}\rho_i (U \sin^2 I$$

$$-W \cos I \sin I + v_{nxo} R \sin^2 I) \tag{2.10}$$

$$j\omega' V \rho_o + \rho_o \dot{v}_{nyo} W = jk_y p_o P - \nu_{ino}\rho_i (V + v_{nyo} R) \tag{2.11}$$

$$j\omega' W\rho_o = -Rg\rho_o - \dot{p}_o P - p_o \dot{P} - \nu_{ino}\rho_i (W \cos^2 I$$

$$-U \cos I \sin I - R\, v_{nxo} \cos I \sin I) \tag{2.12}$$

$$\frac{\rho_o K}{(\gamma-1)m} (j\omega' T_o T + W\dot{T}_o) = \lambda_o (\frac{3}{2} \dot{T}_o T + \frac{5}{2} \dot{T}_o \dot{T} + T_o \ddot{T} - k^2 T_o T)$$

$$+\dot{\lambda}_o (\frac{3}{2} \dot{T}_o T + T_o \dot{T}) + p_o (jk_x U + jk_y V - \dot{W}) + \nu_{ino}\rho_{io} [R(v_{nyo}^2 \tag{2.13}$$

$$+ \nu_{nxo}^2 \sin^2 I) + 2U\, v_{nxo} \sin^2 I + 2 v_{nyo} V - 2W\, v_{nxo} \cos I \sin I]$$

$$-P + R + T = 0 \tag{2.14}$$

In (2.13) no perturbation on Q was assumed. Of course Qis affected by the passage of a GW. One significant part of Q is the term β in equation (2) of Volland's paper (46), representing the heating of the neutrals due to viscous damping. Other effects, such as perturbation changes in solar heating, should also be considered a part of Q. However, since viscosity has been neglected already, it is beyond the scope of this paper to determine even an approximate expression for the perturbation in Q.

Since no derivatives of R, V, and U appear in equations (2.9) through (2.13), they can be eliminated using equations (2.10), (2.11), and (2.14):

$$U = \frac{-j}{\omega'-j\nu\sin^2 I}\left[jk_x gHP-\nu v_{nxo}(P-T)\sin^2 I+(\nu\cos I \sin I - \dot{v}_{nxo})W\right]$$

$$V = \frac{-j}{\omega'-j\nu}\left[jk_y gHP-\nu v_{nyo}(P-T) - \dot{v}_{nyo}W\right]$$

$$R = P - T$$

We are then left with three equations in three unknown field variables. We now introduce a fourth variable, N, defined as

$$N = \frac{\lambda_o T_o}{p_o}\dot{T} + \frac{3}{2}\frac{\lambda_o \dot{T}_o}{p_o}T \tag{2.15}$$

This leaves us with a set of four first-order differential equations in four field variables. In matrix form, the equations

are written as

$$-j[A]\bar{e} + \frac{\partial \bar{e}}{\partial z} = 0 \tag{2.16}$$

where the vector $\bar{e}$ is defined as

$$\bar{e} = \begin{Bmatrix} p_o^{1/2} \frac{W}{gH} \\ p_o^{1/2} p \\ p_o^{1/2} \lambda_o T_o T \\ p_o^{1/2} N \end{Bmatrix}$$

and the matrix [A] has the elements:

$$a_{11} = \frac{-j}{2H} - \frac{jk_x \cos I \sin I}{\omega' - j\nu \sin^2 I} \nu + \dot{w}_1$$

$$a_{12} = -\frac{\omega'}{gH} + \frac{k_x^2}{\omega' - j\nu \sin^2 I} + \frac{k_y^2}{\omega' - j\nu}$$

$$a_{13} = \frac{\omega' - j\nu W_1}{\lambda_o T_o gH}$$

$$a_{21} = -\frac{\omega'(\omega' - j\nu)}{\omega' - j\nu \sin^2 I} + \frac{\dot{v}_{nxo} \nu \cos I \sin I}{\omega' - j\nu \sin^2 I}$$

$$a_{22} = \frac{j}{2H} - \frac{jk_x \nu \cos I \sin I}{\omega' - j\nu \sin^2 I} - \frac{jw_2}{gH} \tag{2.17}$$

$$a_{23} = \frac{j}{\lambda_o T_o H} \left(-1 + \frac{w_2}{g}\right)$$

$$a_{33} = \frac{j}{2H}$$

$$a_{34} = -jp_o$$

$$a_{41} = -j\left(g+\frac{C^2}{\gamma-1}\frac{\dot{H}}{H}\right) - 2\nu\left[v_{nxo}\frac{\dot{v}_{nxo}\sin^2 I+j\omega'\cos I \sin I}{\omega' - j\nu\sin^2 I} + \frac{v_{nyo}\dot{v}_{nyo}}{\omega'-j\nu}\right]$$

$$a_{42} = -\omega' + 2\nu w_1 + \frac{jw_3}{gH}$$

$$a_{43} = -\frac{jk^2}{p_o} + \frac{\omega'\gamma}{(\gamma-1)\lambda_o T_o} - \frac{jw_3}{\lambda_o T_o gH}$$

$$a_{44} = -\frac{j}{2H}$$

$$a_{14} = a_{24} = a_{31} = a_{32} = 0$$

where

$$w_1 = \frac{jk_x v_{nxo}}{\omega'-j\nu\sin^2 I} + \frac{jk_y v_{nyo}}{\omega'-j\nu}$$

$$w_2 = v_{nxo}\nu\cos I \sin I\left(1 + \frac{j\nu\sin^2 I}{\omega'-j\nu\sin^2 I}\right)$$

$$w_3 = \nu(v_{nxo}^2 \sin^2 I + v_{nyo}^2) + 2j\nu^2\left(\frac{v_{nxo}^2 \sin^2 I}{\omega'-j\nu\sin^2 I} + \frac{v_{nyo}^2}{\omega'-j\nu}\right)$$

The matrix [A] has elements which are z-dependent, so the simple method of solution for a system of equations with constant coefficients is not available to us. We follow instead the method described by Volland (47), and use a transformation matrix [B] and a vector $\bar{c}$ such that

$$\bar{e} = [B]\ \bar{c} \tag{2.18}$$

where

$$[B]^{-1}[A][B] = \begin{bmatrix} K_{z1} & 0 & 0 & 0 \\ 0 & K_{z2} & 0 & 0 \\ 0 & 0 & K_{z3} & 0 \\ 0 & 0 & 0 & K_{z4} \end{bmatrix}$$

The elements K_{zj} are defined by the eigenvalue equations

$$\det \left| [A] + K_{zj}[I] \right| = 0, \quad j = 1,2,3,4 \tag{2.19}$$

where [I] is the unit matrix. The four roots K_{zj} in equations (2.19) and (2.21) reduce to the eigenvalues q_i derived by Volland in equation (6) of his paper (47), if ion drag and wind are neglected and suitable transformations are made. However, the symmetry of roots which is apparent in Volland's work, and which he discusses, disappears when either of these conditions exist:

a) Ion drag is present;

b) A nonisothermal slab model is assumed.

Condition a) is apparent from equation (2.21), where $k_1 \neq 0$ if $\nu \neq 0$; and condition b) causes $\dot{H}$ to be greater than zero in (2.21). In either case, (2.21) cannot be written in the form

$$K_z^4 + d_1 K_z^2 + d_2 = 0$$

and no two roots can be chosen such that $K_{zj} = - K_{zi}$, as

was the case in Volland's paper.

The reason for the lack of symmetry involved here is easily found, and it has been pointed out by Liu and Yeh (31) for condition a). In all expressions for gravity wave modes, at least one axis of symmetry is necessarily present: that about the gravitational acceleration vector. The consideration of ion drag introduces a second axis of symmetry along the magnetic field line. Finally, a vertical inhomogenity within the slab exists if temperature is not constant within the slab.

Corresponding to each K_{zj} there will also be an eigenvector, whose elements we will denote as W_j, P_j, T_j, and N_j. From application of matrix algebra theory, [B] can readily be determined:

$$[B] = \begin{vmatrix} W_1 & W_2 & W_3 & W_4 \\ P_1 & P_2 & P_3 & P_4 \\ T_1 & T_2 & T_3 & T_4 \\ N_1 & N_2 & N_3 & N_4 \end{vmatrix}$$

and the vector $\bar{c}$ can be determined from (2.18). Equations (2.16) and (2.18) can now be combined to give

$$-j[B]^{-1}[A][B]\bar{c} + \frac{\partial \bar{c}}{\partial z} + [B]^{-1}\dot{[B]}\bar{c} = 0 \qquad (2.20)$$

The elements of the matrix $[B]^{-1}\dot{[B]}$ are zero in a lossless isothermal atmosphere; in the real atmosphere, they are non-zero, and measure the coupling between wave modes. When

these elements are small compared with the eigenvalues, the mode coupling is small, and the ray theory approximation will be satisfactory. If certain elements become large at given values of z, it would indicate mode coupling and possible mode reflection.

It should be noted that the matrix $[B]^{-1}\dot{[B]}$ as we have defined it so far is not unique. It is necessary that the elements of [B] be normalized and that the main diagonal terms of $[B]^{-1}\dot{[B]}$ be zero, as discussed by Inoue and Horowitz (26), in order for the coupling matrix to be unique.

Volland (46), (47), has examined the importance of the coupling matrix in his full wave treatment of the problem, and concluded that coupling from the ascending GW mode to the other modes at thermospheric heights is not significant. It should be noted that Volland assumed no background wind (an assumption we will eventually use for all results in this paper). Where an ambient wind exists coupling may become very important indeed. We will not repeat Volland's work here, but will simply note one particular case where $[B]^{-1}\dot{[B]}$ may become significant.

Since the term $(\det [B])^{-1}$ is a factor in the coupling matrix, terms in the matrix could become very large if det[B] becomes very small or goes to zero. This would only be likely to occur when two of the eigenvalues become identical, i.e. when K_z goes to zero for either the GW or thermal conduction wave modes. This case, where the wave front is

vertical, has been discussed by Cowling et al.(4) for GW's, and is called the condition for critical coupling.

2.4 Constraints on the Neutral Wind Model

The presence of terms involving v_{nxo} and v_{nyo} in the matrix [A] makes equation (2.19) considerably more difficult to solve. Ordinarily, the only effect of a neutral wind on the GW is considered to be a Doppler shift in frequency of the form $\omega' = \omega - k_x v_{nxo} - k_y v_{nyo}$; however, the inclusion of ion drag introduces an anisotropy in the wind effect. Because this anisotropic effect is difficult to handle mathematically, we will find a set of restrictions on v_{no}, the magnitude of the horizontal wind vector, which permits us to eliminate all wind effect terms from equations (2.17) except the Doppler shift.

The first and most important constraint concerns the Doppler shifted frequency ω'. The condition where $\omega' \to 0$ has been discussed at some length by Cowling et al. (4). When this happens, the wave is asymptotically trapped and dissipated. In order to eliminate the explicit wind effect terms, we have to impose more severe restrictions than simply that $\omega' \neq 0$. First we assume that ω is at least of the order of ν ; if this were not so, that is if $\omega << \nu$, ion drag losses would dominate, and the wave would be quickly dissipated. Then we constrain ω' so that either

$$\omega' >> \nu$$

or if $\omega \sim \nu$, then the Doppler shift must be small, that is

$$\omega >> |k_x v_{nxo} + k_y v_{nyo}|$$

Either condition permits us to neglect the w_1 term in a_{42}. Furthermore, since $v_{no}^2 << c^2$ at ionospheric heights, we can neglect the w_3 term in a_{42} and a_{43} if either of these conditions hold. Also, since $\nu v_{nxo} << g$, the w_2 terms can be neglected in a_{22} and a_{23}. (These statements assume that $v_{no} < 250$ meters/sec - a reasonable assumption (48)).

The second constraint is that wind shear be negligible; that is, $\dot{v}_{no} \simeq 0$. This constraint eliminates all the remaining explicit wind effect terms from (2.17). It should be noted that the $\dot{w}_1$ term in the expression for a_{11} is not automatically negligible under this constaint, since a term involving $\dot{\nu}$ is involved. This term may be neglected if

$$\frac{1}{H} \geq \frac{\dot{\nu}}{\nu}$$

using the first constraint above. This condition is generally a valid one, at and above the F2 peak. Even well below the F2 peak, where the ion density gradient is steepest, computation from typical ion density profiles such as those given in Chapter 5 shows that $\frac{\dot{\nu}}{\nu} \simeq .05$ km^{-1}, or about the same order as 1/H at these altitudes.

If both of these constraints are met, then we can assume that the only effect of the neutral wind will be a Doppler shift of the form described above. However, these are very severe constraints. It is unlikely that the wind shear is

negligible below 200 km; furthermore, for many waves, the Doppler shift can be large enough that $\omega' \to 0$. For mathematical convenience in solving the problem, we assume that the constraints are satisfied. However, in any given real problem involving wind, a careful check of both constraints is necessary, since they are not generally valid.

2.5 The Dispersion and Polarization Relations

In this section we will set down the dispersion and polarization relations which have been derived using the assumptions of the previous section.

Define:

$$\gamma_1 = \frac{\gamma}{\gamma - 1}$$

$$\psi = \frac{\lambda_o T_o}{j\omega' p_o}$$

$$k_1 = \frac{k_x \nu \cos I \sin I}{\omega' - j\nu \sin^2 I}$$

$$c_1 = \frac{\omega'}{gH} - \frac{k_x^2}{\omega' - j\nu \sin^2 I} - \frac{k_y^2}{\omega' - j\nu}$$

$$c_2 = \gamma_1 + k^2 \psi$$

$$c_3 = \frac{\omega'(\omega' - j\nu)}{\omega' - j\nu \sin^2 I}$$

Then equation (2.19) becomes

$$\det\begin{bmatrix} K_z - \frac{j}{2H} - jk_1 & -c_1 & \frac{\omega'}{gH} & 0 \\ -c_3 & K_z + \frac{j}{2H} - jk_1 & \frac{-j}{H} & 0 \\ 0 & 0 & \lambda_o T_o (K_z + \frac{j}{2H}) & -jp_o \\ -jg(1+\gamma_1 \dot{H}) & -\omega' & \omega' c_2 & K_z - \frac{j}{2H} \end{bmatrix} = 0$$

which can be written as

$$\psi K_z^4 - 2jk_1 \psi K_z^3 + K_z^2 \left[c_2 + \psi\left(\frac{1}{2H^2} - k_1^2 - c_1 c_3\right)\right]$$

$$+ jK_z\left(-2k_1 c_2 - 2\frac{k_1 \psi}{4H^2} + \gamma_1 \frac{\dot{H}}{H}\right) + \frac{\psi}{4H^2}\left(\frac{1}{4H^2} - k_1^2 - c_1 c_3\right) + \frac{c_2}{4H^2}$$

$$- c_1 c_2 c_3 - c_2 k_1^2 - \frac{1}{H^2} + \frac{\omega' c_3}{gH} + \frac{c_1 g}{\omega' H} + \gamma_1 \frac{\dot{H}}{H}\left(-\frac{1}{2H} + k_1 + \frac{c_1 g}{\omega'}\right)$$

$$= 0 \qquad (2.21)$$

This is a fourth-order equation in K_z, and its solution will yield four roots. These roots correspond to four characteristic waves: two gravity waves, one upgoing and one downgoing, and two thermal conduction waves, also one upgoing and one downgoing. If the matrix $[B]^{-1}[\dot{B}]$ is sufficiently small at all altitudes, so that coupling between modes is minimal, the upgoing GW will be the only mode present. In the numerical solution to be discussed later, we will in fact assume that the upgoing GW mode is the only one present, and will solve (2.21) numerically for this root of K_z.

The selection of the proper root of (2.21) is an important, but not a difficult, task. The upgoing GW mode must have a

negative imaginary part of K_z (since the wave is attenuated as it goes upward). This makes it easy to eliminate the two downgoing waves, and we only need to separate the upgoing GW from the upgoing thermal conduction wave. Volland (47) has already done this; for equation (6) of his paper is equivalent to equation (2.21) above (if we set $\nu = \dot{H} = 0$); by using this form of (2.21), that is,

$$K_z^4 + d_1 K_z^2 + d_2 = 0$$

the GW root is given by (from Volland):

$$K_z = \left[-\frac{d_1}{2} - \left(\frac{d_1^2}{2} - 4d_2\right)^{1/2} \right]^{1/2}$$

The GW root was approximated initially using this equation, followed by an iterated solution to 2.21 with ν and $\dot{H}$ included.

With K_z thus determined, we use it to find the polarization relations from equation (2.16):

$$P = \frac{\omega'^2(\gamma-1)}{\sqrt{p_o}} \left\{ \left(K_z - \frac{j}{2H} - jk_1\right)\left[c_2 + \psi\left(K_z^2 + \frac{1}{4H^2}\right)\right] + \frac{j(1+\gamma_1\dot{H})}{H} \right\}$$

$$W = \frac{\omega'^2(\gamma-1)}{\sqrt{p_o}} \left\{ c_1 gH\left[c_2 + \psi\left(K_z^2 + \frac{1}{4H^2}\right)\right] - \omega' \right\}$$

$$T = \frac{\omega'(\gamma-1)}{\sqrt{p_o}} \left[jc_1 g(1+\gamma_1 \dot{H}) + \omega'(K_z - \frac{j}{2H} - jK_1)\right]$$

$$R = P - T$$

$$U = \frac{1}{\omega' - j\nu \sin^2 I} \left[k_x gHP + \nu \cos I \sin I W\right]$$

These are used to determine the perturbed magnitudes of ρ, T_n, and $\bar{v}_n$ as discussed in section 3.5. They reduce to the dispersion and polarization relations of Hines (17) for the lossless isothermal case; that is, if we set

$$\nu \equiv \psi \equiv \dot{H} \equiv 0 \quad .$$

In the non-isothermal lossless atmosphere, ($\nu = \psi = 0$), equation (2.21) reduces to equation (10) of Hines' paper (19) for the same case. For the case of an isothermal atmosphere with ion drag neglected ($\nu = \dot{H} = 0$), equation (2.21) reduces (after some transformation of variables) to equation (6) of Volland's (47). Finally, in an isothermal atmosphere with thermal conductivity neglected ($\dot{H} = \psi = 0$) we obtain equation (20) of Liu and Yeh (31) from (2.21).

2.6 Energy Flux

In this section, for notational convenience, we will write perturbed quantities as

$$p = p_o + p_1 + p_2 + \ldots$$

$$\bar{v}_n = \bar{v}_o + \bar{v}_1 + \bar{v}_2 + \ldots$$

...etc.

where the subscript indicates the perturbation order. We assume here that $\bar{v}_o \equiv 0$.

For an isothermal atmosphere, the instantaneous flux of wave energy, which we will call $\bar{F}_w$, has been written as (21), (47)

$$\bar{F}_w = p\bar{v}_n$$

and the time average of such a flux is usually written as

$$\langle \bar{F}_w \rangle = \frac{1}{2} p_1 \bar{v}_1^* \tag{2.22}$$

where the asterisk indicates a complex conjugate and the <>the time average. In (2.22) p_1 and v_1 are complex,in contrast to our usual notation. This is not a correct expression to begin with, as Eckart (8) and Jones (28) have pointed out; and its indiscriminate application to a nonisothermal atmosphere can lead to a physically unacceptable growth in energy flux with altitude in an upgoing wave. The chief problem is that second-order perturbation quantities, which we have excluded from consideration, should properly be included in equation (2.22).

In order to avoid becoming involved with second order perturbation equations, we will use an approach which Eckart has discussed (8). We rewrite the first-order equivalent of equations (2.1) through (2.4) in the following form:

$$\frac{\partial \rho_1}{\partial t} + \nabla \cdot (\rho_o \bar{v}_1) = 0 \tag{2.23}$$

$$\rho_o \frac{\partial \bar{v}_1}{\partial t} = \rho_1 \bar{g} - \nabla p_1 - \nu_{in} \rho_i (\bar{v}_1 - \bar{v}_{i1}) \tag{2.24}$$

$$\frac{\partial p_1}{\partial t} + \nabla \cdot (p_o \bar{v}_1) = (\gamma-1)[Q_1 + \nabla \cdot (\lambda \nabla T_n)_1 - p_o \nabla \cdot \bar{v}_1] \tag{2.25}$$

$$\frac{p_1}{p_o} = \frac{T_1}{T_o} + \frac{\rho_1}{\rho_o} \tag{2.26}$$

where we have used a combination of equations (2.1), (2.3), and(2.4) in writing (2.25). We now multiply (2.23) by

$$s_1 = \frac{\gamma p_o \frac{\rho_1}{\rho_o} - p_1}{\gamma p_o \frac{(v_1 \cdot \nabla \rho_o)}{\bar{v}_1 \cdot \nabla p_o} - \rho_o}$$

and multiply (2.25) by

$$\frac{1}{\gamma p_o} (p_1 - \rho_o s_1)$$

then add the resulting two expressions to the dot product of (2.24) with $\bar{v}_1$. The resulting equation, after some simplification, is

$$\frac{\partial}{\partial t}\left[\frac{\rho_o v_1^2}{2} + \frac{p_1^2}{2\gamma p_o} + \frac{(p_1 - c^2\rho_1)^2}{2\gamma p_o(\gamma-1+H)}\right] + \nabla \cdot (p_1 \bar{v}_1)$$
$$= \frac{1}{1+\gamma_1 H}\left(\frac{T_1}{T_o} + \frac{p_1}{p_o} H\right)[Q_1 + \nabla \cdot (\lambda \nabla \bar{T}_n)_1] - \nu_{in}\rho_i \bar{v}_i (\bar{v}_1 - \bar{v}_{i1}) \tag{2.27}$$

Equation (2.27) is an energy conservation equation similar in many ways to equation (21-1) of Eckart's (8). The time derivative term is called the external energy, and

includes the second-order kinetic energy ($\frac{1}{2}\rho_o v_1^2$), the elastic energy ($\frac{1}{2} p_1^2/\gamma p_o$), and the thermobaric energy. Of course, this is not a true energy conservation equation, since source or sink terms are present on the right hand side of (2.27).

In the lower thermosphere, where a steep positive gradient of temperature exists, equation (2.27) gives an apparent increase in energy flux with altitude. However, we can verify that the time average vertical flux of (2.27) -- that is, the flux given by equation (2.27) in the z direction-- will be constant in an isothermal lossless atmosphere, and a steadily decreasing function of altitude in an isothermal lossy atmosphere. For the lossless case, the polarization relations give

$$p_1 = \sqrt{p_o}\,\omega'^2(\gamma K_z - \frac{j}{2H})A' \exp\left(-j\int_o^z K_z dz\right)$$

$$(v_1)_z = \frac{\omega'}{\sqrt{p_o}}(\omega'^2 - k^2c^2)\,A' \exp\left(-j\int_o^z K_z dz\right)$$

then

$$\langle F_w\rangle_z = \frac{\omega'^3}{2}\left[(\gamma K_z - \frac{j}{2H})(\omega' - k^2c^2)\right]|A'|^2 \cdot \exp j\int_o^z (K_z^* - K_z)dz \qquad (2.28)$$

If K_z is real (no loss), the integrand above is zero and the exponential factor is unity. All the other terms in (2.28) are constant in an isothermal atmosphere, so the vertical flux is constant also.

If K_z is complex due to the presence of losses, other terms will be present within the brackets in (2.28). However, (2.28) can be considered a reasonable approximation for our purposes. The term of primary importance is the exponential factor: If $K_z = K_{zr} + jK_{zi}$, it becomes

$$\exp\left(2\int_o^z K_{zi}\,dz\right)$$

and since K_{zi} is negative for losses in an upgoing GW, this factor decreases steadily as z increases. The vertical energy flux is therefore a steadily decreasing function of altitude in a lossy isothermal atmosphere. Thus equation (2.27) can be used as a qualitative measure of vertical energy flux in the upper part of the F region (where neutral temperature is nearly constant); it should not be considered as an exact quantitative measure, since we have neglected the term $p_o v_2$ in computing (2.27).

3. IONIZATION DENSITY VARIATIONS IN TIME AND SPACE

3.1 Introduction

The ionization density in the ionosphere satisfies the equation of continuity, which is a parabolic partial differential equation of the second order. We shall use it in the form developed by Pound and Yeh (35) and Fritz and Yeh (11). This equation, with attendant boundary conditions, is then solved by numerical methods to give a profile of ionization density as a function of height and time.

The equation, as they derive it, has limitations which make it unsuitable for application to an atmosphere containing neutral winds and waves. In particular, it is assumed that:

a) the atmosphere is isothermal;

b) no neutral gas velocity exists;

c) no quantities have a spatial variation in the horizontal plane.

Cho and Yeh (48) have modified the numerical approach to remove restrictions a) and b), but their model still did not provide for the existence of a wave structure. While the derivation to follow parallels their work in many ways, we will remove all the restrictions cited above. The resulting partial differential equation, after we make an appropriate transformation of variables, reduces to an equation in two variables, time and the transformed spatial variable; nevertheless, the wave induced horizontal gradient is taken into account. The final form of the equation is especially well

suited for numerical solution.

3.2 Development of the Equation of Continuity

The equation of continuity for ion number density is

$$\frac{\partial N}{\partial t} + \nabla \cdot (N\bar{v}_i) = q - L \tag{3.1}$$

The ionization velocity $\bar{v}_i$ is determined by a balance of three forces: gravitation, partial pressure (diffusion), and the "frictional" force due to collisions with neutral particles:

$$\bar{v}_i = \{\bar{v}_n \cdot \hat{B}_o - \frac{g \sin I}{\nu_{in}} - \frac{K\hat{B}_o \cdot \nabla[N(T_i+T_e)]}{m_i \nu_{in} N}\} \hat{B}_o \tag{3.2}$$

so that

$$\nabla \cdot (N\bar{v}_i) = \sin I \frac{\partial}{\partial z} \{N(v_{nx}\cos I + v_{nz}\sin I)$$

$$- \frac{Ng}{\nu_{in}} \sin I - \frac{K}{m_i \nu_{in}} [\cos I \frac{\partial}{\partial z} N(T_i+T_e) + \sin I \frac{\partial}{\partial z} \cdot$$

$$N(T_i+T_e)]\} + \cos I \frac{\partial}{\partial x} \{N(v_{nx}\cos I + v_{nz}\sin I) - \frac{Ng}{\nu_{in}} \sin I$$

$$- \frac{K}{m_i \nu_{in}} [\cos I \frac{\partial}{\partial x} N (T_i+T_e) + \sin I \frac{\partial}{\partial z} (T_i+T_e)N]\} \tag{3.3}$$

The assumptions made in writing (3.2) are that (i) the ions can move only along the magnetic field lines, (ii) the magnetic field lines are straight in the portion of the ionosphere of interest, and (iii) the dynamo field can be ignored. Of course, the approximation of locally straight magnetic field

lines having a constant dip angle is not a good one at the equator. To avoid this difficulty, we shall apply the theory only to the non-equatorial ionosphere. The constancy of dip permits us to transform (3.3) to the normal or canonical form by the linear transformation of variables

$$\xi = x \sin I - z \cos I$$

$$\zeta = z$$

$$y = y$$

This is a non-orthogonal transformation of the coordinate system. The coordinate ξ is perpendicular to the magnetic field line in the x-z plane. In a solution of the equation in the transformed coordinate system, we hold ξ and y constant, so that motion in space will be along the field line. Under this transformation, (3.3) becomes

$$\nabla \cdot (N\bar{v}_i) = \sin I \frac{\partial}{\partial \zeta} \{ - \frac{K \sin I}{m_i \nu_{in}} \frac{\partial}{\partial \zeta} [N(T_i+T_e)] - \frac{Ng}{\nu_{in}} \cdot \sin I + N(v_{nx} \cos I + v_{nz} \sin I) \} \tag{3.4}$$

We can then combine (3.1) and (3.4) to obtain the complete equation in a form that is particularly well suited to application of the numerical approach:

$$\frac{\partial N}{\partial t} = q - L + \sin I \left[G_1 \frac{\partial^2 N}{\partial \zeta^2} + \left(\frac{\partial G_1}{\partial \zeta} + G_2 \right) \frac{\partial N}{\partial \zeta} + N \frac{\partial G_2}{\partial \zeta} \right] \tag{3.5}$$

where

$$G_1 = \frac{K \sin I (T_i+T_e)}{m_i \nu_{in}}$$

$$G_2 = \frac{g \sin I}{\nu_{in}} + \frac{K \sin I}{m_i \nu_{in}} \frac{\partial}{\partial \zeta} (T_i+Te) - v_{nx} \cos I - v_{nz} \sin I$$

A great advantage of this approach to the continuity equation is its generality. No assumption has been made about the form of any of the parameters in equation (3.5), except the restriction that $I \neq 0$. We are free to include a neutral wind or a neutral wave structure without loss of generality; one simply makes appropriate changes in the computed profiles of the two variable parameters G_1 and G_2.

3.3 Boundary and Initial Conditions

The solution of (3.5) requires that we specify two boundary conditions and an initial condition. Following the previous work in this area, we choose the boundary conditions

$$N(0,t) = 0 \tag{3.6}$$

and

$$\lim_{\zeta \to \infty} (N\bar{v}_i)\ \hat{z} = \Gamma_\infty\ (t) \tag{3.7}$$

Equation (3.7) states that the flux out of the ionosphere at the upper boundary (we use the height of 700 km above the earth's surface) is a given function of time. It may be rewritten in the form

$$\lim_{\zeta \to \infty} \sin I\ \left(G_1\ \frac{\partial N}{\partial \zeta} + G_2 N\right) = -\Gamma_\infty(t) \tag{3.8}$$

The exact form of $\Gamma_\infty(t)$ is still under investigation, and no well defined model is available to us. Several different

phenomena contribute to the flux, including thermal expansion and contraction, the thermospheric neutral wind, and the diurnal change in ionization production. So far, no theory has been able to include all of the phenomena in a resulting expression for flux. We only know that there exists a positive flux (out of the ionosphere) during the daytime, and a negative flux at night. Both fluxes have observed magnitudes of order $10^8 cm^{-2} sec^{-1}$ (10). The flux expression used in our computation is

$$\Gamma_\infty(t) \doteq \Gamma_0 N_{0pk}[T_\infty(t) - T_\infty(avg)]$$

where Γ_0 is a constant, N_{0pk} the peak ambient ion density, and $T_\infty(avg)$ the average value of exospheric temperature.

The initial condition for the ambient ionosphere problem is chosen to represent a profile of the ionosphere at some fixed time t_o:

$$N_o(\zeta,t_o) = N_o(\zeta) \tag{3.9}$$

When (3.5) is solved for the density in the absence of a GW, t_o is 1200 hours local time, and $N_o(\zeta)$ is a simple Chapman layer, given by the equation

$$N_o(\zeta) = \{\frac{q_m}{\alpha} \exp\ [1 - \frac{z_m}{H} - \exp\ (- \frac{z_m}{H \cos\ \chi})]\}^{1/2}$$

where q_m is the production rate at the height of peak production z_m. Having begun computing the non-GW ionosphere profile at time t_o, we introduce a GW into the system at a later time t_1. The initial condition for this computation is

the computed ambient ion density at time t_1. Thus we have in effect "switched on" the wave at time t_1; it did not exist prior to this time. We therefore would expect to observe some kind of transient response, and it is noticeable in some cases. However, the transient response is always small, and a steady state is reached in no more than three computation cycles in the observed computer results.

3.4 Ionization Production and Loss

The loss term L in (3.5) is generally written as

$$L = \frac{\alpha\beta}{\beta + \alpha N} N^2 \tag{3.10}$$

where α is assumed constant, and β is a function of ξ, ζ, y, and t, in the presence of a wave structure. β is proportional to the number density $n(N_2)$ of molecular nitrogen:

$$\beta = \beta_o n(N_2)$$

where β_o is a constant. Since a perturbation change in $n(N_2)$ is approximately proportional to a perturbation change in the neutral density ρ, we can write the perturbed value of β as

$$\beta = \beta_o n_o(N_2)(1 + A'R) \tag{3.11}$$

using the notation of section 2.3, $n_o(N_2)$ being the unperturbed number density of N_2.

The production term q can be dealt with in similar fashion. In a nonisothermal atmosphere, it may be written as

$$q = \sigma_{io} n(O) S \tag{3.12}$$

where S is the intensity of ionizing solar radiation flux, σ_{io} is the effective ionization cross section of atomic oxygen, and n(O) is the number density of atomic oxygen. A GW affects S, as Hooke has noted (25), but the primary (and most predictable) effect of a neutral wave structure is the perturbation change in n(O). This may be taken as proportional to changes in ρ, with little loss of accuracy. A reasonable approximation to the production term is therefore

$$q = Q_i(\zeta,\chi)(1 + A'R) \tag{3.13}$$

χ being the solar zenith angle. Q_i is computed from the results of Cho and Yeh, using equation (3.12). Their model depends on the determination of the optical depths of atomic oxygen and molecular nitrogen, which are given by

$$\tau_O = \sigma_{ao} \int_L n(O) ds$$
$$\tau_{N_2} = \sigma_{aN} \int_L n(N_2) ds$$

L being the ray path of solar radiation from the top of the atmosphere to the point under concern, and σ_{aO} and σ_{aN} being the absorption cross sections of O and N_2, respectively. When the optical depths are computed, S is found from

$$S = S_\infty \exp(-\tau_O - \tau_{N_2})$$

S_∞ being the intensity of solar ionizing radiation at the top of the atmosphere.

3.5 The Effect of Gravity Waves on a Computation of Ion Density

Equation (3.5), with its attendant equations (3.6) and (3.8) through (3.11), plus (3.13), may be solved numerically to find $N(\xi,y,\zeta,t)$. If no wave structure is assumed, the solution is straightforward and will yield $N(\zeta,t)$--a profile of the unperturbed ionosphere. A neutral wind model is easily selected and included in this solution.

We, however, are interested in including the effect of an acoustic-gravity wave which is assumed to propagate in the neutral atmosphere. Following the results of Chapter 2, suppose that f is any atmospheric or ionospheric parameter which is perturbed by the passage of the GW. (This of course excludes N, which is not a perturbed quantity.) Then

$$f(\xi,y,\zeta_n,t) = f_o(\zeta_n,t) + f_o(\zeta_n,t)\ \text{Real}\ \{FA \exp j[\omega t - \frac{k_x\xi}{\sin I} - k_y y - \sum_{m=1}^{n} (K_{zm}+k_x \cot I)\Delta\zeta_m]\} \qquad (3.14)$$

where the m (or n) subscript denotes a quantity at the m^{th} (or n^{th}) level. $f(\xi,y,\zeta_n,t)$ is real. This equation gives the approximate value of f at the n^{th} level, assuming the atmosphere to be divided into slabs of thickness $\Delta\zeta_m$ at the m^{th} level. F is determined from the polarization relations. We will use (3.14) in computing the values of β, q, G_1 and G_2 which are needed to solve equation (3.5). Thus β and q are given by equations 3.11 and 3.12; and in computing G_1 and G_2, we use

$$\nu_{in} = \nu_{ino}(1+A'R)$$

$$(T_i+T_e) = (T_i+T_e)_o(1+A'T)$$

$$v_{nx} = v_{nxo} + A'U$$

$$v_{nz} = WA'$$

The rationale for these approximations is given in Chapter 2, except for the implicit assumption above that T_i and T_e vary as the neutral temperature under wave perturbations. This is a good assumption in the case of ion temperature, which depends on the neutral temperature (and is identical to it below about 300 km). It may not be a good assumption for the electron temperature in the daytime, when solar phenomena affect T_e more than the neutral temperature does; however, the error introduced by the assumption is probably quite small. Computations indicated no significant difference when the temperature was held at its ambient value during wave passage.

3.6 Temporal Effects and Perturbed Variables

Suppose we rewrite (3.14) so that only time variation is expressly shown (in complex notation):

$$f = f_o(t)(1 + FA_1e^{j\omega t}) \tag{3.15}$$

then the time derivative of f is

$$\frac{\partial f}{\partial t} = \frac{\partial f_o}{\partial t}(1 + FA_1e^{j\omega t}) + j\omega f_o FA_1e^{j\omega t}$$

An examination of equations (2.9) through (2.13) makes it apparent that we have neglected $\frac{1}{f_o}\frac{\partial f_o}{\partial t}$ in comparison with $j\omega$ in all cases. Since the winds are not expressed in the exact form of (3.15), we note that

$$\frac{1}{U}\frac{\partial v_{nxo}}{\partial t} \quad \text{and} \quad \frac{1}{V}\frac{\partial v_{nyo}}{\partial t}$$

are neglected in comparison with $j\omega$. We will now check the accuracy of each of these approximations for waves of frequency $\omega \geq .001$ radians/sec, since this is about the lower bound of observed TID frequencies. We will consider each variable in turn below.

Temperature: From CIRA 1965 (5), it can be determined that changes in neutral temperature of 100°K per hour seldom occur, even during periods of high solar activity. Based on a temperature of 1000°K,

$$\frac{1}{T_o}\left|\frac{\partial T_o}{\partial t}\right| < .00003 \text{ sec}^{-1};$$

therefore, the inequality

$$\frac{1}{T_o}\left|\frac{\partial T_o}{\partial t}\right| << \omega$$

is valid.

Neutral density: Again using CIRA 1965, we find that for mean solar activity, during the morning at 300 km altitude, the time gradient of density is near its diurnal maximum. Then

$$\frac{1}{\rho_o} \left|\frac{\partial \rho_o}{\partial t}\right| < .00004 \text{ sec}^{-1}$$

so

$$\frac{1}{\rho_o} \left|\frac{\partial \rho_o}{\partial t}\right| << \omega$$

Wind: Using the results of Cho and Yeh (48), we observe that a change of speed of 100 meters/sec in two hours for either the east-west or north-south component is about the largest likely variation. Therefore

$$\left|\frac{\partial v_{nxo}}{\partial t}\right| \text{ and } \left|\frac{\partial v_{nyo}}{\partial t}\right| < .015 \text{ meters/sec}^2$$

Numerical computations indicate that for typical GW's with frequency $\omega = .001$ radians/sec, horizontal velocities increase from about 15 meters/sec at 700 km to 50 meters/sec at the peak of GW amplitude. Therefore, typically,

$$\frac{1}{U}\left|\frac{\partial v_{nxo}}{\partial t}\right| \text{ and } \frac{1}{V}\left|\frac{\partial v_{nyo}}{\partial t}\right| < .001 \text{ sec}^{-1}$$

These terms are therefore sometimes of the same order as ω and their neglect is not always justified.

This does not tell the full story, however. It is clear that the magnitudes of U and V depend on ϕ, the GW azimuth of propagation. As an example of the problem we face, consider an eastward propagating wave. The north-south diurnal change in wind speed could completely mask the relatively weak north-south gas parcel motion which is caused by the GW.

Nor does our problem disappear for shorter period GW's, since U and V decrease with increasing frequency.

An attempt to remove this approximation introduces problems which are better not considered at this point. In any event, we will not be using neutral winds in computation of results for this paper, though provision is made for them in the program. Therefore the validity of the approximation will not be considered further. This section is primarily intended as a warning to users of the computer program that the inclusion of a neutral wind may be fraught with difficulties.

Ionization Density: We have not assumed that N is a perturbed quantity, and therefore did not assume that $N(t) \propto e^{j\omega t}$; however this assumption is used by some authors, so let us consider the validity of such an approximation.

For a wintertime sunrise, when the time gradient of N_o is at its annual peak, N_o can increase as much as sixfold in a four hour period. Then

$$\left|\frac{1}{N_o}\frac{\partial N_o}{\partial t}\right| \simeq .00035$$

therefore, the approximation

$$\left|\frac{1}{N_o}\frac{\partial N_o}{\partial t}\right| << |j\omega|$$

is not always valid, especially during disturbed conditions such as those associated with magnetic storms. However, it appears to be a reasonable approximation for most times and

for shorter wavelengths. This approximation is not used in this work, as we solve the equation using $\frac{\partial N}{\partial t}$, where N is the total electron density, including wave-induced variations.

4. ION DRAG EFFECTS

4.1 Introduction

A considerable amount of work has recently been done on the effect of ion drag, also referred to as ohmic loss, for GW's at ionospheric heights. Gershman and Grigor'yev first developed an approach to the problem (15); the limitations of this approach were pointed out in a qualitative analysis by Hines (24). In a more general approach to the ion drag problem, Liu and Yeh (31) followed the development given by Hines (17) with the inclusion of an ion-neutral collision effect term in the equation of motion, as in our equation (2.2). In these approaches, constraints are set by choosing some parameters as purely real and others as complex. For the approach which is to be used here, where stratified horizontal layers are used, the constraint is that the horizontal wave numer k and azimuth ϕ be real and constant throughout the region.

With k_x and k_y constrained to be real, two conclusions are apparent on examination of the dispersion relation, equation (2.21). One is that, for fixed k, the imaginary part of K_z changes as ϕ is varied. Second, it is obvious that this variation in K_{zi}, which implies a variation in the loss rate of GW energy, is due to the presence of ion drag; the variation vanishes as $\nu \to 0$. We are then led to expect a change in energy loss of the GW as ϕ changes; and this effect, caused

by ion drag, should lead to preferred directions of propagation. In this chapter, we will examine the consequences of this expectation.

4.2 The Effect of Gas Parcel Orbits on Ion Damping

Midgley and Liemohn (32) have developed graphs of the neutral gas parcel orbits as a function of frequency and horizontal phase velocity. We will be interested in the orbits portrayed in figure (4-1), which is an extract from their work. This is the graph for waves whose sources lie below the ionosphere--the type which are of primary interest to us.

Ion drag is caused by the fact that, in the F region, the ion gyrofrequency is much larger than the ion-neutral collision frequency; the ionization is therefore constrained to move along the magnetic field lines, and ions will resist or impede the flow of neutrals across field lines.

Minimum drag will occur, for a given frequency and wave front inclination, in the case of a wave propagating northward or southward ($\phi = 0°$ or $180°$), where the plane of the orbit ellipse is aligned with the earth's magnetic field. Within this plane, a further minimum of drag will occur when the major axis of the ellipse lies along the field line. The drag will be zero only when the gas parcel orbit is a straight line. For internal waves, the zero drag condition almost never occurs, contrary to an assumption which is sometimes made in studies of the problem. Its occurrence would require that

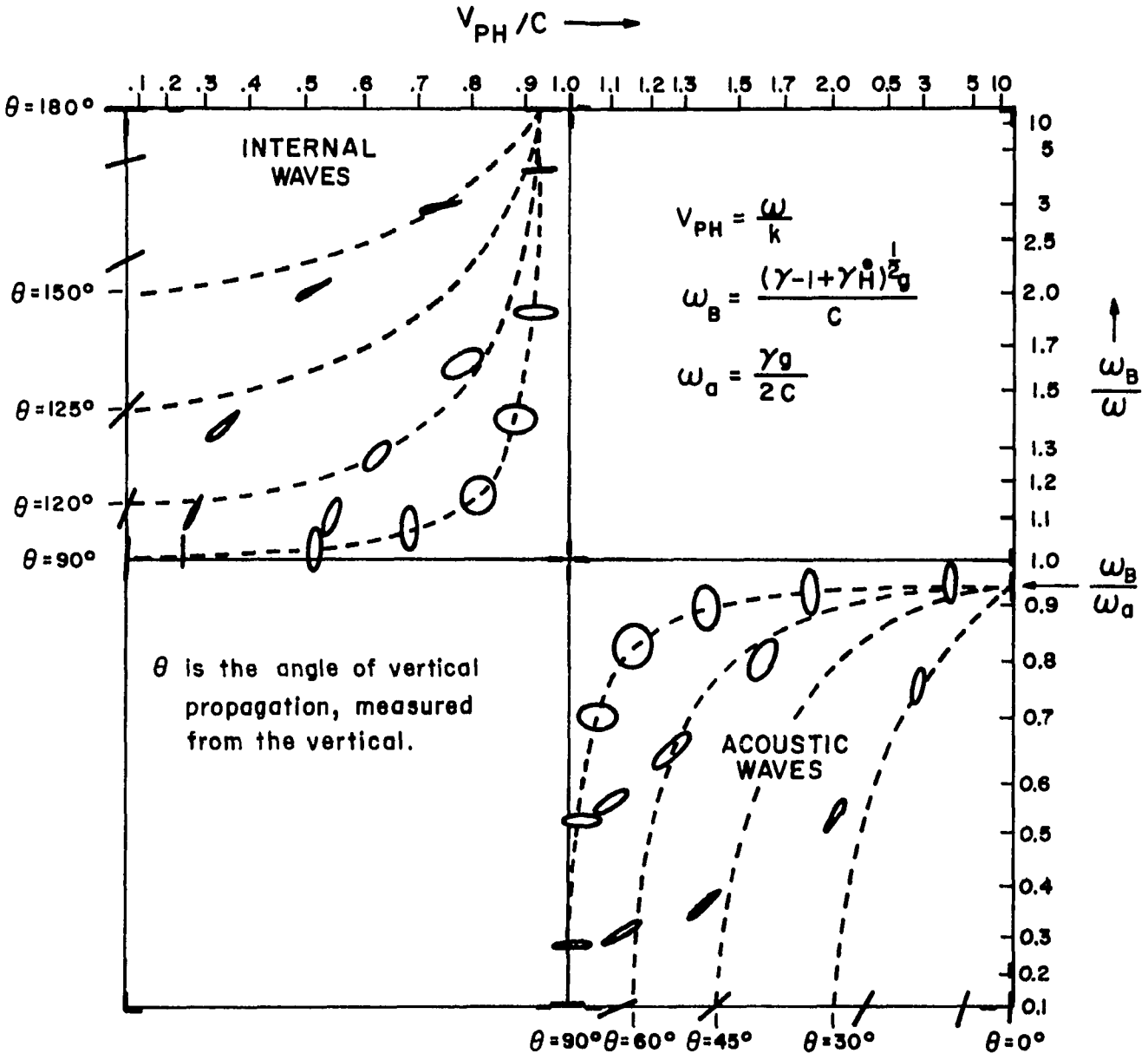

Fig. 4-1

NEUTRAL GAS PARCEL ORBITS FOR WAVES ORIGINATING BELOW THE IONOSPHERE

(from Midgley & Liemohn, 1965)

either $\omega \to 0$ or the horizontal phase velocity $v_{ph} \to 0$, neither case being of interest. For acoustic waves, the zero drag condition occurs in the limiting case of sound waves, or for the case of vertically propagating waves at the magnetic pole.

4.3 The Relative Importance of Ion Drag and Thermal Conduction

We have previously indicated that we would consider the two loss mechanisms of ion drag and thermal conduction. It is common practice in GW analysis to neglect ion drag, just as viscous damping was neglected in comparison with thermal conductivity. This appears to be an unwise step for two reasons: a) ion drag is a highly directional loss effect, as discussed in section 2.2; we also can observe that it appears in equation (2.21) in the form of the terms c_1, c_3, and k_1, which are definitely dependent on azimuth of wave propagation. Thermal conduction, in contrast, acts isotropically in the horizontal plane. b) Ion and thermal conduction damping are two different types of loss mechanism, and the conditions under which each may be important are different. For example, from equation (2.21), we can determine that thermal conduction is significant when

$$\psi \sim \frac{\gamma_1}{k^2}$$

Ion damping, however, is important when ω and ν are of the same order of magnitude. Depending on the values of ω, k, z, or N_o, one of these effects might be negligible, the other

significant; the only certain way to determine what effects are important is to solve the dispersion relation for each case. We can state with certainty that thermal conductivity will become the predominant loss mechanism if one goes sufficiently far up in altitude; but this altitude will be different for different wave parameters. By retaining the ion drag loss in equation (2.21), we can compare its effect to that of thermal conductivity in numerical computation of K_{zi}, the imaginary part of K_z.

4.4 Comparison with Experimental Observations

At least two problems exist in any attempt to reconcile TID observations with the ion drag theory explained in this chapter. First, by measuring perturbations in the ionization density we are most likely to observe exactly those waves which suffer least from ion drag; that is, a TID whose gas parcel orbits move along the magnetic field lines. Conversely, if the orbits are perpendicular to the field lines, no motion of the ionization would be observed. This problem does not exist at all, of course, in direct neutral density measurements such as those of Newton et al. (33). A more serious problem is that of the source of the disturbance. One can establish the preferred direction of wave propagation at a given station without too much difficulty, simply by averaging the direction of propagation over many observations; but the direction so established may be more closely related to a preferred geographical source than to the constraints of ion drag. This

appears to be the case, for example, in the observations of Bowman (3).

Notwithstanding the difficulties cited above, it is significant that most observations of TID's show a tendency for the waves to propagate in a north-south direction. This is particularly true for stations with a low magnetic dip angle, for which the anisotropy with respect to ϕ is greater. To cite a few examples, the observations of Sterling (39) and Thome (41) agree with the results we have discussed. However, the amount of data published to date is not sufficient for this tendency to be labeled as conclusive.

Perhaps the best confirmation of the ion drag theory comes from the data of Newton et al. (33). They observe a tendency for waves to travel in a north-south direction, in general the direction in which ion drag causes the least loss. While their observations do not depend on ionization motion, as we noted above, they do encounter the source problem. They indicate that a possible source region is the polar front.

Waves originating in an impulse disturbance, where the source is well defined, do not fit the plane wave theory used here. However, the motion of the gas parcels should be about the same, so ion drag effects should be much the same as for plane waves. It is instructive to examine the results reported by Albee and Kanellakos (1) for TID's due to a low altitude nuclear explosion. The waves depicted in figure 1 of their paper are far above perturbation magnitude, and nonlinear

effects predominate; nonetheless, it is significant that at Maui, (ϕ = 240°) the disturbance is weaker than at Tonga (ϕ = 0°), though Tonga is twice the distance from the explosion. Such a result is consistent, for plane waves at least, with the ion drag theory.

5. EXPERIMENTAL RESULTS AND NUMERICAL COMPUTATIONS

5.1 Introduction

The numerical computation program described in the appendix has been used to compute altitude profiles of a number of ionospheric parameters in the presence of gravity waves. The program is based on the results of chapters 2 and 3. In addition, the program has been modified to selectively eliminate certain dynamic effects or loss mechanisms (such as ion drag, production, loss, and diffusion perturbations, etc.) in order to permit us to evaluate the significance of the particular effect over a number of cases. We took this approach for a reason: some controversy exists concerning the relative importance of different effects. The primary object of this research work was to determine what effects should be considered in a mathematical treatment of GW propagation; and if a particular effect is not generally significant, to determine the conditions on its significance, insofar as possible. In this chapter, we will therefore present computational results concerning the assumptions discussed below.

In chapter 2, we included both ion drag and terms involving $\dot{H}$ in deriving the dispersion and polarization relations. Both of these effects are frequently neglected in the literature. We further discussed ion drag in some detail in chapter 4. In section 5.5, we make comparisons of the relative losses suffered by GW's with and without the inclusion of ion drag. In section 5.6, the effect of $\dot{H}$ terms is similarly examined.

In chapter 3, we included the effect of perturbations in diffusion, production, and loss, as well as directed neutral velocity, in setting up an equation for N, which was not treated as a perturbed variable. Because the current work in this area follows the lead of Hooke (25), who treated N as a perturbed quantity and considered directed neutral velocity to be the dominant effect of a GW on ion density, we will examine the relative importance of these different effects in section 5.3 by comparing their magnitudes for different cases. In this section we will also consider the desirability of treating ion density as a perturbed quantity. In section 5.4, the closely related topic of phase relationships between different variables is examined.

Finally, in section 5.2, we present the results of a numerical computation and its comparison with an experimentally observed wave. Except for the wave discussed in section 5.2, all computations used the following parameters:

$\Delta\zeta$ = 2 km

Δt = 1/2 hour (in computation of the ambient ionosphere)
= (wave period)/20 (in computing the wave-disturbed ionosphere)

β = .008 sec^{-1} at 120 km

$\alpha = 10^{-8} cm^{-3} sec^{-1}$

HL = 700 km (upper boundary in computations)

I = -70°

λ_o = 324 dyne-cm^2/sec-°K (This is higher than the correct

thermal conductivity coefficient by a factor of 9/5 to allow for viscous effects.)

$F_{10.7} = 1.5 \cdot 10^{-20}$ watt - sec/meter^2 (solar radiation flux at 10.7 cm)

sun's declination = 0

latitude = 40° N

y = 0

T = 1500°K (max); 1000°K (min).

T_{120} = 355°K

(T_e) = 2500°K (max); 1000°K (min)

$\rho_o = .2461\ 10^{-10}$ gm/cm^3 at 120 km

TABLE 1

Horizontal Wave Number	Wave Period	Azimuth	Amplitude
.02 km^{-1}	20 min.	90°	$2 \cdot 10^8$ dynes$^{1/2}$sec^2
.02	"	0°	10^9
.03	"	0°	"
.01	30 min.	0°	"
.01	"	0°	"
.01	"	180°	"
.01	60 min.	0°	"
.01	60 min.	270°	"
.005	"	0°	"
.004	"	90°	$2 \cdot 10^9$
.005	120 min.	0°	10^9

The flux was chosen to have a peak of $2.2 \cdot 10^8$cm^{-2}sec^{-1}. All of the other physical constants and altitude profiles needed

are computed. The models used for computation are discussed in subroutine ZPROFL in the appendix. The series of waves shown in Table 1 was computed, using different times of day and different ionization density profiles. When graphs using one of these waves are presented in this chapter, the pertinent wave parameters listed above are given on the graph.

Though N is computed along the magnetic field line, all of the altitude-time contour graphs to follow have been plotted with a correction factor to give the wave profile in the vertical direction, not along a field line, at a given time.

5.2 Comparison with Experimental Observations

It is helpful to be able to compare wave profiles predicted by the program with those actually observed for TID's in the ionosphere having the same wave parameters. Unfortunately, examples of such TID's where complete wave data is available are rather scarce at non-equatorial latitudes. (Of course, our program is not valid at the magnetic equator). One exception to this statement is a 1966 observation by Georges (13), and we will compare this observation qualitatively with the result computed using our program.

Georges has presented results of TID observations deduced from vertical sounding data. Based on the data he obtained, the wave and site parameters are:

sun's declination	-23°
dip angle I	-67°
k	.005 km^{-1}

coordinates of site	93°W, 37°N
wave period	30 min.
phase velocity	768 meters/sec.
azimuth	173° (ϕ = 187°)
time	2300 - 0200 local time

Georges portrayed his results in the form of a graph of iso-ionic density contours as a function of altitude and time. The graph is reproduced in figure 5-1. For comparison, a wave structure was computed using the parameters described above, or where a parameter is not listed, using the parameters in the introduction. The result is shown in figure 5-2. The curves on this graph are contours of constant ion density, drawn as functions of altitude and time. The magnitude of the density of each contour, in number/cm^3, is shown on the graph. Thus, while the units used to describe the contours are different in figures 5-1 and 5-2, the contours in both graphs represent curves of constant ion (electron) density.

Of course, there are differences in the two graphs due to a difference in the height of the F2 peak between the computed and observed models. However, the similarity in the shape of the contours is striking. Furthermore, the wave-front tilts of the computed and measured waves compare reasonably well (75° to 78° tilt for the computed wave, and 83° tilt for the observed wave). Also, both waves show an amplitude growth with increasing altitude, though the growth is smaller and difficult to measure in the case of the observed TID.

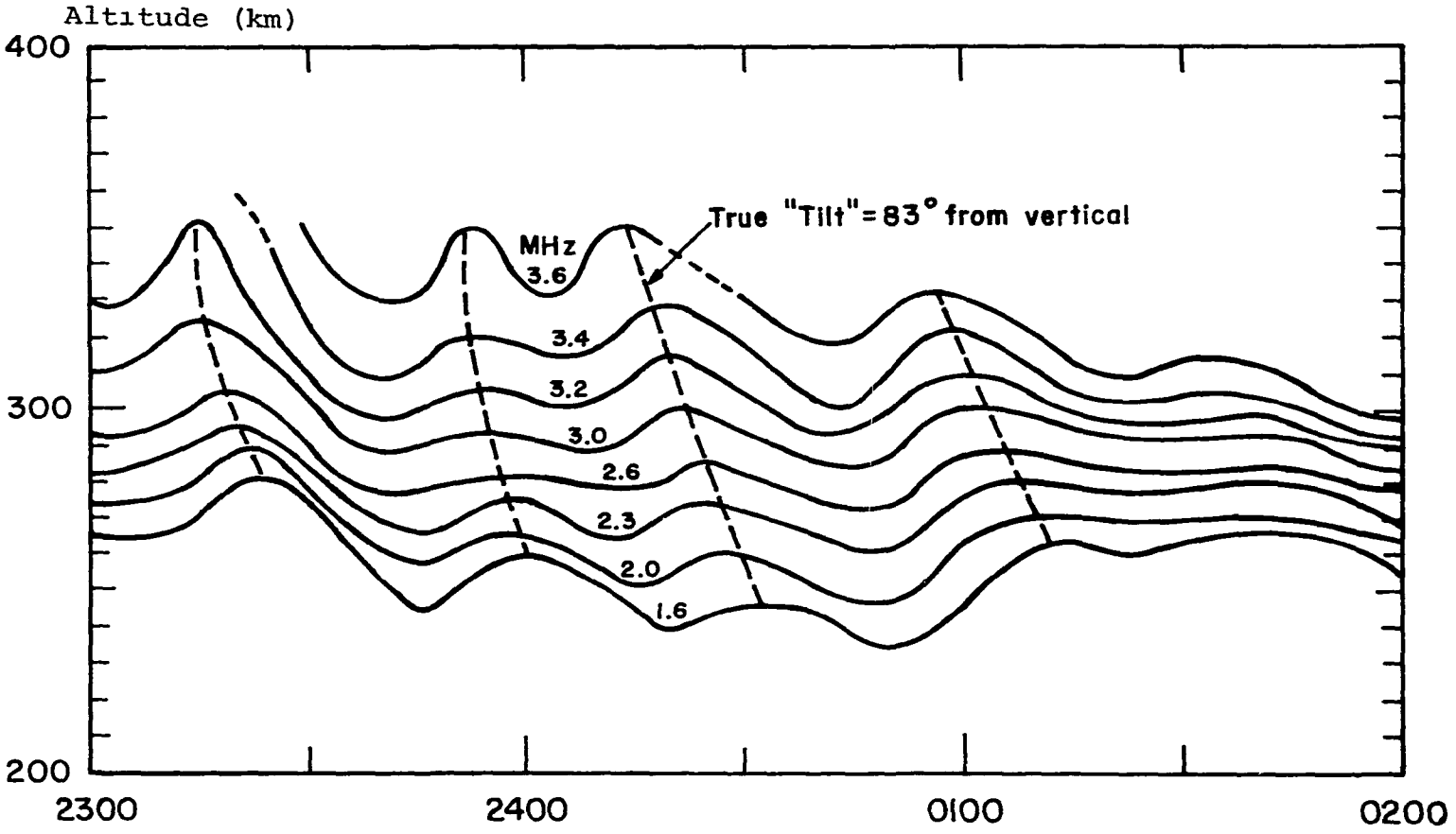

Figure 5-1.

Constant Ion Density Contours for a GW
(from Georges, 1967)

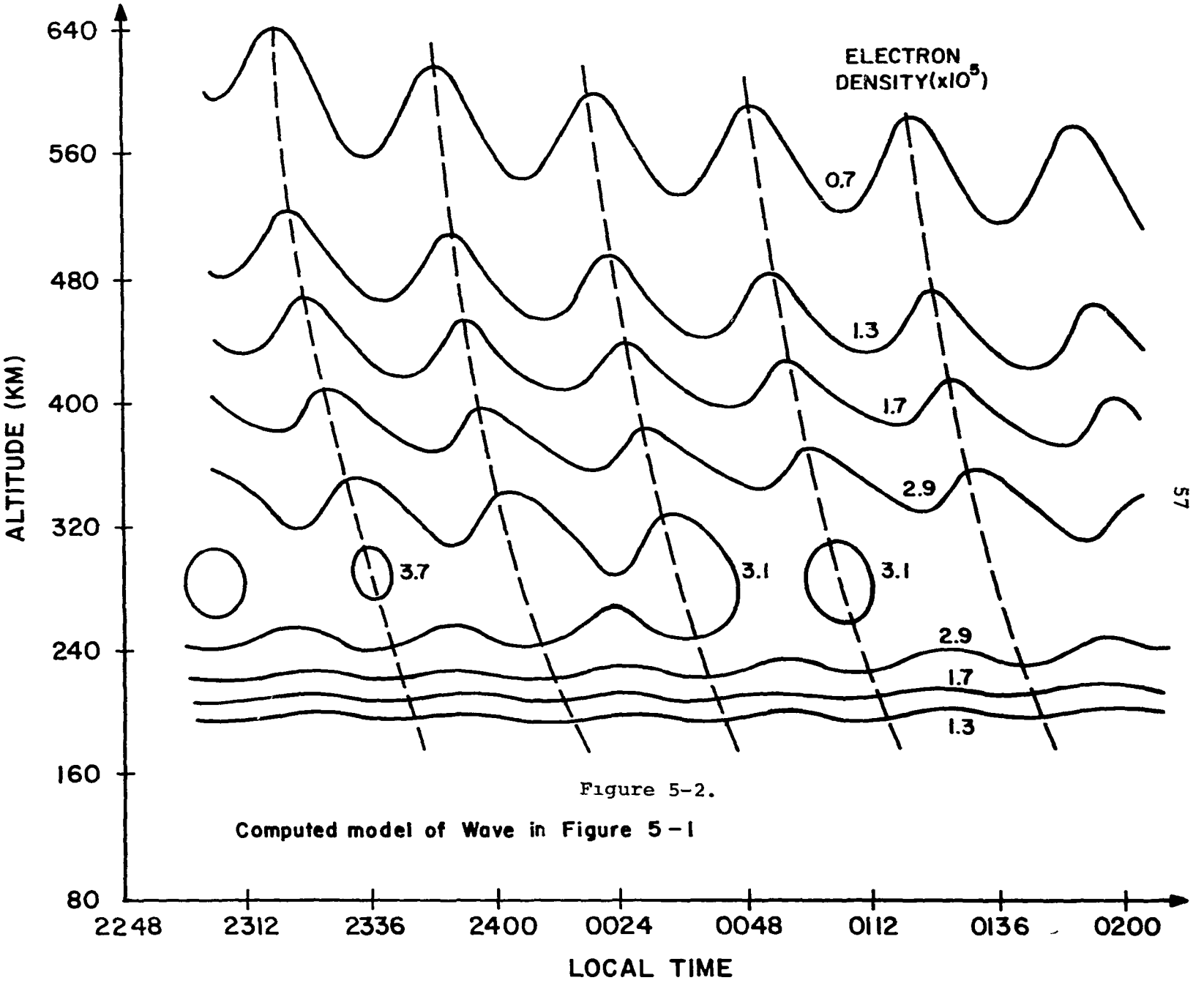

Figure 5-2.

Computed model of Wave in Figure 5-1

5.3 The Relative Importance of Perturbed Parameters

In section 3.5, we discussed the different variables which are perturbed in the presence of a GW. Three of these, ν_{in}, q, and β, were considered to follow the neutral density variations in magnitude and phase. The sum of ion and electron temperature, $T_i + T_e$, was considered to follow the neutral temperature fluctuations. The remaining parameter, which we will call $\bar{v}_g$, the neutral gas directed velocity along the magnetic field line, has a variation given by

$$\bar{v}_g = (\bar{v}_n \cdot \hat{B}_o)\ \hat{B}_o = (v_{nx}\cos I + v_{ny}\sin I)\ \hat{B}_o$$

Because $\bar{v}_g$ does not have an ambient value (its magnitude is zero in the absence of a GW, if we assume no background wind), we cannot readily compare its fluctuations with those of neutral density and temperature to determine its relative importance. We instead find it necessary to resort to the selective removal of certain perturbations to determine their effect on the resulting TID. This procedure is discussed later in this section.

We can, however, compare the perturbed quantities with each other; and if we write the total ion density as the sum of an ambient and a fluctuating quantity,

$$N = N_o + \Delta N \qquad (5.1)$$

we can express the percentage fluctuation of ion density as $|\Delta N/N_o|$ (in percent). It can then readily be compared with the fluctuations in neutral density, $|\rho_1/\rho_0|$, and in neutral

temperature, $|T_1/T_0|$, both expressed as percentage of deviation.

Such a comparison is shown for several typical GWs in figures 5-3 and 5-4. The wave and ionospheric parameters are given beside each graph. Two of these need some explanation. The peak ion density, N_{pk}, is given in number/cm^3. The ion density profiles all follow the pattern given in figures 5-11 through 5-14. θ_B is the acute angle between the magnetic field line and the major axis of the gas parcel orbit ellipse which is discussed in chapter 4. θ_B was determined to within 5° using figure 4-1, and was measured in the plane determined by the field line and the ellipse major axis. Thus the larger the angle θ_B, the less effective the particular wave is in moving ionization along the field lines. Of course, this statement is not valid in comparing different waves, since one wave may have a parcel orbit which is nearly a straight line, while it could be nearly a circle with a different wave.

The results shown in figures 5-3 and 5-4, which are typical of all waves listed in section 5.1, lead us to two conclusions:

1. Neutral density variations are generally smaller than the ion density variations which the GW produces.

2. Temperature variations are even smaller. Note that the only exception to rule 1 occurs for case 3, where the gas parcel orbit major axis is nearly perpendicular to $\hat{B}_o$. In this case, $|v_g|$ is small compared to $|\bar{v}_n|$. Case 4 is similar to case 3, case 1 being more typical for the average GW. A different picture of cases 1 and 3 is given in figures 5-5 and

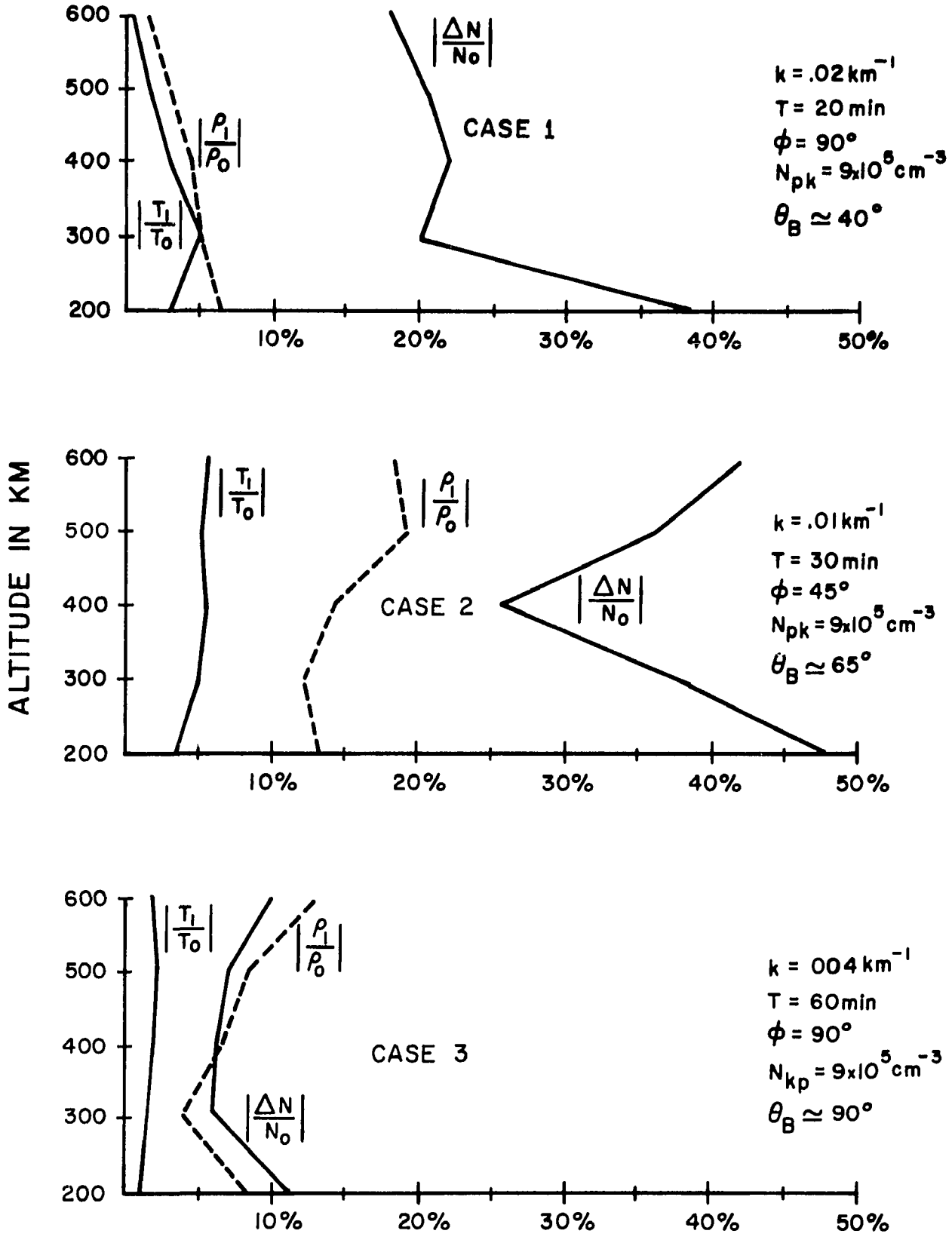

Relative Magnitude of Wave Parameters

Figure 5-3

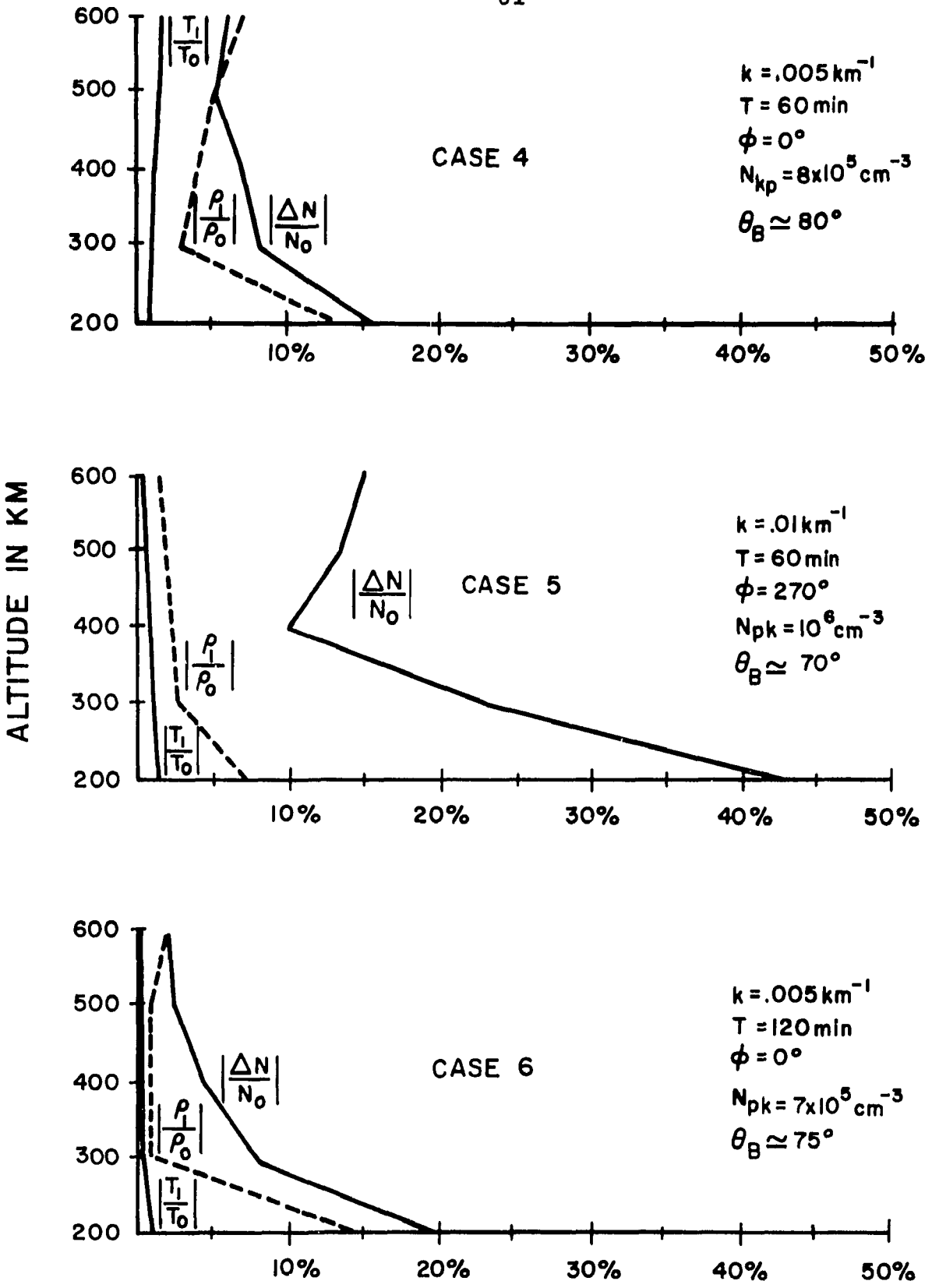

Relative Magnitude of Wave Parameters

Figure 5-4

5-6, where ion density contours of these cases are shown. In those cases where the gas parcel orbit and the magnetic field lines were nearly parallel, a 10% density perturbation corresponded to a 90% (or better) variation in ion density. It was considered pointless to plot these curves, since TIDs of this magnitude are not normally observed.

Based on the results given, and on the fact that the largest observed TIDs (whose parcel orbits presumably are nearly field aligned) typically have about a 25% variation in N (25), we are led to believe that GWs seldom have more than a 5% variation in ρ. (This is a rather arbitrary figure, and should not be taken as the upper limit; a good case can be made for a figure of less than 5%.) It therefore appears that GWs in the ionosphere are generally well within perturbation magnitude.

In order to further assess the importance of various perturbed parameters, the program described in the appendix was modified to remove perturbations in q, β, (T_e+T_i), and ν_{in}. This was done by setting PT(K), PN(K), PX(K), QP(K), and BETAL equal to their unperturbed values in subroutine COFCAL. The waves listed in table 1 were then recomputed with no other changes. The results were striking; No noticeable change in the ion density contours (like those in figure 5-2) was observed in any case! It is apparent that perturbations in these four variables usually contribute almost nothing to the resulting ion density fluctuations. One case which may

well be an exception to this rule is the case where the solar rays are parallel to wave phase fronts; Hooke (25) discussed this case in detail, but no test of it was attempted here. Our result concerning the insignificance of perturbations of q, β, $(T_e + T_i)$ and ν_{in} was correctly predicted by Hooke. It results, in part, from the fact that production and loss perturbations, both being proportional to neutral density fluctuations, tend to cancel each other out generally. However, even at night, when only loss is present, no difference was noticed when loss perturbations were removed, so the cancellation probably is not too important anyway. Perturbations in ν_{in} and (T_e+T_i) only cause perturbations in the diffusion velocity, as we discuss later; and these perturbations are small compared to the effect of directed neutral velocity, as Hooke has pointed out. Our next step is to consider what effects <u>are</u> important.

To begin with, let us write the total velocity $\bar{v}_i$ of the ions as the sum of a diffusion velocity $\bar{v}_d$ and the directed velocity $\bar{v}_g$, where

$$\bar{v}_d = \bar{v}_{do} + \bar{v}_{d1} + \cdots$$

the subscripts indicating the order of perturbation. Then we can write, to the first order,

$$\nabla\cdot(\bar{v}_i N)_1 = \nabla\cdot\ (N_o\bar{v}_g + \Delta N\ \bar{v}_{do} + N_o\bar{v}_{d1}) \qquad (5.2)$$

Here we treat N as a perturbed quantity, in contrast to our approach throughout this paper; ΔN is the first order perturbation. We will continue to treat N as perturbed in this section

(though, as we indicated earlier, a value of 25% for $\Delta N/N_o$ is not unusual), for convenience in comparing our work to that of Hooke (25).

Hooke, in addition to treating N as perturbed, neglected the last two terms on the right hand side of (5.2), as well as neglecting production and loss perturbations. These assumptions lead to equation (49) of his paper, which may be written as, in complex notation,

$$\Delta N = \frac{j}{\omega} (v_{nx}\cos I + v_{nz}\sin I)\left[\frac{\partial N_o}{\partial \zeta} \sin I - j(k_x \cos I + K_z \sin I) N_o\right] \tag{5.3}$$

The physical perturbed density is just the real part of the complex expression given above. A number of wave profile computations were made using equations (5.3) and (5.1) to determine N as a function of height and time. These computed profiles were compared with the profiles for identical waves which were computed using the appendix program (the waves in table 1), under identical ionospheric and atmospheric conditions. The only difference is that one set of profiles was computed using (5.3) and (5.1); the other set involved a full solution of equation (3.5) with boundary conditions, as described in the appendix. The resulting wave profiles differed markedly in all cases where the two sets of results were compared. Two typical cases are shown in figures 5-5 and 5-6. The solid lines in each figure are the constant density profiles, the numbers near each contour giving the ion density ($X \cdot 10^5$ cm^{-3}) of the contour, just as in figure 5-2. The dashed lines are

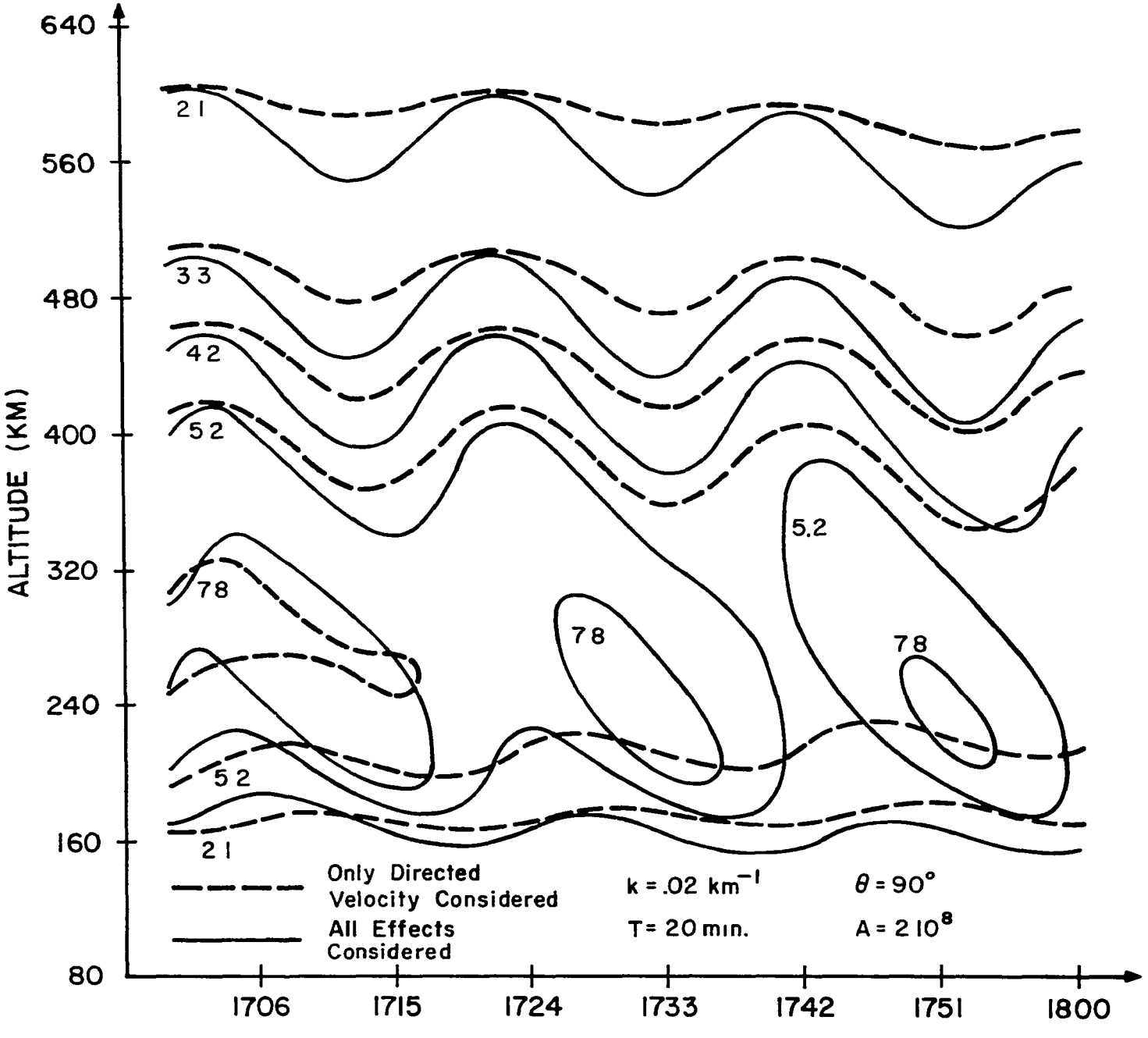

Figure 5-5. Directed Neutral Velocity Effects

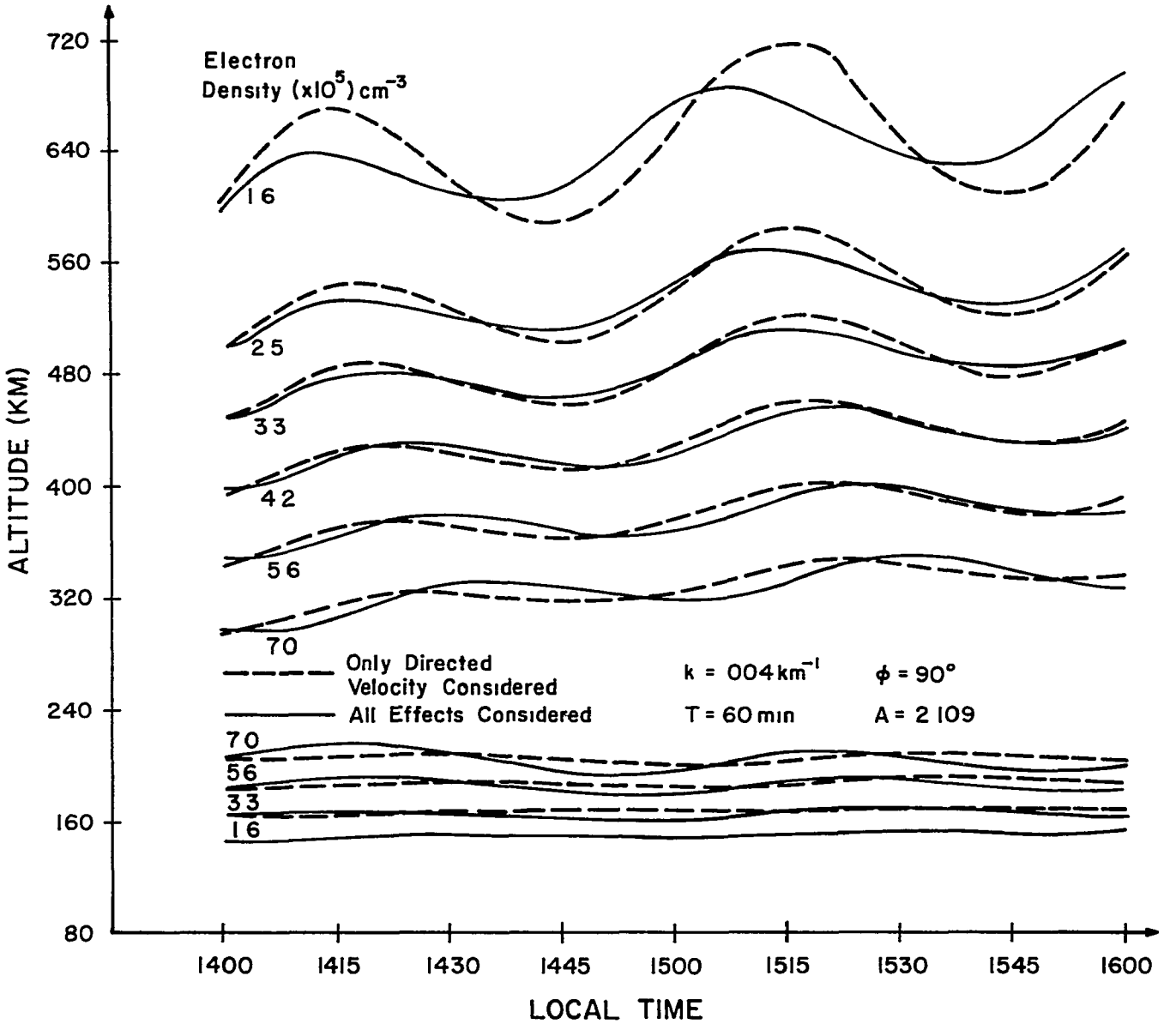

Figure 5-6.

Directed Neutral Velocity Effects

the same-value contours computed using equations (5.3) and (5.1). In the 20 minute period wave, only a magnitude change is noticeable (at least at higher altitudes); in the one hour period wave, both magnitude change and phase shifting are observed.

Clearly, equation (5.3) does not represent the complete solution for GW effects. Yet, as we have indicated, perturbation in production, loss, and diffusion velocity (i.e., in ν_{in} and $T_i + T_e$) do not normally affect the resulting ionization fluctuations to a significant degree. What effects are left to consider?

The neglect of perturbations in ν_{in} and $(T_i + T_e)$ eliminates the last term on the right-hand side of (5.2). One can readily see this if he takes the first-order perturbation equivalent of equation (3.4) assuming N is perturbed, and compares the result to equation (5.2). In formulating (5.3), Hooke neglects the last term in (5.2) too; but he also neglects the next to last term, and this step cannot be justified. The neglect of the $\Delta N\ \bar{v}_{do}$ term in (5.2) is the source of the difference which shows up in figures 5-5, 5-6, and all the computed results. The rationale which Hooke used to neglect this term is that it is small compared to the term $N_o \bar{v}_g$. Computations of the ratio

$$\left| \frac{v_{do} \Delta N}{v_g N_o} \right|$$

show that this is simply not so. Such computations were made

at 100 km steps for seven typical GWs with periods ranging from 20 minutes to two hours. The computational results are shown in figure 5-7. Each wave plot is numbered, with the parameters of the wave listed by the corresponding number in the table on the graph. It can be seen that the ratio drops below the 0.1 level (where the neglect of the $N \bar{v}_{do}$ term would indeed by justified) only at one point for one wave. In general, the two terms are of the same order of magnitude over the altitude range considered (200 to 600 km). The generally rapid increase in the ratio above about 400 km altitude is due to a large increase in ambient diffusion velocity above that altitude.

We must conclude that, if a perturbation approach such as that of equation (5.2) must be used, the $\Delta N \bar{v}_{do}$ term must be kept. However, the use of (5.2) is not really desirable, because N is not generally a perturbed quantity, even though the GW itself is of perturbation magnitude. The effect of this conclusion is to render the assumption that

$$\bar{v}_i = (\bar{v}_n \cdot \hat{B}_o)\, \hat{B}_o$$

which was made in section 2.2, untenable. However, because the use of the assumption permits a ready solution to the problem which was posed, no attempt was made to find a better approximation. Because $\bar{v}_i$ only appears in equation (2.2) and (2.3) in conjunction with $\bar{v}_n$, the assumption would only lead to inaccuracy in cases where

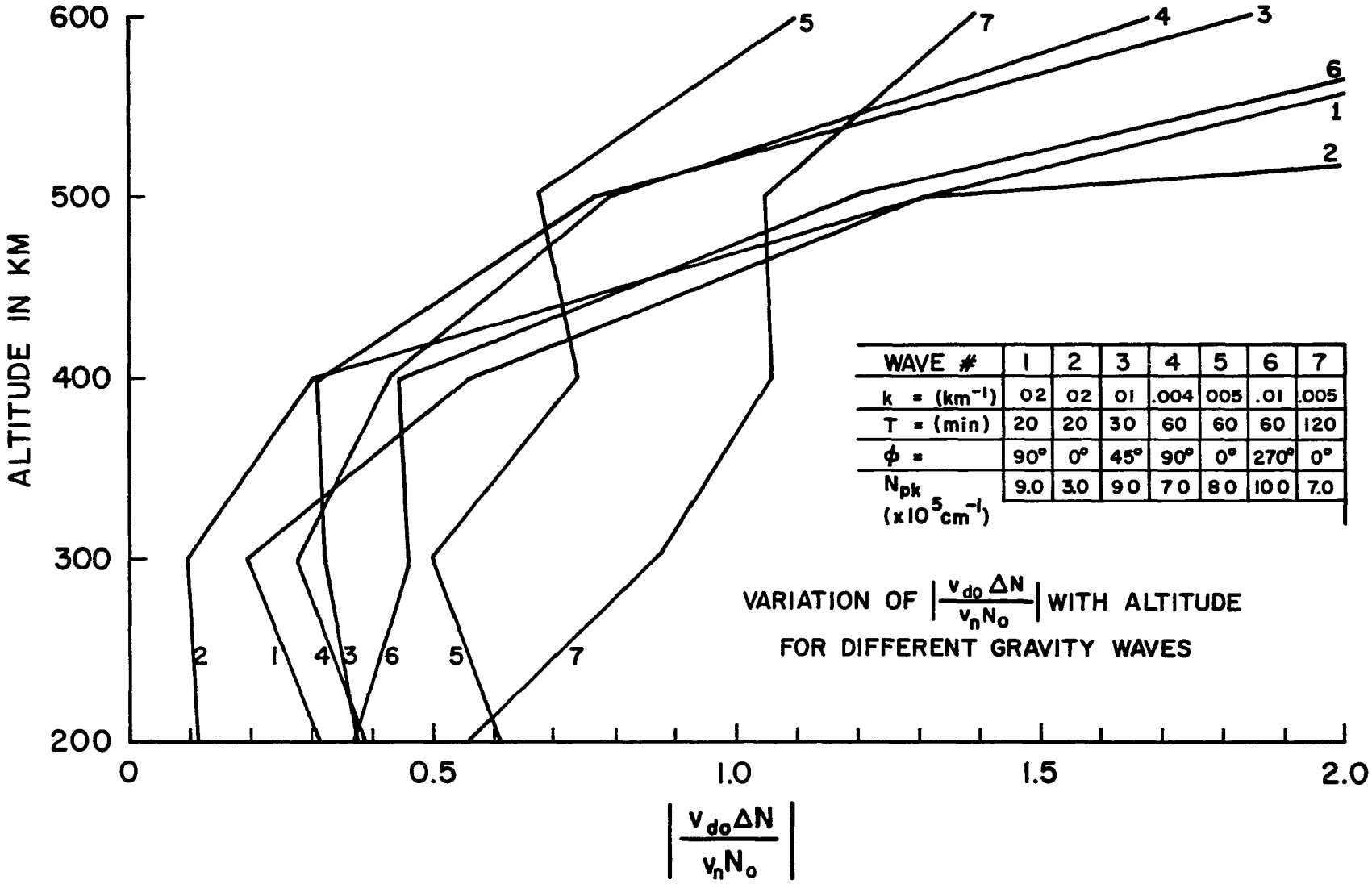

WAVE #	1	2	3	4	5	6	7
k = (km^{-1})	02	02	01	.004	005	.01	.005
T = (min)	20	20	30	60	60	60	120
ϕ =	90°	0°	45°	90°	0°	270°	0°
N_{pk} ($\times 10^5 cm^{-1}$)	9.0	3.0	90	70	80	100	7.0

Figure 5-7

$$| \bar{v}_n - (\bar{v}_n \cdot \hat{B}_o)\hat{B}_o |$$

was small compared to

$$| \bar{v}_{do} \frac{\Delta N}{N_o} | \quad .$$

This would seldom occur except when the major axis of the gas parcel orbit ellipse lay along or near the magnetic field line (i.e., when $\bar{v}_n \simeq v_n \hat{B}_o$).

5.4 Phase Relationships Between Wave Parameters

One area of GW theory where little or no results have been published is the phase relationship between the ion density fluctuations and the corresponding neutral gas parameter perturbations. The output of our numerical program includes data which permits the study of phase, as well as amplitude, relationships at a fixed point in space over a period of time. Figures 5-8 and 5-9 show examples of this capability for two waves at a fixed point 300 km above the earth's surface. We can readily compare the phase (and amplitude) of N/N_o, ρ/ρ_o , T_n/T_o, and v_g/C (v_g is the directed neutral velocity along the field lines, defined earlier; it is normalized by dividing it by the speed of sound C).

We can go further and study the altitude profiles of phase relationships for different waves. The result of this study is presented in figure 5-10 for six typical waves. In this graph, the 0° phase line vertically is the phase of N/N_o, taken as the reference. In order to make the results

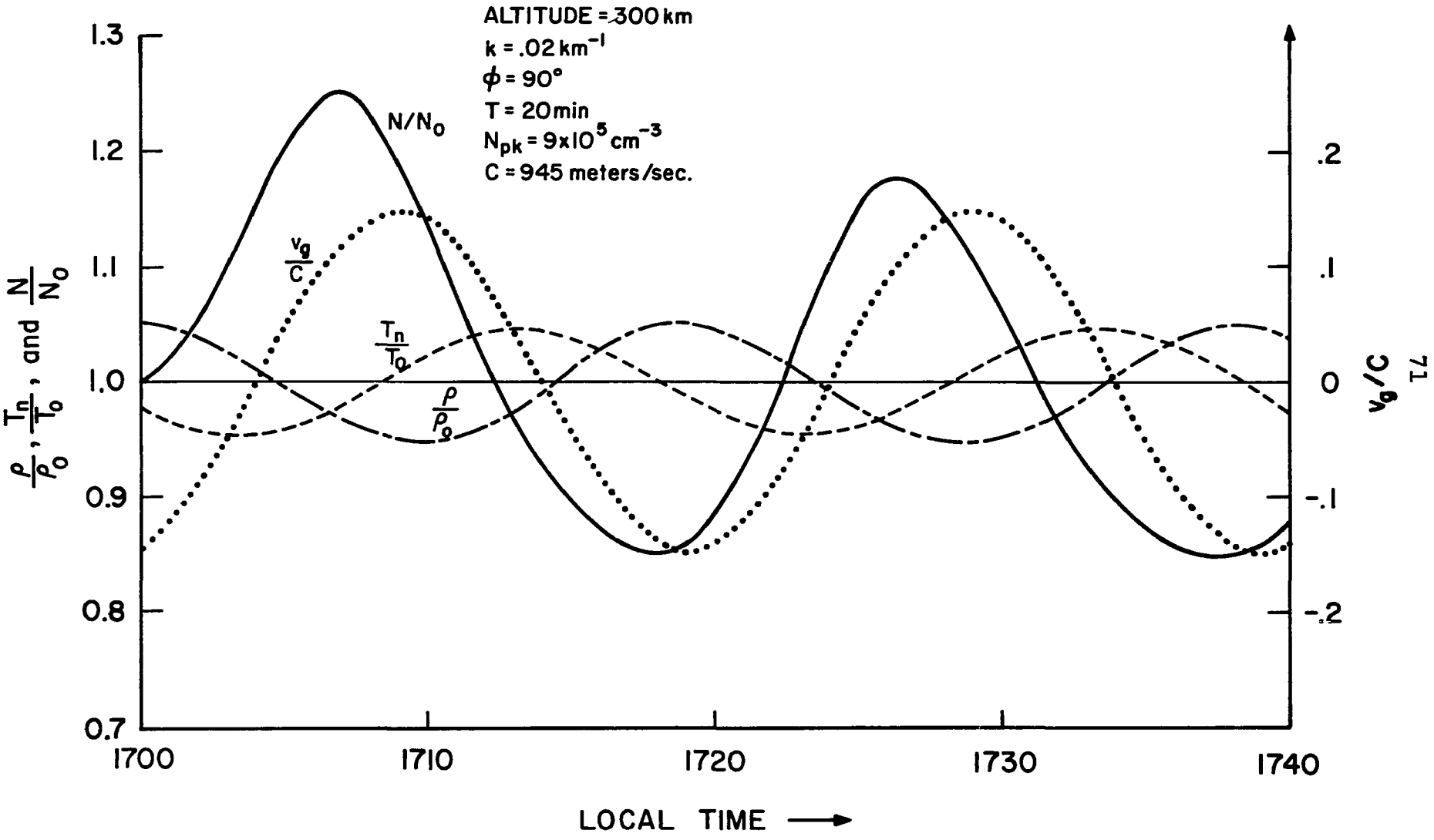

Figure 5-8.

Phase and Magnitude of Parameters for a Typical GW

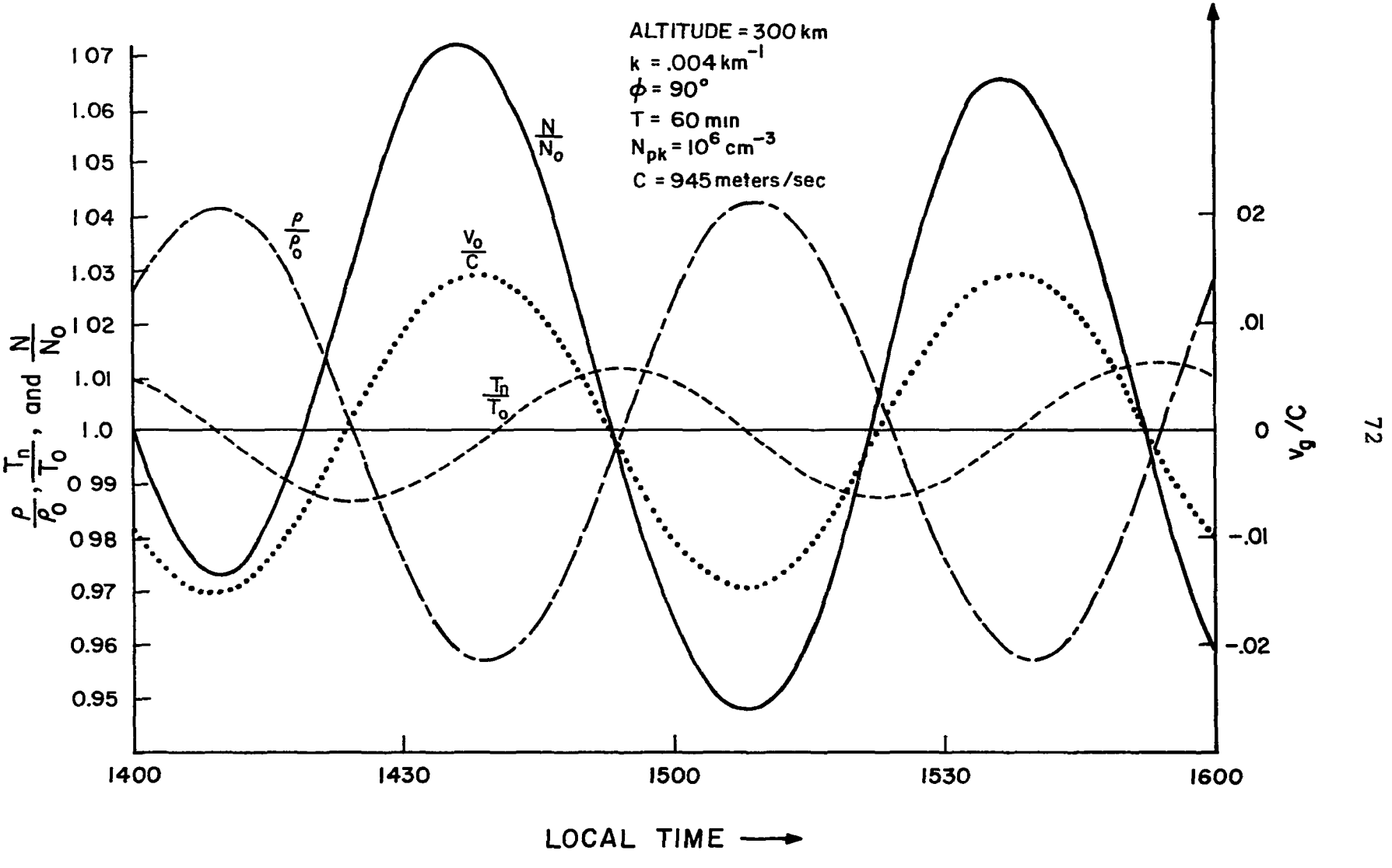

Figure 5-9.

Phase and Magnitude of Parameters for a Typical GW

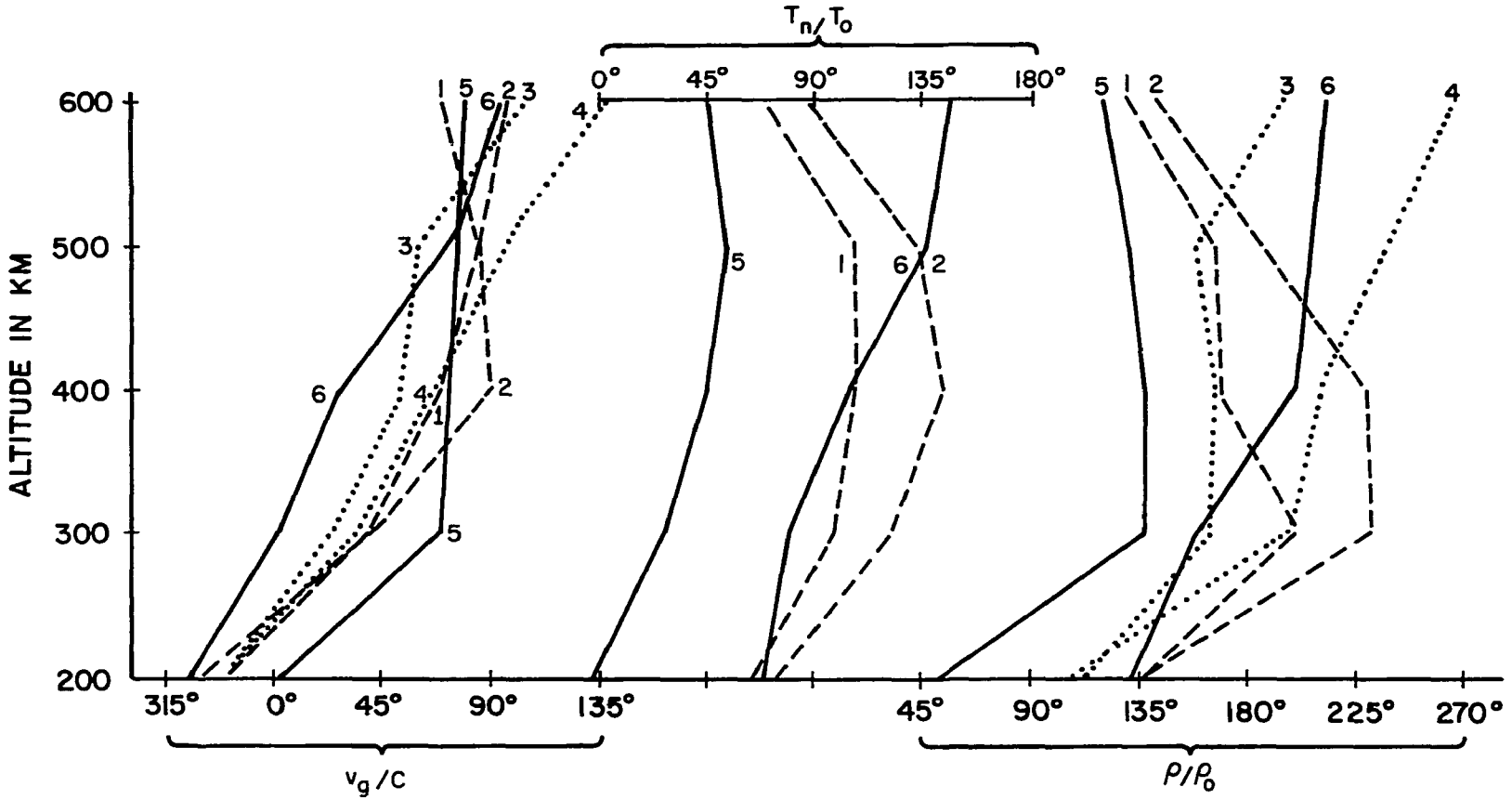

WAVE #	1	2	3	4	5	6
k =	.02	.02	.01	.01	005	004
T = (min)	20	20	30	30	60	60
ϕ =	0°	90°	45°	180°	0°	90°
N_{pk} ($\times 10^5 cm^{-1}$)	35	90	95	30	80	90

Figure 5-10.

Phase Profiles with Respect to $\Delta N/N_o$ for Typical Waves

easier to follow and to avoid crowding of lines, three separate phase scales were set up. Thus v_g/C phase is plotted from 315° to 135° on the left, T_n/T_o phase is plotted from 0° to 180° in the center, and ρ/ρ_o phase is plotted from 45° to 270° on the right. The lines in each group are further drawn distinctively according to wave period. Generally, the points on the graph are accurate to within 5° of phase, and to within 15° of phase for the T_n/T_o lines. Two T_n/T_o lines are not shown; the temperature fluctuations were too small to permit the ready measurement of phase.

One should exercise caution in making any general statements about phase relationships based on figure 5-10; though the results shown are typical of all waves studies, they are computed for one specific location and magnetic dip angle. However, two definite tendencies were noted in all waves:

1. The phase of v_g/C, the normalized neutral velocity along the field line, increased with altitude; it was nearly in phase with N/N_o in the F1 region (around 200 km) and increased to about a 90° lag behind N/N_o above the F2 peak.
2. ρ/ρ_o tended to lag T_n/T_o in phase by about 90° in all cases.

5.5 The Significance of Ion Drag

Following the discussion of section 4.3, we have computed K_{zi}, the imaginary part of K_z, with and without ion drag. Curves giving the amplitude of neutral density fluctuations as

a function of altitude, for each of these two cases, were drawn for all waves considered. Typical curves for four different frequencies are shown in figures 5-11 through 5-14, with a plot of the ambient electron density profile superimposed on each graph. The two amplitude curves have a magnitude given by the horizontal scale along the bottom of each graph; however, this scale is not important, because we are only interested in the relative magnitude of the two waves for comparison of ion drag effects. Wave magnitudes should not be compared from one graph to another.

Both curves show a $1/\sqrt{\rho_o}$ growth in amplitude near the bottom of the region considered, at first; but the rate of growth drops off as thermal conductivity begins to take effect with increasing height. The curve $\nu \neq 0$ has a slower rate of growth because ion drag losses are included as well as thermal conductivity losses. Finally, at the point where the $(p_o)^{-1/2}$ growth rate just matches the exp $(K_{zi}z)$ attenuation rate, the curves peak (at different altitudes, since K_{zi} is larger in magnitude when ν is included). Above this altitude, the attenuation rate is larger than the growth rate, and the amplitude decreases. Two major results are apparent from a study of the graphs, and are discussed in the next two paragraphs.

First, we observe that ion drag is frequency dependent in its effect. This conclusion was expected, since ion drag appears primarily in the form of the terms $\omega' - j\nu$

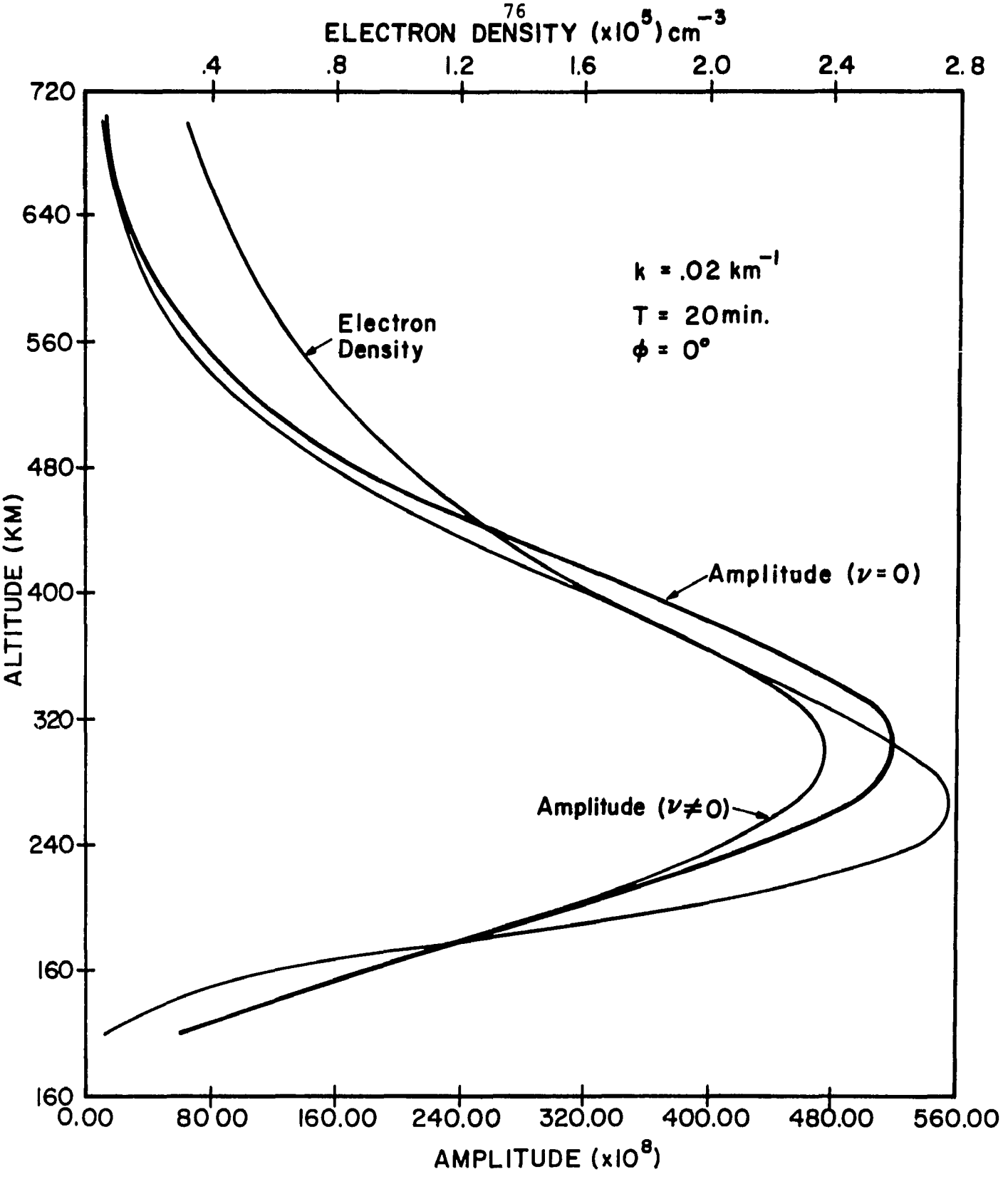

Amplitude Profile of Neutral Density Fluctuations

Figure 5-11

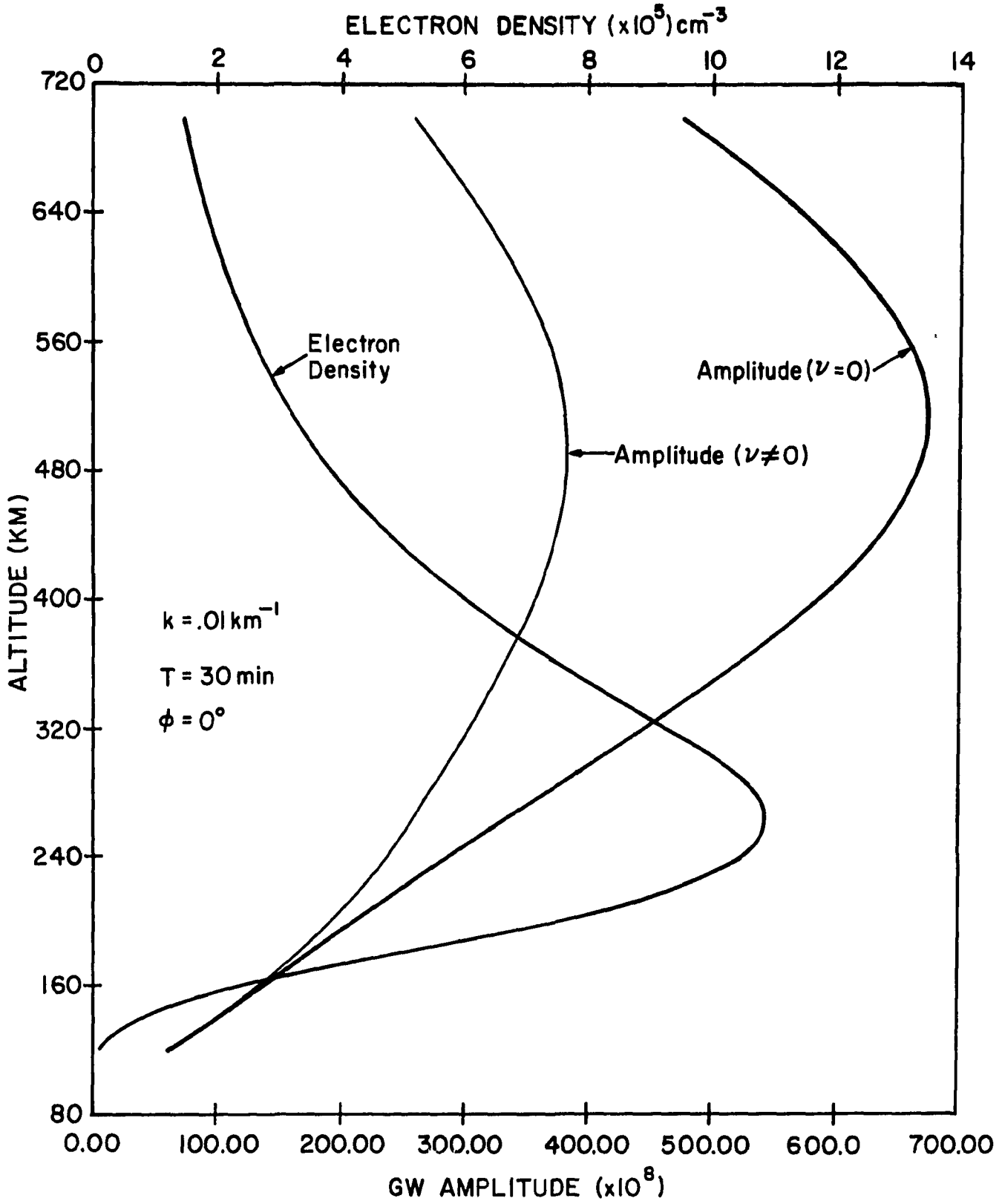

Amplitude Profile of Neutral Density Fluctuations
Figure 5-12

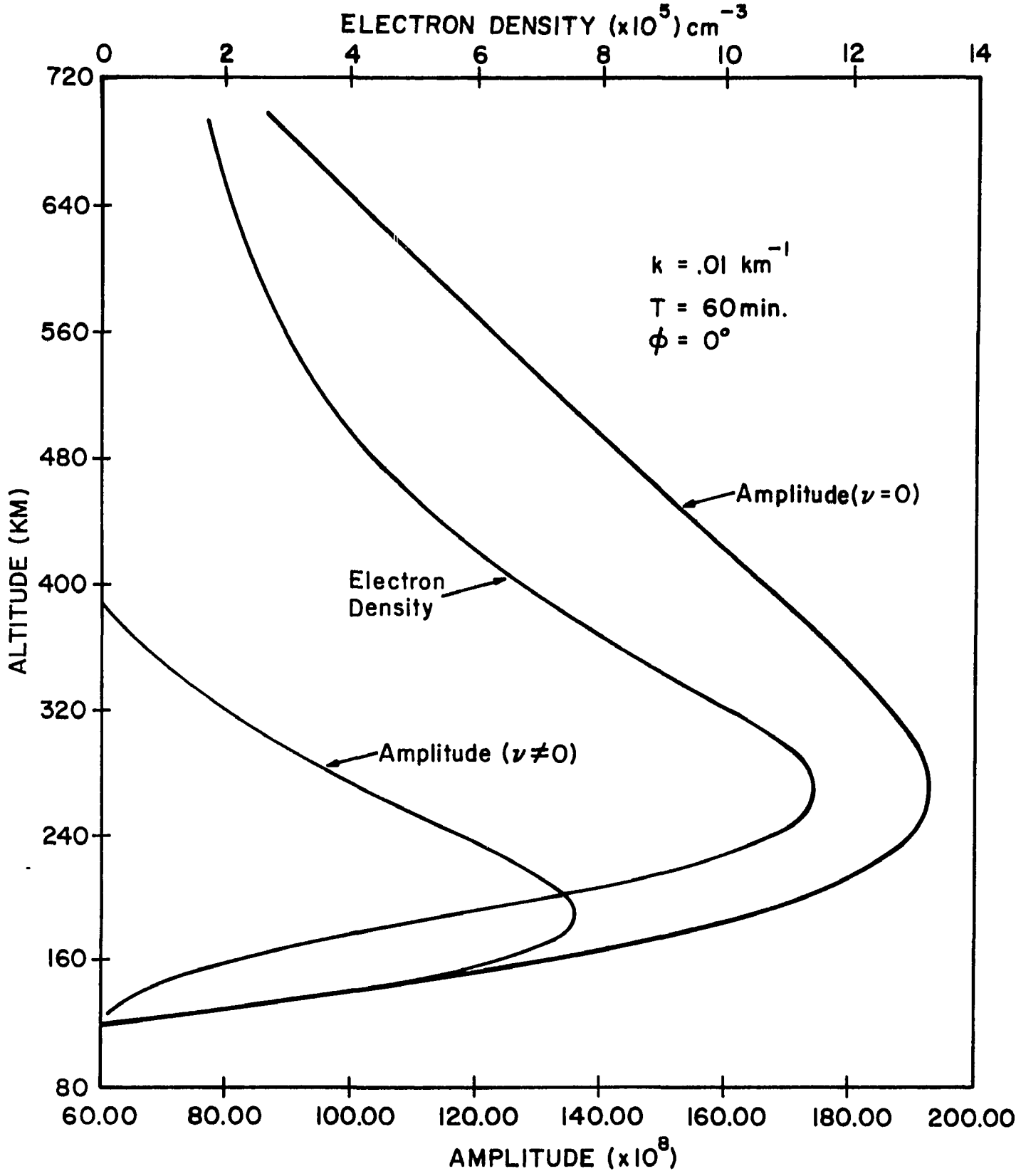

Amplitude Profile of Neutral Density Fluctuations
Figure 5-13

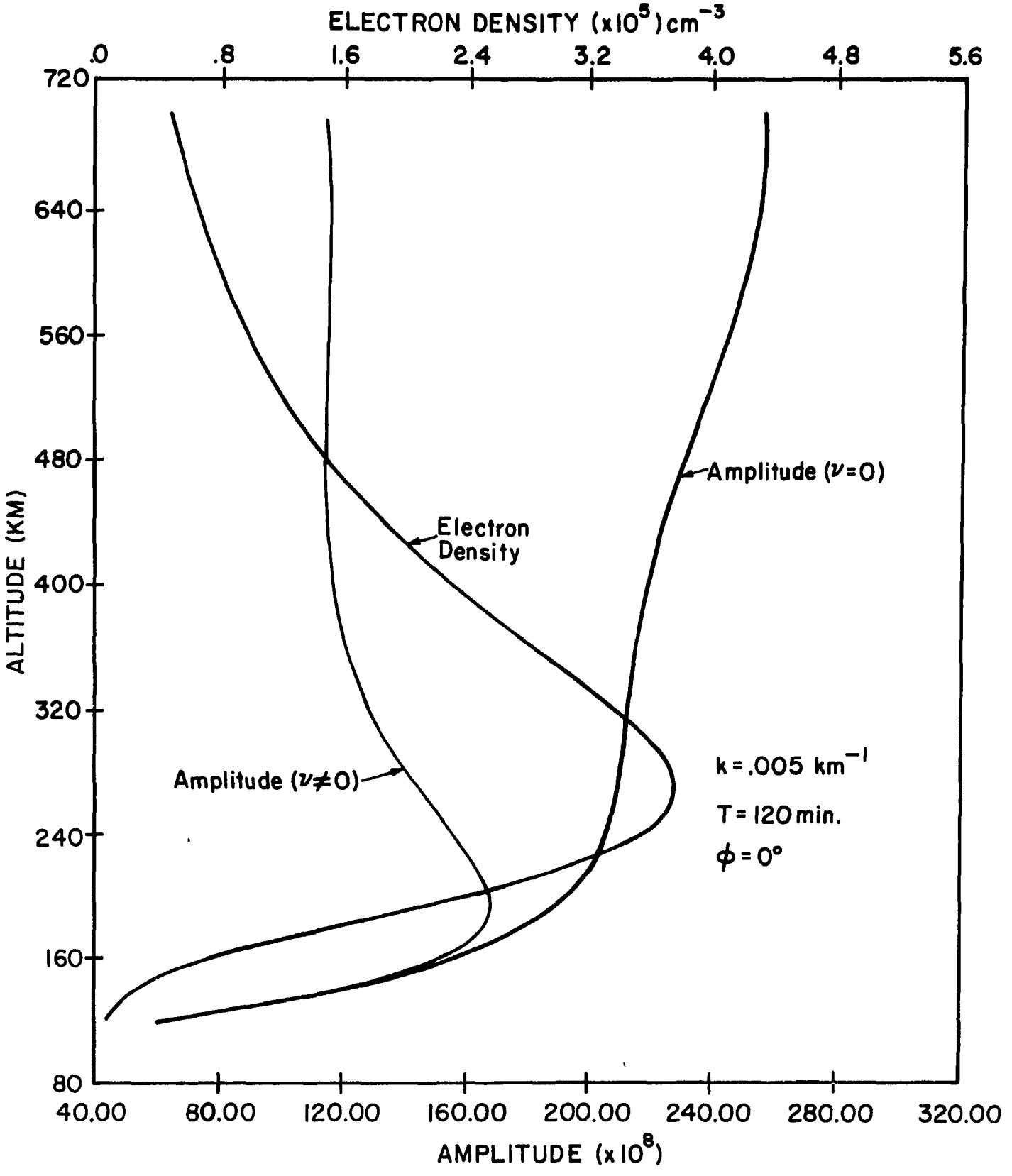

Amplitude Profile of Neutral Density Fluctuations
Figure 5-14

and $\omega' - j\nu \sin^2 I$, and in both terms an increase in ω reduces the relative importance of ν . Because the effect of thermal conductivity is also somewhat dependent on ω (since $\psi' \propto \frac{1}{\omega}$), the decrease in ion drag with increasing frequency is not as apparent as it would otherwise be.

Second, we see that ion drag has two effects on the wave amplitude: (1) A decrease in amplitude of about 50% (for lower frequency waves) compared to the amplitude predicted by thermal conductivity alone; and (2), a reduction in the altitude of the wave peak by as much as 100 km for low frequency waves.

It is apparent from these results that ion drag is a significant loss mechanism, especially at the lower GW frequencies.

5.6 Importance of the $\dot{H}$ Term

As noted in chapter 2, the derivative of ρ_o with respect to z involves a term in $\dot{H}$, which is sometimes ignored in the consideration of a nonisothermal atmosphere. In order to test this approximation, test computations were made with $\dot{H}$ set equal to zero. The results of these computations were then compared with otherwise identical wave computations where the $\dot{H}$ term was retained in the dispersion and polarization relations. The only difference in the two programs was that we set GRADH(K) = 0 in subroutine ZPROFL in the appendix program.

The difference in the results was noticeable only in the value of K_z which the two programs computed. A typical plot

of K_{zi} as a function of altitude is shown in figure 5-15, with our usual program computation ($\dot{H} \neq 0$) shown by the solid line. The two curves differed perceptibly below 200 km, but the difference was slight above 150 km. We expect a noticeable difference to occur from 120 to 150 km, if it occurs at all, since there is a very steep temperature gradient in this region. The fact that no perceptible difference occurs in either the wave amplitude plot (like figure 5-12) or the ion density contour plot (similar to figure 5-2) indicates that the $\dot{H}$ term is relatively unimportant in its effect on the resulting TID.

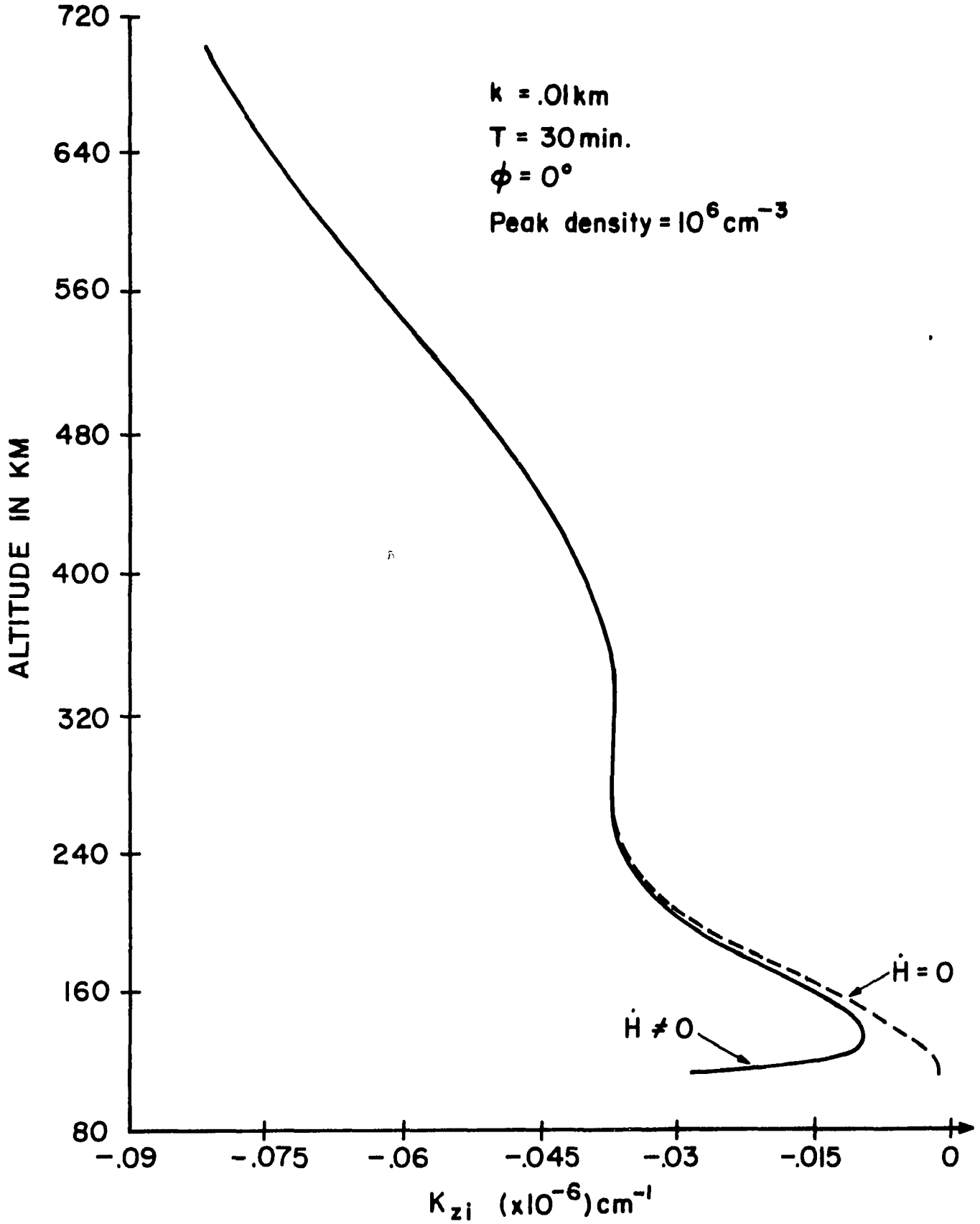

Typical Altitude Profile of K_{zi} with and without the $\dot{H}$ Term

Figure 5-15

6. CONCLUSION

Klostermeyer (29) concluded that ion drag was the dominant loss mechanism for GW's in the F region. Volland (47) contended that thermal conductivity was most important. One major finding of this paper is that both statements are partly right, and that either statement, in the typical ionosphere, can be misleading. At higher frequencies, thermal conduction (including viscous damping) is clearly predominant; but when the GW periods exceed about thirty minutes, ion drag may significantly decrease both the amplitude of the wave and the altitude of its peak, compared to the conditions which exist when ion drag is not present. A key factor in determining how important ion drag can be is the angular relation between the gas parcel orbit and the magnetic field lines.

On the other hand, the $\dot{H}$ correction term, which has been considered by Hines and others to be a necessary element in deriving a dispersion relation for the nonisothermal atmosphere GW, was found to be unimportant so far as the structure of the resulting TID is concerned. However, in studies such as the ray tracing program of Cowling (4), or work of a similar nature where such effects tend to be cumulative, it would be well to keep the $\dot{H}$ term in the dispersion relation.

Probably the most important result of this investigation concerns the relative importance of perturbed parameters, discussed in section 5.3. First, the results obtained clearly indicate that it is inappropriate to treat ion density as a

perturbed quantity; the response of the ionosphere to a neutral gas wave of perturbation magnitude may be ion density fluctuations well above such a magnitude. It was also noted that perturbations in production, loss, and diffusion velocity were generally unimportant in the production of ion density fluctuations. This result confirms the conclusion of earlier work in this area (25). However, the interaction of ion density fluctuations with the ambient ambipolar diffusion velocity produce a term (or terms) which compares to the directed neutral velocity in its significance in producing ionization variations. It therefore cannot in general be assumed that ion velocity is simply the component of neutral velocity along the magnetic field lines. Diffusion velocity effects must be taken into account in some manner.

Finally, a study of phase relationships between perturbed parameters (section 5.4) showed that a definite phase relationship exists between ion density fluctuations and the neutral velocity component along the magnetic field lines. For the -70° dip angle used in our study (presumed typical of temperate latitudes), the velocity phase showed a lag, steadily increasing with altitude, behind N/N_o phase; it varied from 0° near 120 km to about 90° lag above the F2 peak. A consistent relationship between neutral temperature and density phases was also observed, density lagging temperature by about 90° at all altitudes in our study.

A considerable number of approximations were made to give the results which we have presented. Most of the approxi-

mations were discussed earlier, but it is appropriate at this point to summarize some of them.

One assumption implicit in our treatment is that the atmosphere above 500 km is similar in nature to the atmosphere at, say, 300 km. Yet significant differences do exist. Between 500 and 700 km, the mean free path of gas particles approaches in magnitude both the scale height and the wavelength of a typical GW. The hydromagnetic equations are not strictly applicable, and indeed there is some question whether a neutral gas wave can exist under these conditions. Furthermore, coupling to the viscosity wave modes can be important above 500 km (46). This problem is not of serious concern in general, since we are usually not interested in what happens to the GW or the TID much above the F2 peak. It would be very unwise, in any event, for one to rely on the graphs in chapter 5 at altitudes above 500 km.

A variational scheme was assumed for the perturbed parameters which is not strictly correct. Thus ν_{in}, q and β were presumed to follow the neutral gas density variations in magnitude and phase. Yet ν_{in} is also dependent on temperature to some extent (section 2.3). β is proportional to the density of N_2, not to the neutral gas density (eqn. 3.11). q is proportional to the density of atomic oxygen (eqn. 3.12) and further dependent on fluctuations in solar ionizing radiation (25). Furthermore, we assumed that the ion and electron temperatures fluctuated in the same manner as the neutral temperature, though the electron temperature might be

more affected by the solar flux, for example (sec. 3.5). However, though all of these assumptions are in error to a greater or lesser degree, it turns out that none of them affect our computed results significantly; as we noted earlier, the perturbations themselves are not of primary importance in determining the total ion density.

A number of other effects have been neglected, or included only with simplifying assumptions about their nature, for the sake of mathematical convenience. For example, we neglect perturbations in Q (section 2.3) because we do not know what sort of expression to use for a perturbed Q. We neglect viscosity so that equation (2.21) will not be of eighth order in K_z, and take it into account by increasing the thermal conductivity coefficient (though the two loss processes are not identical in nature). Finally, we place severe constraints on the wind model (section 2.4) in order to simplify the terms in equations (2.17). The constraints cause no problem in the present study, because we assume no wind in the computations; but even this is a questionable assumption, since in the real ionosphere a no-wind condition is unlikely to exist.

We assume that the latitude is constant in computation, and compute such latitude-dependent variables as ion production for a fixed point above the earth's surface. This is a good approximation at temperate and higher latitudes, where the latitudinal change as we move along a field line is not great. Where the dip angle is small, nearer the equator, the approximation is not as good.

The assumption that

$$v_i = (\bar{v}_n \cdot \hat{B})\ \hat{B}_o$$

turned out to be a poor approximation; its shortcomings were outlined in chapter 5. A significant part of $\bar{v}_i$ results from the ambient ion diffusion velocity. However, this approximation does not generally appear to affect the end result, as we noted in section 5.3. We were able to make a better approximation to ρ_i in solving the neutral gas equations, by using the value of ρ_i computed at the previous time step. This technique introduces only a slight error, since the time increments were taken to be small (1/20 of the wave period).

Finally, we assume that the background atmosphere and ionosphere are slowly varying media. The validity of this approximation for different parameters is discussed in section 3.5.

One should note, in closing, that the computer program described in the appendix, which has been used extensively to support this investigation, has yet untapped capabilities. For example, provisions have been made to include the effect of a neutral wind on GW's, and this would be well worth a separate investigation. Also, the production function could easily be modified to include the effect of neutral gas density fluctuations on solar ionizing radiation. This would provide an interesting test of the production function effect discussed by Hooke (25) when the solar rays lie in the plane of wave phase fronts.

LIST OF REFERENCES

1. Albee, P. R., and Kanellakos, D. P., "A Spatial Model of the F-Region Ionospheric Traveling Disturbance Following a Low-Altitude Nuclear Explosion," J. Geophys. Res., 73, 1039-1053 (1968).

2. Banks, P. M., "The Thermal Structure of the Ionosphere," Proc. IEEE, 57, 258-281 (1969).

3. Bowman, G. G., "Further Studies of 'Spread F' at Brisbane", Planet. Space Sci., 2, 133-156 (1960).

4. Cowling, D. H., Webb, H. D., and Yeh, K. C., "A Study of Traveling Ionospheric Disturbances in the Ionosphere," Tech. Report No. 38, Ionosphere Radio Laboratory, Univ. of Ill. (1970).

5. Committee on Space Research, CIRA 1965, North-Holland, Amsterdam, 1965.

6. Cunnold, D. M., "F Region Ionization Perturbations Produced by Transport Effects Associated with Acoustic Gravity Waves," Research Report #534, Applied Research Lab., Sylvania Electronic Systems, Waltham, Mass. (1967).

7. Dalgarno, A., and Smith, F. J., "The Thermal Conductivity and Viscosity of Atomic Oxygen," Planet. Space Sci., 9, 1-2 (1962).

8. Eckart, C., Hydrodynamics of Oceans and Atmospheres, Pergamon Press, Oxford (1960).

9. Evans, J. V., "The Heating of the Protonosphere," Space Research VIII, North-Holland, Amsterdam 717-727 (1967).

10. Evans, J. V., Brockelman, R. A., Julian, R. F., Reid, W. A., and Carpenter, L. A., "Determination of F-region vertical drifts at Millstone Hill," Radio Science, 5, 27-38 (1970).

11. Fritz, J. H., and Yeh, K. C., "An Investigation of F2 Region Ionospheric Behavior by Computer Methods," Ionosphere Radio Laboratory Tech. Report #35, EERL, Univ. of Ill. (1968).

12. Geisler, J. E., "On the Limiting Daytime Flux of Ionization into the Protonosphere," J. Geophys. Res., 72, 81-85 (1967).

13. Georges, T. M., "Ionospheric Effects of Atmospheric Waves," ESSA Tech. Report IER 57-ITSA 54, Institute for Telecommunications Sciences and Aeronomy, Boulder, Col. (1967).

14. Georges, T. M., Acoustic-Gravity Waves in the Atmosphere, Symposium Proceedings, ESSA and ARPA (1968).

15. Gershman, B. N. and Grigor'yev, G. I., "Theory of Moving Ionospheric Disturbances (magnetohydrodynamic absorption)," Geomagnetism and Aeronomy, 5, 656-660 (1965).

16. Herman, J. R., and Chandra, S., "The Influence of Varying Solar Flux on Ionospheric Temperatures and Densities: A Theoretical Study," Planet. Space Sci., 17, 815-840 (1969).

17. Hines, C. O., "Internal Atmospheric Gravity Waves at Ionospheric Heights," Can. J. Phys., 38, 1441-1481 (1960).

18. Hines, C. O., "Corrections to 'Internal Atmospheric Gravity Waves at Ionospheric Heights'," Can. J. Phys., 42, 1424-1427 (1964).

19. Hines, C. O., "Atmospheric Gravity Waves: A New Toy for the Wave Theorist," Radio Science, 69D, 375-380 (1965).

20. Hines, C. O., "Dynamical Heating of the Upper Atmosphere," J. Geophys. Res., 70, 177-183 (1965).

21. Hines, C. O., and Reddy, C. A., "On the Propagation of Atmospheric Gravity Waves Through Regions of Wind Shear," J. Geophys. Res., 72, 1015-1034 (1967).

22. Hines, C. O., Some Consequences of Gravity-Wave Critical Layers in the Upper Atmosphere, J. Atmosph. Terr. Phys. , 30, 837-843 (1968).

23. Hines, C. O., "An Effect of Molecular Dissipation in Upper Atmospheric Gravity Waves," J. Atmosph. Terr. Phys., 30, 845-849 (1968).

24. Hines, C. O., "An Effect of Ohmic Losses in Upper Atmospheric Gravity Waves," J. Atmosph. Terr. Phys. 30, 851-856 (1968).

25. Hooke, W. H., "Ionospheric Irregularities Produced by Internal Atmospheric Gravity Waves," J. Atmosph. Terr. Phys., 30, 795-823 (1968).

26. Ihoue, Y., and Horowitz, S., "Magneto-Ionic Coupling in an Inhomogeneous Anisotropic Medium," Radio Science, 1, 427-440 (1966).

27. Jacchia, L. G., "Static Diffusion Models of the Upper Atmosphere with Empirical Temperature Profiles," Smithsonian Contributions of Astrophysics, V. 8, No. 9, Smithsonian Institution, Washington, D. C. (1965).

28. Jones, W. L., "The Transport of Energy by Internal Waves," Tellus XXI, 2, 177-184 (1969).

29. Klostermeyer, J., "Gravity Waves in the F Region," J. Atmosph. Terr. Phys., 31, 25-45 (1969).

30. Kohl, H. King, J. W., and Eccles, D., "Some Effects of Neutral Air Winds on the Ionospheric F Layer," J. Atmosph. Terr. Phys., 1733-1744 (1968).

31. Liu, C. H., and Yeh, K. C., "Effect of Ion Drag on Propagation of Acoustic-Gravity Waves in the Atmospheric F Region," J. Geophys. Res., 74, 2248-2255 (1969).

32. Midgley, J. E., and Liemohn, H. B., "Gravity Waves in a Realistic Atmosphere," J. Geophys. Res., 71, 3729-3748 (1966).

33. Newton, G. P., Pelz, D. T., and Volland, H., "Direct In Situ Measurements of Wave Propagation in the Neutral Thermosphere," J. Geophys. Res., 74, 183-196 (1969).

34. Pitteway, M. L. V., and Hines, C. O., "The Viscous Damping of Atmospheric Gravity Waves," Can. J. Phys. 41, 1935-1948 (1963).

35. Pound, T. R., and Yeh, K. C., "Response of Ionospheric Electron Density to a Change of Electron Temperature," Ionospheric Radio Propagation Lab., EERL, Univ. of Ill. (1966).

36. Reid and Sherwood, The Properties of Gases and Liquids, McGraw Hill, N. Y. (1966).

37. Rishbeth, H., "On Explaining the Behavior of the Ionospheric F Region," Rev. Geophys., 6, 33-71 (1968).

38. Smith, F. L. III, "Electron Production and Loss Rates in the F Region," J. Geophys. Res., 73, 7385-7398 (1968).

39. Sterling, D. L., "Traveling Disturbances Observed at Jicamarca," Aeronomy Report #19, EE Dept., University of Illinois, 178-183 (1967).

40. Stubbe, P., "Frictional Forces and Collision Frequencies Between Moving Ion and Neutral Gases," J. Atmosph. Terr. Phys., 30, 1965-1985 (1968).

41. Thome, G. D., "Incoherent Scatter Observations of Traveling Ionospheric Disturbances," J. Geophys. Res., 69, 4047 (1964).

42. Thome, G. D., and Rao, P. B., "Comparison of Acoustic-Gravity Wave Theory with HF and UHF Observations," Final Report, Raytheon Co., spencer Lab., Burlington, Mass. (1969).

43. Titherige, J. E., "Periodic Disturbances in the Ionosphere," J. Geophys. Res., 73, 243-252 (1968).

44. Vincent, R. A., "A Criterion for the Use of the Multilayer Approximation in the Study of Acoustic-Gravity Wave Propagation," J. Geophys. Res., 74, 2996-3001 (1969).

45. Volland, H., "Heat Conduction Waves in the Upper Atmosphere," J. Geophys. Res., 72, 2831-2841 (1967).

46. Volland, H., "The Upper Atmosphere as a Multiple Refractive Medium for Neutral Air Motions," J. Atmosph. Terr. Phys., 31, 491-514 (1969).

47. Volland, H., "Full Wave Calculations of Gravity Wave Propagation Through the Thermosphere," J. Geophys. Res., 74, 1786-1795 (1969).

48. Yeh, K. C., Flaherty, B. J., and Cho, H. R., "Studies of the Ionosphere at Geomagnetically Conjugate Stations" (appendix c), Tech. Report No. 37, Ionosphere Radio Laboratory, The Univ. of Ill. (1969).

APPENDIX

THE NUMERICAL COMPUTATION PROGRAM

In this appendix a program is described which numerically solves equation (3.5), with attendant boundary conditions. The solution may be either the perturbed or unperturbed ion density distribution.

Main Program

First, four cards are read, and the data so obtained are used to compute the physical parameters of the F region. They are:

Card 1

HNSTEP: Thickness of the horizontally stratified layers in km; usually 2.0.

DELTME: Time increment Δt in hours for the unperturbed ionosphere computation; usually 0.5.

QPO: The 10.7 cm solar flux in units of 10^{-22} watts/m^2-Hz.

BETAO: Magnitude of the loss coefficient β at 120 km.

ALPHA: The recombination coefficient α in $cm^{-3}sec^{-1}$.

FLUX: A parameter used in computing $\Gamma_\infty(t)$.

CONTV: Another parameter used in computing $\Gamma_\infty(t)$.

Card 2

HL: The upper boundary height in km; usually 700.

DIP: The magnetic dip angle, I, in degrees, measured positive upward.

DECL: Sun's declination in degrees, measured positive north of the equator.

RLAT: Observer's latitude in degrees, measured positive north of the equator.

Y: Horizontal distance from the observer, positive toward geomagnetic west; normally set equal to zero.

Card 3

TXMAX: Diurnal exospheric temperature maximum, in °K.

TXMIN: Dirunal exospheric temperature minimum, in °K.

T120: Temperature at 120 km in °K; normally 355.

TEEMAX: Diurnal exospheric electron temperature maximum in °K.

TEEMIN: Diurnal exospheric electron temperature minimum in °K.

After computing some constants and initializing some parameters, the program begins at 1200 local time to compute unperturbed electron density, first reading data card 4 which gives information about the first gravity wave.

Card 4 (and subsequent)

AMPLO: GW amplitude in $dyne^{1/2}\text{-}sec^2$

THERMC: Coefficient of thermal conductivity, λ_o, in $dyne\text{-}cm^2/sec\text{-}°K$

WVN: Horizontal wave number in km^{-1}

PERIOD: GW period in minutes.

PHI: ϕ in degrees.

TINT: Time of start of the GW in hours (must be greater than 12.0 or the last TERM read, and an even multiple of DELTME).

TERM: Time of GW termination, in hours (must be greater than TINT and an even multiple of DELTME).

The program then computes an initial electron density profile (in subroutine ZPROFL) and begins computing a dynamic unperturbed profile until time TINT. It then begins computing and plotting a perturbed profile at a reduced time interval until time TERM is reached. At this time the next data card, having the same information as card 4 above, is read and the unperturbed profile computations resume until a new TINT is reached. This process continues until a card having a TERM greater than 98.00 is read, at which time the program terminates.

Subroutine ZPROFL

This subroutine computes the physical constants and altitude profile of the atmosphere at a given time. A number of the expressions used are empirical, chosen only because they fit observed data. The parameters computed are listed below in order of appearance, followed by their subroutine names and an explanation including the applicable computation formula.

χ(CHI): The sun's zenith angle in radians. It depends on the observer's latitude and local apparent time, and on the solar declination.

$$\chi = \cos^{-1}[\sin(\text{lat.})\sin(\text{dec.}) + \cos(\text{lat.})\cos(\text{dec.})\cos\left(\frac{15(\text{time} - 12.)}{57.296}\right)]$$

T_∞ (TEMPEX) and $T_{e\infty}$ (TEEX): The exospheric neutral and electron temperatures, both functions of time, are determined by the input values of TXMAX and TXMIN (or TEEMAX and TEEMIN) and by χ :

T_∞ = TXMIN + (TXMAX - TXMIN)[cos(χ - .7854 + .20944sin (χ + .7854))$^{1/2}$]$^{2.5}$

$T_{e\infty}$ has the same formula, with TEEMIN and TEEMAX in place of TXMIN and TXMAX.

T_n(TEMP(K)): The neutral temperature, computed using TIME, T_∞, T120, and the equation of Jacchia (21).

m(WM(K)): The mean molecular mass of the atmosphere. Computed using the empirical formula

$$m = 20 - 5.0448\tan^{-1}\left(\frac{z - .100}{25}\right) \quad \text{for ALT(K)} \leq 180$$

$$m = 25.106 - 7.9357\tan^{-1}\left(\frac{z-60}{140}\right) \quad \text{for ALT(K)} > 180$$

ζ + 120 or z + 120 (ALT(K)): The altitude in kilometers of each stratified layer above the earth's surface. ALT (1) = 120 km; ALT (J) = HL (usually 700 km).

ξ(X(K)): The horizontal distance toward magnetic north from the observer:

$$\xi = z \cos I/\sin I$$

g (GC(K)): The acceleration due to gravity in cm/sec^2:

$$g = \frac{980.665}{\left(1+ \frac{z+120}{6356.77}\right)^2}$$

v_{nxo}(VNXO(K)) and v_{nyo}(VNYO(K)): The horizontal wind components in cm/sec.

H(HK(K)): The neutral gas scale height in km, computed from

$$H = \frac{831.44\ T_n}{mg}$$

HO: The scale height of atomic oxygen in km.

HN2: The scale height of molecular nitrogen in km.

T_e(TE(K)): The electron temperature, computed empirically from

$$T_e = T_n + (\text{TEEX-TEMPEX}) \exp\left(-\frac{80}{z+1}\right)$$

T_i(TI(K)): The ion temperature, set equal to the neutral temperature for altitudes less than ALITRN, and set equal to

$$T_e + (T_n - T_e)\exp\left(1 - \frac{z+120}{\text{ALITRN}}\right)$$

for altitudes greater than ALITRN.

ρ(DENN(K)): The neutral density in gm/cm^3.

$$= (\text{DEN120})\ \frac{T_n}{T120}\ \exp - \sum_{i=1}^{K} \left(\frac{\Delta\zeta}{H_i} + \dot{H}_i\right)$$

β (BETALO(K)): The linear loss coefficient.

$$\beta = \text{BETAO} \exp\left(-\sum_{i=1}^{K} \frac{\Delta\zeta}{HN2_i}\right)$$

$\dot{H}$ (GRADH(K)): The gradient of scale height.

$$\dot{H} = \left(\frac{HK(K+1)}{HK(K)} - 1\right)/\Delta\zeta$$

ν_{in}(COLFN): The ion-neutral collision frequency in sec^{-1}.

$$\nu_{in} = 1.565 \cdot 10^{15}\ \rho/m^{1.5}$$

Γ_∞(VLB): The flux out of the ionosphere at height HL, in $cm^{-2}sec^{-1}$. We compute the peak electron density (CONT) and assume that the flux is proportional to (1) the peak electron density and (2) the difference between the exospheric temperature and its daily mean. The constants FLUX and CONTV are

proportionality constants. This is a purely empirical expression, and matches observed flux reasonably well.

DENO(K): The number density of atomic oxygen.

$$DENO(K) = DENO(O)\ \frac{T_n}{T120}\ \exp\ (-\sum_{i=1}^{K}\ \frac{\Delta\zeta}{HO}\ )$$

q_o(CHAP(K)): The ion production function in $cm^{-3}sec^{-1}$. Generated by a call to subroutine PRODUC.

N (DEN(K)): Here, the initial value of N, from

$$N = \left(\frac{q_o}{\alpha}\right)^{1/2}$$

PN(K), PT(K), PX(K), and PZ(K) are the parameters necessary to compute the unperturbed coefficients of equation (3.5). They are discussed in subroutine COFCAL.

Subroutine COFCAL (IMPL)

This subroutine has as its primary inputs the parameters (PN(K), PT(K), PX(K) and PZ(K) which were computed in subroutine ZPROFL. If the index number IMPL is equal to 1, these parameters are used unmodified. If IMPL > 1, the modified parameters computed in subroutine FACALG for the presence of a GW are used. The output, which is used by subroutine TRIDIA to compute $N(\zeta)$, is the terms A(K), B(K), C(K), D, E, QP(K), and BETA(K). A description of the terms, their equivalents in the main part of this paper, and dimensions follows.

Program Term	Text Expression	Dimension
PT(K)	$T_i + T_e$	°K
PN(K)	$\frac{\partial}{\partial \zeta}(T_i + T_e)$	°K/cm
PX(K)	$\sin I/\nu_{in}$	sec
PZ(K)	$v_{nx}\cos I + v_{nz}\sin I$	cm/sec
TC, TC1	G_1	cm^2/sec
SC,SC1	G_2	cm/sec
GRADTC	$\frac{\partial G_1}{\partial \zeta}$	cm/sec
GRADSC	$\frac{\partial G_2}{\delta \zeta}$	sec^{-1}
BETAL	β	sec^{-1}
ALPHN	αN	sec^{-1}
A(K)	$G_1 \sin I$	cm^2/sec
B(K)	$(\frac{\partial G_1}{\partial \zeta} + G_2)\sin I$	cm/sec
C(K)	$\frac{\partial G_2}{\partial \zeta}$	sec^{-1}
QP(K)	q	$cm^{-3}sec^{-1}$
BETA(K)	$\frac{\alpha\beta N}{\alpha N+\beta}$ or β	sec^{-1}
D	$-G_1 \sin I$	cm^2/sec
E	$-G_2 \sin I$	cm/sec

Subroutine FACALG

This subroutine uses the results of chapter 2 in the text to compute the values of K_z and the polarization relations.

The principal inputs are the altitude profile computed in subroutine ZPROFL and the data read from the input cards.

Program Term	Text Expression	Dimension
H	j or $\sqrt{-1}$	--
AMPL	A	$dynes^{1/2}\text{-}sec^2$
G1	$\gamma - 1$	--
G2	$\gamma_1 = \frac{\gamma}{\gamma-1}$	--
WVN	k	cm^{-1}
HNSCM	$\Delta\zeta$	cm
DELTIM	Δt	hours
SINISQ	$\sin^2 I$	--
CSINI	cos I sin I	--
WVNSQ	k^2	cm^{-2}
PHI	ϕ	radians
WVNX	k_x	cm^{-1}
WVNXSQ	k_x^2	cm^{-2}
WVNY	k_y	cm^{-1}
WVNYSQ	k_y^2	cm^{-2}
FREQ	ω	sec^{-1}
FRTIM	$\omega' t$	--
TDELO	k_x/ω'	hours/cm
PSIO	$\omega' t - k_y y - \sum_i K_{zi}\Delta\zeta_i$	--
G	g	cm/sec^2

HKK	H	cm
GHK	gH	cm^2/sec^2
DENK	N	cm^{-3}
TK	T_n	°K
HKI2	$\frac{1}{2H}$	cm^{-1}
HKSQ	$1/H^2$	cm^{-2}
HKSQ4	$1/(4H^2)$	cm^{-2}
COLLIF	ν	sec^{-1}
PRESS	p_o	$dynes/cm^2$
G2H	$\gamma_1 \dot{H}$	--
G1H	$1 + \gamma_1 \dot{H}$	--
FRQ	$\omega' = \omega - k_x v_{nxo} - k_y v_{nyo}$	sec^{-1}
FRQSQ	$(\omega')^2$	sec^{-2}
WGH	ω'/gH	sec/cm^2
F1	$j\nu$	sec^{-1}
F2	$\omega' - j\nu$	sec^{-1}
F3	$\omega' - j\nu\sin^2 I$	sec^{-1}
PRESQ	$1/\sqrt{p_o}$	$cm/dynes^{1/2}$
THERMK	ψ	cm^2
THERM2	2ψ	cm^2
Z1	k_1	cm^{-1}
C1	c_1	sec/cm^2
C2	c_2	---
C3	c_3	sec^{-1}
W2GH	ω'^2/gH	cm^{-2}
GKWH	$k^2 g/\omega'^2 H$	cm^{-2}

Z4	$\frac{1}{2H} - \frac{\omega'^2}{gH} + k^2$	cm^{-2}
Z6	$c_2 + \psi/4H^2$	--
WVNZ	K_z	cm^{-1}
WVNT	K_z (where $\nu \neq 0$)	cm^{-1}
Z5	$\frac{1}{4H} - k_1^2 - c_1 c_3 - 2jk_1 K_z$	cm^{-2}
WNVZTI(K)	Im(WVNT)	cm^{-1}
WVNZTR(K)	Re(WVNT)	cm^{-1}
PSIK	$\omega' t - k_x \xi - k_y y - \sum_1^K K_{zi} \Delta\zeta_i$	--
Z2	$\psi(K_z^2 + \frac{1}{4H^2})$	--
Z3	$K_z - j(\frac{1}{2H} + k_1)$	cm^{-1}
C4	$\omega'^2(\gamma-1)/\sqrt{p_o}$	$\frac{\text{cm-dynes}^{-1/2}}{\text{sec}}$
WVNZR(K)	Re(K_z)	cm^{-1}
WVNZI(K)	Im(K_z)	cm^{-1}
PPK	P	$dynes^{-1/2} sec^{-2}$
PZK	W	$cm\text{-}dynes^{-1/2} \cdot sec^{-3}$
PTK	T	$dynes^{-1/2} \cdot sec^{-2}$

PNK	R	$dynes^{-1/2}sec^{-2}$
PXK	U	$cm\text{-}dynes^{-1/2} \cdot sec^{-3}$
TDELAY(K)	$k_x\xi/\omega'$	hours
FACT5	A'	$dynes^{1/2}sec^{2}$
AMPGW(K)	1 + Re(RA')	--
AMPLG(K)	|A'|	$dynes^{1/2}sec^{2}$
EFLUX(K)	$1/2Re[p_oPA'(WA')^*]$	dynes/cm-sec
AMPLH(K)	A' for $\nu = 0$	$dynes^{1/2}sec^{2}$

Subroutine DENPLT

This subroutine plots curves of computed quantities as functions of altitude. The curves are, in order of plotting:

1. K_{zi}, where ion drag is not included (series of X'es) and with ion drag (solid line).
2. K_{zr}, under the same conditions as (1) above.
3. The amplitude, including phase variations, of the neutral density with altitude. The vertical line amplitude = 1.0 represents ambient density.
4. Energy flux 1/2 Re $(p'v_z^*)$
5. The amplitude of the gravity wave, |A'| , with no phase variation, under the same conditions as (1).
6. The ambient electron density profile.
7. Curves of constant electron density as functions of altitude and local time. The solid line is the curve of peak electron density. All other curves have the magnitude of ambient electron density at specified levels at time TINT. These magnitudes are printed out in subroutine PRINTA.

Subroutine SORT(TINT)

This subroutine merely determines the altitudes and times at which the different constant electron density contours, including the peak density contour, occur at each time step. In here also is computed COLF(K), the GW-affected electron density, for use in subroutine COFCAL(2).

The subroutine works like this: Each point [V(K), ALT(K)] is checked to see if it is the closest point to a predetermined density (DENA through DENF) or to the density peak (DENG). If so, it is stored as a point on that density contour, with coordinates of altitude [PTA(MA) through PTG(MG)] and time [PA(MA) through PG(MG)]. In this program, DENA through DENF are the ambient densities at 600, 500, 450, 400, 350, and 300 km, respectively, at time TINT.

Subroutine PRINTA

This subroutine simply prints out data stored in the machine for every 100 km of altitude as a check on the program's operation. The labels are generally self-explanatory, except that two "EL DEN=" labels are used; the first is the ambient, and the second the GW-affected, density.

Subroutine TRIDIA

This is a condensed version of the TRIDIA used by Fritz and Yeh (11) and Pound and Yeh (35). It solves the tridiagonal matrix to give V(K), the total electron density. It is well explained in the work of Fritz and Yeh cited.

Subroutines PRODUC and CHAPMN

These subroutines were developed by Cho (48). They

solve for the production function, q, in a nonisothermal atmosphere, and are used here with his kind permission.

FORTRAN IV G LEVEL 1, MOD 4 MAIN DATE = 70153 14/50/21

```
0001            COMMON HNSTEP,QPO, HK(300),DEN(300),DENN(300),ALT(300),TEMP(300)
0002            COMMON X(300),VNXO(300),DELTIM,HCON,J,SINI,COSI,Y,  AMPL,COLF(300)
0003            COMMON WVNZR(300),WVNZI(300),WVNZTR(300),WVNZTI(300),AMPGW(300)
0004            COMMON BETALO(300),TE(300),TI(300),CHAP(300),BCO,TIME,ALPHA,ALITRN
0005            COMMON HO,CHI,TXMIN,TXMAX,TEEMIN,TEEMAX,T120,HOQ,DEN120,VNYO(300)
0006            COMMON II, GC(300),BETAO,DECLR,RLATR,AMPLO(300),AMPLH(300),IPRT
0007            COMMON VOB,VLB,FLUX,CONTV,V(300),TDELAY(300),GRADH(300),EFLUX(300)
0008            COMMON/COMB/AMPLO,THERMC,WVN,PERIOD,PHI,TINT,TERM
0009            DATA RAD,BC/57.296,1.3805E-16/
0010            READ 2,HNSTEP,DELTME,QPO,BETAO,ALPHA,FLUX,CONTV
0011       2    FORMAT(3F10.5,4E12.4)
0012            READ  4,HL,DIP,DECL,RLAT,Y
0013       4    FORMAT(5F10.5)
0014            READ  5,TXMAX,TXMIN,T120,TEEMAX,TEEMIN
0015       5    FORMAT(5F10.4)
           C    COMPUTE GENERAL PROGRAM CONSTANTS
0016            ALITRN = 300.
0017            DEN120 = .2461E-10
0018            HCON = 1.E-5
0019            DIP = DIP/RAD
0020            BCO = BC/.2656E-22
0021            SINI = SIN (DIP)
0022            COSI = COS (DIP)
0023            AJ = (HL-120.)/HNSTEP + 1.
0024            J = AJ
0025            VOB = 0.
0026            IPRT = 0
0027            ITER = 500
0028            TIME = 12.
0029            AMPL = 0.
0030            TERM = 11.50
0031            DECLR = DECL/RAD
0032            RLATR = RLAT/RAD
0033            DO 30 II = 1,ITER
0034            IF (IPRT.NE.0) GO TO 47
0035            DELTIM = DELTME
0036            TIME = TERM + DELTIM
0037            READ 8, AMPLO,THERMC,WVN,PERIOD,PHI,TINT,TERM
0038       8    FORMAT (3E12.6,4F8.2)
0039            PRINT 40,AMPLO,THERMC,WVN,PERIOD,PHI
0040       40   FORMAT(1H1,'AMPL=',E12.6,'THERM=',E12.6,'WVN=',E12.6,'PERIOD=',Fd.
                12,'PHI=',F8.2/)
0041            IF (TERM.GT.98.) GO TO 99
0042       47   CONTINUE
0043            CALL ZPROFL
0044            CALL COFCAL(1)
0045            CALL TRIDIA
0046            DO 20 K=1,J
0047       20   DEN(K) = V(K)
0048            DEN(J+1) = DEN(J)
0049            IF (TIME.LT.TINT) GO TO 19
0050            CALL FACALG
0051            IF (TIME.EQ.TINT) GO TO 18
0052            CALL COFCAL(2)
0053            CALL TRIDIA
0054       18   CALL SORT(TINT)
0055       19   CONTINUE
0056            CALL PRINTA
```

FORTRAN IV G LEVEL 1, MOD 4 MAIN - DATE = 70153 - 14/50/21

```
0057                TIME = TIME + DELTIM
0058                IF (TIME-TERM) 30,30,29
0059          29    CALL DENPLT
0060          30    CONTINUE
0061          99    CONTINUE
0062                STOP
0063                END
```

FORTRAN IV G LEVEL 1, MOD 4 ZPROFL DATE = 70153 14/50/21

```
0001            SUBROUTINE ZPROFL
0002            COMMON HNSTEP,QPO, HK(300),DEN(300),DENN(300),ALT(300),TEMP(300)
0003            COMMON X(300),VNXO(300),DELTIM,HCON,J,SINI,COSI,Y, AMPL,COLF(300)
0004            COMMON WVNZR(300),WVNZI(300),WVNZTR(300),WVNZTI(300),AMPGW(300)
0005            COMMON BETALO(300),TE(300),TI(300),CHAP(300),BCO,TIME,ALPHA,ALITRN
0006            COMMON HO,CHI,TXMIN,TXMAX,TEEMIN,TEEMAX,T120,HOQ,DEN120,VNYO(300)
0007            COMMON II, GC(300),BETAO,DECLR,RLATR,AMPLG(300),AMPLH(300),IPRT
0008            COMMON VOB,VLB,FLUX,CONTV,V(300),TDELAY(300),GRADH(300),EFLUX(300)
0009            COMMCN/COMA/ PN(300),PT(300),PX(300),PZ(300)
0010            DIMENSION WM(300),DENO(300)
0011            CHI=ARCOS(SIN(RLATR)*SIN(DECLR)+COS(RLATR)*COS(DECLR)*COS((TIME-
                112.)*15./57.296))
0012            TCOSC =(COS((CHI-.7854+.20944*SIN(CHI+.7854))*.5))**2.5
0013            TEMPEX = TXMIN + (TXMAX - TXMIN)*TCOSC
0014            TEEX = TEEMIN + (TEEMAX - TEEMIN)*TCOSC
0015            TEX800 =(TEMPEX - 800.)**2
0016            SSS = .0291*EXP(-.5*TEX800/((750.+(1.722E-4)*TEX800)**2))
0017            TEMSUB = TEMPEX- T120
0018            IF(II.GT.1) GO TO 25
0019            X(1) = 0.
0020            XSTEP = HNSTEP*COSI/(SINI*HCON)
0021            CHZ=ARCOS(SIN(RLATR)*SIN(DECLR)+COS(RLATR)*COS(DECLR)*COS((19.-
                112.)*15./57.296))
0022            TCOSZ =(COS((CHZ-.7854+.20944*SIN(CHZ+.7854))*.5))**2.5
0023            TCEAC = TCOSC - TCOSZ
0024            PHOFLU = 6.8E8*QPO
0025            ALT(1) = 120.
0026            GC(1)=980.665/((1.+120./6356.77)**2)
0027        25  CONTINUE
0028            CCNT = 0.
0029            JJ = J+1
0030            CO 273 K=1,JJ
0031            ALTEP = ALT(K)
0032            G = GC(K)
0033            TEMP(K) = TEMPEX -TEMSUB*EXP((120.-ALTEP)*SSS)
0034            IF(ALT(K).NE.200.) GO TO 243
0035            IPRT = K
0036        243 CONTINUE
0037            IF(II.GT.1)GO TO 26
0038            IF (ALTEP.LE.180.) GO TO 270
0039            WM(K) = 25.106 - 7.9357*ATAN((ALTEP-180.)/140.)
0040            GO TO 271
0041        270 WM(K) = 20.- 5.0448*ATAN((ALTEP-220.)/25.)
0042        271 CONTINUE
0043            VNXO(K) = 0.
0044            VNYO(K) = 0.
0045            ALT(K+1) = ALTEP + HNSTEP
0046            X(K+1) = X(K) + XSTEP
0047            GC(K+1) = 980.665/((1.+ALT(K+1)/6356.77)**2)
0048        26  HCOF1 = 831.44*TEMP(K)/G
0049            HK(K) = HCOF1/WM(K)
0050            HO = HCOF1/16.
0051            HN2 = HCOF1/28.
0052            TE(K) = TEMP(K)+(TEEX-TEMPEX)*EXP(-80./(ALTEP-119.))
0053            IF (ALITRN.GT.ALT(K)) GO TO 69
0054            TI(K) = TE(K) +(TEMP(K)-TE(K))*EXP(1.-ALTEP/ALITRN)
0055            GO TO 122
0056        69  TI(K) = TEMP(K)
```

FORTRAN IV G LEVEL 1, MOD 4 ZPROFL DATE = 70153 14/50/21

```
0057      122   CONTINUE
0058            PT(K) = TI(K) + TE(K)
0059            IF (K.GT.1) GO TO 123
0060            DENN(K) = DEN120
0061            DENO(1) = 7.6E10
0062            BETALO(K) = BETAO
0063            GO TO 124
0064      123   PN(K-1) =(PT(K) -PT(K-1))*HCON/HNSTEP
0065            BETALO(K) = BETALO(K-1)*EXP(-HNSTEP/HN2)
0066            GRADH(K-1) = (HK(K)/HK(K-1) - 1.)/HNSTEP
0067            DENN(K)=DENN(K-1)*EXP(-HNSTEP/HK(K)-GRADH(K-1))*TEMP(K-1)/TEMP(K)
0068            DENO(K) = DENO(K-1)*EXP(-HNSTEP/HO)*TEMP(K-1)/TEMP(K)
0069      124   CONTINUE
0070            COLFN    = 1.565E15*DENN(K)/(WM(K)**1.5)
0071            PX(K) = SINI/COLFN
0072            PZ(K) = VNXO(K)*COSI                                          0001
0073            IF (II.EQ.1) GO TO 273
0074            IF (DEN(K).LT.CONT) GO TO 273
0075            CONT = DEN(K)
0076      273   CONTINUE
0077            CALL PRODUC(CHAP,7.6E10,4.E11,TXMIN,355.,.28,2.5,0.,0.,CHI,1.3805E
               1 -16,2.6512E-23,3.6829E-23,GC(20),6356.77,120.,HNSTEP,JJ,DENO,
                 17.32E-18,14.1E-18,PHOFLU)
0078            IF (II.GT.1) GO TO 120
0079            DO 119 K=1,JJ
0080      119   DEN(K) = SQRT(CHAP(K)/ALPHA)
0081      120   CONTINUE
0082            PN(JJ) = PN(J)
0083            GRADH(JJ) = GRADH(J)
0084            VLB = FLUX*CONT*(TCOSC-TCOSZ)/(TCFAC*CONTV)
0085      37    CONTINUE
0086            RETURN
0087            END
```

FORTRAN IV G LEVEL 1, MOD 4 COECAL DATE = 70153 14/50/21

```
0001            SUBROUTINE COECAL (IMPL)
0002            COMMON HNSTEP,QPO, HK(300),DEN(300),DENN(300),ALT(300),TEMP(300)
0003            COMMON X(300),VNXO(300),DELTIM,HCON,J,SINI,COSI,Y,  AMPL,COLF(300)
0004            COMMON WVNZR(300),WVNZI(300),WVNZTR(300),WVNZTI(300),AMPGW(300)
0005            COMMON BETALO(300),TE(300),TI(300),CHAP(300),BCO,TIME,ALPHA,ALITRN
0006            COMMON HO,CHI,TXMIN,TXMAX,TEEMIN,TEEMAX,T120,HOQ,DEN120,VNYO(300)
0007            COMMON II, GC(300),BETAO,DECLR,RLATR,AMPLG(300),AMPLH(300),IPRT
0008            COMMON VOB,VLB,FLUX,CONTV,V(300),TDELAY(300),GRADH(300),EFLUX(300)
0009            COMMON/COMA/ PN(300),PT(300),PX(300),PZ(300)
0010            COMMON/COMD/QP(300),BETA(300),A(300),B(300),C(300),D,E
0011            HNSTPG = HNSTEP/HCON
0012            HTRAN = 200.
0013            DELTIS = 3600*DELTIM
0014            TC1 = BCO*PX(1)*PT(1)
0015            SC1 = GC(1)*PX(1)+BCO*PX(1)*PN(1) - PZ(1)
0016            DO 52 K = 1,J
0017            QP(K) = CHAP(K)
0018            ALTEP = ALT(K)
0019            TC = TC1
0020            SC = SC1
0021            TC1 = BCO*PX(K+1)*PT(K+1)
0022            SC1 =          BCO*PX(K+1)*PN(K+1)-PZ(K+1)+GC(K+1)*PX(K+1)
0023            GRADTC = (TC1 -TC)/HNSTPG
0024            GRADSC = (SC1 - SC)/HNSTPG
0025            A(K) = TC*SINI
0026            B(K) = (GRADTC + SC)*SINI
0027            C(K) = GRADSC*SINI
0028            IF (IMPL.EQ.1) GO TO 47
0029            DENK = COLF(K)
0030            QP(K) = QP(K)*AMPGW(K)
0031            BETAL = BETALO(K)*AMPGW(K)
0032            GO TO 48
0033      47    CONTINUE
0034            DENK = DEN(K)
0035            BETAL = BETALO(K)
0036      48    CONTINUE
0037            IF (ALTEP.GT.HTRAN) GO TO 50
0038            ALPHN = ALPHA*DENK
0039            BETA(K) = ALPHN*BETAL/(BETAL + ALPHN)
0040            GO TO 51
0041      50    BETA(K) = BETAL
0042      51    CONTINUE
0043            C(K) = C(K) - 1./DELTIS
0044            QP(K) = QP(K) + DENK  /DELTIS
0045      52    CONTINUE
0046            D =-A(J)
0047            E = -SC*SINI
0048            RETURN
0049            END
```

```
FORTRAN IV G LEVEL 1, MOD 4            FACALG        DATE = 70153      14/50/21

0001                  SUBROUTINE FACALG
                C     THIS PROGRAM SOLVES THE DISPERSION EQUATION FOR KZ AND THE
                C     POLARIZATION RELATIONS.
0002                  COMPLEX F1,F2,F3,C1,C2,C3,Z1,Z2,Z3,Z5,Z6,H,BB,CC,WVNZ,THERMK,WVNT,
                     1THERM2,CSQRT,CEXP,PPK,PXK,PZK,PNK,PTK,PSIO,PSIK,FACT5,CONJG,CMPLX
0003                  COMMON HNSTEP,QPO, HK(300),DEN(300),DENN(300),ALT(300),TEMP(300)
0004                  COMMON X(300),VNXO(300),DELTIM,HCON,J,SINI,COSI,Y,  AMPL,COLF(300)
0005                  COMMON WVNZR(300),WVNZI(300),WVNZTR(300),WVNZTI(300),AMPGW(300)
0006                  COMMON BETALO(300),TE(300),TI(300),CHAP(300),BCU,TIME,ALPHA,ALITRN
0007                  COMMON HO,CHI,TXMIN,TXMAX,TEEMIN,TEEMAX,T120,HOQ,DEN120,VNYO(300)
0008                  COMMON II, GC(300),BETAO,DECLR,RLATR,AMPLG(300),AMPLH(300),IPRT
0009                  COMMON VOB,VLB,FLUX,CONTV,V(300),TDELAY(300),GRADH(300),EFLUX(300)
0010                  COMMON/COMA/ PN(300),PT(300),PX(300),PZ(300)
0011                  COMMON/COMB/AMPLO,THERMC,WVN,PERIOD,PHI,TINT,TERM
0012                  COMMON/COMF/PA(200),PB(200),PC(200),PD(200),PE(200),PTA(200),
                     1PTB(200),PTC(200),PTD(200),PTE(200),MA,MB,MC,MD,ME
0013                  COMMON/COMF/PF(200),PG(200),PTF(200),PTG(200),MF,MG
0014                  DATA H/(0.,1.)/,COI/.84992E-9/,RAD/57.296/,GAMMA/1.4/
                C     COMPUTE CONSTANTS FOR GRAVITY WAVE PROGRAM
0015                  IF (AMPL.GT.0 ) GO TO 44
0016                  AMPL = AMPLO
0017                  G1 = GAMMA - 1.
0018                  C2 = GAMMA/G1
0019                  IS = 0
0020                  WVN = WVN*HCON
0021                  HNSCM = HNSTEP/HCON
0022                  DELTIM = PERIOD/1200.
0023                  SINISQ = SINI**2
0024                  CSINI = COSI*SINI
0025                  WVNSQ = WVN**2
0026                  PHI = PHI/RAD
0027                  WVNX = WVN*COS(PHI)
0028                  WVNXSQ = WVNX**2
0029                  WVNY = WVN*SIN(PHI)
0030                  WVNYSQ = WVNSQ - WVNXSQ
0031                  FREQ = .104719/PERIOD
0032             44   CONTINUE
0033                  AMPLHF = 0.
0034                  IS = IS + 1
0035                  JJ = J+1
0036                  DO 3 K=1,JJ
0037                  G = GC(K)
0038                  HKK = HK(K)/HCON
0039                  GHK = G*HKK
0040                  DENK = DEN(K)
0041                  TK = TEMP(K)
0042                  HK12 = .5/HKK
0043                  HKSQ = 1./(HKK*HKK)
0044                  HKSQ4 = HKSQ/4.
0045                  COLLIF = COI*DENK
0046                  PRESS = DENN(K)*GHK
0047                  G2H = G2*GRADH(K)
0048                  G1H = 1. + G2H
0049                  FRQ = FREQ - VNXO(K)*WVNX - VNYO(K)*WVNY
0050                  FRTIM =  FRQ*TIME*3600.
0051                  TDELO = WVNX/( FRQ*3600.)
0052                  PSIO = -Y*WVNY + FRTIM
0053                  FRQSQ = FRQ**2
```

```
0054                WGH = FRQ/GHK
0055                F1 = H*COLLIF
0056                F2 = FRQ - F1
0057                F3 = FRQ -F1*SINISQ
0058                PRESQ = 1./SQRT(PRESS)
0059                THERMK = -H*THERMC*(TK**2.5)/((TK+245.4)*PRESS*FRQ)
0060                THERM2 = 2.*THERMK
0061                Z1 = WVNX*COLLIF*CSINI/F3
0062                C1 = WGH - WVNXSQ/F3 - WVNYSQ/F2
0063                C2 = G2 + WVNSQ*THERMK
0064                C3 = FRQ*F2/F3
0065                W2GH = FRQ*WGH
0066                GKWH = WVNSQ*HKSQ/W2GH
0067                Z4 = HKI2/HKK - W2GH + WVNSQ
0068                Z6 = C2 + THERMK*HKSQ4
0069                IF (TIME.NE.TINT) GO TO 5
0070             -- IF (K.GT.1) GO TO 7
0071                WVNZ = -CSQRT(CMPLX(-WVNSQ-HKSQ4+W2GH/GAMMA+GKWH/G2,0.))
0072                WVNT = WVNZ
0073          7     CONTINUE
0074                BB = C2 + THERMK*Z4
0075                CC =Z6*(HKSQ4+WVNSQ-W2GH)+G2H*(HKI2/HKK-GKWH+H*WVNT/HKK)-GKWH+W2GH
0076                WVNT = -CSQRT((-BB+CSQRT(BB**2-4.*CC*THERMK))/THERM2)
0077                CC =Z6*(HKSQ4+WVNSQ-W2GH)+G2H*(HKI2/HKK-GKWH+H*WVNT/HKK)-GKWH+W2GH
0078                WVNT = -CSQRT((-BB+CSQRT(BB**2-4.*CC*THERMK))/THERM2)
0079                Z5 = HKSQ4-Z1**2-C1*C3-2.*H*Z1*WVNT
0080                BB = C2 + THERMK*(Z5+HKSQ4)
0081                CC = Z6*Z5+G2H*(Z1-HKI2+H*WVNT)/HKK+G1H*C1*HKSQ/WGH-HKSQ+WGH*C3
0082                WVNZ = -CSQRT((-BB+CSQRT(BB**2-4.*CC*THERMK))/THERM2)
0083                WVNZTI(K) = AIMAG(WVNT)
0084                WVNZTR(K) = REAL(WVNT)
0085                GO TO 9
0086          5     WVNZ = WVNZR(K) + H*WVNZI(K)
0087          9     Z5 = HKSQ4-Z1**2-C1*C3-2.*H*Z1*WVNZ
0088                BB = C2 + THERMK*(Z5+HKSQ4)
0089                CC = Z6*Z5+G2H*(Z1-HKI2+H*WVNZ)/HKK+G1H*C1*HKSQ/WGH-HKSQ+WGH*C3
0090                WVNZ = -CSQRT((-BB+CSQRT(BB**2-4.*CC*THERMK))/THERM2)
0091                WVNZR(K) = REAL(WVNZ)
0092                WVNZI(K) = AIMAG(WVNZ)
0093                PSIO = PSIO-WVNZ*HNSGM
0094                PSIK = PSIO - WVNX*X(K)
0095                Z2 = (WVNZ*WVNZ+HKSQ4)*THERMK
0096                Z3 = WVNZ-H*(HKI2+Z1)
0097                C4 = FRQSQ*G1*PRESQ
0098                PPK = C4*(Z3*(C2+Z2)+H*G1H/HKK)
0099                PZK = C4*(C1*GHK*(C2+Z2)-FRQ)
0100                PTK = C4*(H*C1*G*G1H/FRQ + Z3)
0101                PNK = PPK - PTK
0102                PXK = (WVNX*GHK*PPK+COLLIF*CSINI*PZK)/F3
0103                TDELAY(K) = TDELO*X(K)
0104                FACT5 = AMPL*CEXP(H*PSIK)
0105                AMPGW(K) = 1.+REAL(FACT5*PNK)
0106                PZ(K) = PZ(K) + COSI*REAL(FACT5*PXK) + SINI*REAL(FACT5*PZK)
0107                PX(K) = PX(K)/AMPGW(K)
0108                PT(K) = PT(K)*(1.+REAL(FACT5*PTK))
0109                IF (K.EQ.1) GO TO 4
0110                PN(K-1) = (PT(K)-PT(K-1))/HNSGM
0111          4     CONTINUE
```

FORTRAN IV G LEVEL 1, MOD 4 FACALG DATE = 70153 14/50/21

```
0112                IF (IS.NE.10) GO TO 3
0113                EFLUX(K) = .5*PRESS*REAL(PZK*FACT5*CONJG(PPK*FACT5))
0114                AMPLG(K) = CABS(FACT5)*PRESQ
0115                AMPLHF = AMPLHF+HNSCM*WVNZTI(K)
0116                AMPLH(K) = AMPL*EXP(AMPLHF)*PRESQ
0117          3     CONTINUE
0118                PN(JJ) = PN(J)
0119                RETURN
0120                END
```

FORTRAN IV G LEVEL 1, MOD 4 DENPLT DATE = 70153 14/50/21

```
0001            SUBROUTINE DENPLT
0002            COMMON HNSTEP,QPO, HK(300),DEN(300),DENN(300),ALT(300),TEMP(300)
0003            COMMON X(300),VNXO(300),DELTIM,HCON,J,SINI,COSI,Y,  AMPL,COLF(300)
0004            COMMON WVNZR(300),WVNZI(300),WVNZTR(300),WVNZTI(300),AMPGW(300)
0005            COMMON BETALO(300),TE(300),TI(300),CHAP(300),BCO,TIME,ALPHA,ALITRN
0006            COMMON HO,CHI,TXMIN,TXMAX,TEEMIN,TEEMAX,T120,HOQ,DEN120,VNYO(300)
0007            COMMON II, GC(300),BETAO,DECLR,RLATR,AMPLG(300),AMPLH(300),IPRT
0008            COMMON VOB,VLB,FLUX,CONTV,V(300),TDELAY(300),GRADH(300),EFLUX(300)
0009            COMMON/COMF/PA(200),PB(200),PC(200),PD(200),PE(200),PTA(200),
               1PTB(200),PTC(200),PTD(200),PTE(200),MA,MB,MC,MD,ME
0010            COMMON/COMF/PF(200),PG(200),PTF(200),PTG(200),MF,MG
0011            DIMENSION TX(2),TY(2),TU(2),TV(2),TW(2),TZ(2)
0012            CALL CCP1PL(2.,1.,-3)
0013            CALL CCP4SC(ALT,8.0,J,1,TY)
0014            CALL CCP4SC(WVNZI ,8.0,J,1,TU)
0015            CALL CCP4SC(WVNZTI,8.0,J,1,TV)
0016            CALL CCP4SC(WVNZR ,8.0,J,1,TW)
0017            CALL CCP4SC(WVNZTR,8.0,J,1,TZ)
0018            CALL CCP5AX(0.,0.,9HKZ (IMAG),-9,8.,0.,TU)
0019            CALL CCP5AX(0.,0.,8HALTITUDE,8,8.,90.,TY)
0020            CALL CCP6LN(WVNZI,ALT,J,1,TU,TY)
0021            ALT(J+1) = TY(1)
0022            ALT(J+2) = TY(2)
0023            WVNZTI(J+1) = TV(1)
0024            WVNZTI(J+2) = TV(2)
0025            CALL LINE(WVNZTI,ALT,J,1,-1,03)
0026            CALL CCP1PL(9.,0.,-3)
0027            CALL CCP5AX(0.,0.,9HKZ (REAL),-9,8.,0.,TW)
0028            CALL CCP5AX(0.,0.,8HALTITUDE,8,8.,90.,TY)
0029            CALL CCP6LN(WVNZR,ALT,J,1,TW,TY)
0030            WVNZTR(J+1) = TZ(1)
0031            WVNZTR(J+2) = TZ(2)
0032            CALL LINE(WVNZTR,ALT,J,1,-1,03)
0033            CALL CCP1PL(9.,0.,-3)
0034            CALL CCP4SC(AMPGW,8.0,J,1,TX)
0035            CALL CCP5AX(0.,0.,9HAMPLITUDE,-9,8.,0.,TX)
0036            CALL CCP5AX(0.,0.,8HALTITUDE,8,8.,90.,TY)
0037            CALL CCP6LN(AMPGW,ALT,J,1,TX,TY)
0038            CALL CCP1PL(9.,0.,-3)
0039            CALL CCP4SC(EFLUX,8.0,J,1,TX)
0040            CALL CCP5AX(0.,0.,11HENERGY FLUX,-9,8.,0.,TX)
0041            CALL CCP5AX(0.,0.,8HALTITUDE,8,8.,90.,TY)
0042            CALL CCP6LN(EFLUX,ALT,J,1,TX,TY)
0043            CALL CCP1PL(9.,0.,-3)
0044            CALL CCP4SC(AMPLH,8.0,J,1,TX)
0045            AMPLH(J+1) = TX(1)
0046            AMPLH(J+2) = TX(2)
0047            CALL CCP5AX(0.,0.,9HAMPLITUDE,-9,8.,0.,TX)
0048            CALL CCP5AX(0.,0.,8HALTITUDE,8,8.,90.,TY)
0049            CALL CCP6LN(AMPLG,ALT,J,1,TX,TY)
0050            CALL LINE(AMPLH,ALT,J,1,-1,03)
0051            CALL CCP1PL(10.,0.,-3)
0052          3 CALL CCP4SC(DEN,8.0,J,1,TX)
0053            CALL CCP5AX(0.,0.,7HDENSITY,-9,8.,0.,TX)
0054            CALL CCP5AX(0.,0.,8HALTITUDE,8,8.,90.,TY)
0055            CALL CCP6LN(DEN,ALT,J,1,TX,TY)
0056            CALL CCP1PL(9.,0.,-3)
0057            CALL CCP4SC( PA,10.,MA,1,TX)
```

FORTRAN IV G LEVEL 1, MOD 4 DENPLT DATE = 70153 14/50/21

```
0058                CALL CCP5AX(0.,0.,4HTIME,-4,10.,0.,TX)
0059                CALL CCP5AX(0.,0.,8HALTITUDE,8,8.,90.,TY)
0060                PA(MA+1) = TX(1)
0061                PA(MA+2) = TX(2)
0062                PTA(MA+1) = TY(1)
0063                PTA(MA+2) = TY(2)
0064                PB(MB+1) = TX(1)
0065                PB(MB+2) = TX(2)
0066                PTB(MB+1) = TY(1)
0067                PTB(MB+2) = TY(2)
0068                PC(MC+1) = TX(1)
0069                PC(MC+2) = TX(2)
0070                PTC(MC+1) = TY(1)
0071                PTC(MC+2) = TY(2)
0072                PD(MD+1) = TX(1)
0073                PD(MD+2) = TX(2)
0074                PTD(MD+1) = TY(1)
0075                PTD(MD+2) = TY(2)
0076                PE(ME+1) = TX(1)
0077                PE(ME+2) = TX(2)
0078                PTE(ME+1) = TY(1)
0079                PTE(ME+2) = TY(2)
0080                PF(MF + 1) = TX(1)
0081                PF(MF + 2) = TX(2)
0082                PTF(MF+1) = TY(1)
0083                PTF(MF+2) = TY(2)
0084                CALL LINE(PA,PTA,MA,1,-1,03)
0085                CALL LINE(PB,PTB,MB,1,-1,04)
0086                CALL LINE(PC,PTC,MC,1,-1,02)
0087                CALL LINE(PD,PTD,MD,1,-1,01)
0088                CALL LINE(PE,PTE,ME,1,-1,00)
0089                CALL LINE(PF,PTF,MF,1,-1,05)
0090                CALL CCP6LN(PG,PTG,MG,1,TX,TY)
0091                CALL CCP1PL(13.,-1.,-3)
0092                ALT(J+1) = ALT(J) + HNSTEP
0093                IPRT = 0
0094                AMPL = 0.
0095                RETURN
0096                END
```

FORTRAN IV G LEVEL 1, MOD 4 SORT DATE = 70153 14/50/21

```
0001            SUBROUTINE SORT(TINT)
0002            COMMON HNSTEP,QPO, HK(300),DEN(300),DENN(300),ALT(300),TEMP(300)
0003            COMMON X(300),VNXO(300),DELTIM,HCON,J,SINI,COSI,Y, AMPL,COLF(300)
0004            COMMON WVNZR(300),WVNZI(300),WVNZTR(300),WVNZTI(300),AMPGW(300)
0005            COMMON BETALO(300),TE(300),TI(300),CHAP(300),BCO,TIME,ALPHA,ALITRN
0006            COMMON HO,CHI,TXMIN,TXMAX,TEEMIN,TEEMAX,T120,HOQ,DEN120,VNYO(300)
0007            COMMON II, GC(300),BETAO,DECLR,RLATR,AMPLG(300),AMPLH(300),IPRT
0008            COMMON VOB,VLB,FLUX,CONTV,V(300),TDELAY(300),GRADH(300),EFLUX(300)
0009            COMMON/COMF/PA(200),PB(200),PC(200),PD(200),PE(200),PTA(200),
               1PTB(200),PTC(200),PTD(200),PTE(200),MA,MB,MC,MD,ME
0010            COMMON/COMF/PE(200),PG(200),PTF(200),PTG(200),MF,MG
0011            COMMON/COMG/DENA,DENB,DENC,DEND,DENE,DENF,DENG
0012            IF (TIME.GT.TINT) GO TO 1
0013            MA = 0
0014            MB = 0
0015            MC = 0
0016            MD = 0
0017            ME = 0
0018            MF = 0
0019            MG = 0
0020            INH = 100./HNSTEP
0021            INJ = INH/2
0022            IPPP = IPRT + INH
0023            DENF = DEN(IPPP)
0024            IPPP = IPPP + INJ
0025            DENE = DEN(IPPP)
0026            IPPP = IPPP + INJ
0027            DEND = DEN(IPPP)
0028            IPPP = IPPP + INJ
0029            DENC = DEN(IPPP)
0030            IPPP = IPPP + INJ
0031            DENB = DEN(IPPP)
0032            IPPP = IPPP + INH
0033            DENA = DEN(IPPP)
0034            IF (DENF.GT.DENE) GO TO 1
0035            IF (DENE.GT.DEND) GO TO 4
0036            ARX = DEND
0037            DEND = DENF
0038            DENF = ARX
0039            GO TO 1
0040       4    ARX = DENE
0041            DENE = DENF
0042            DENF = ARX
0043       1    CONTINUE
0044            COLF(1) = V(1)
0045            DENG = DENB
0046            K=1
0047       2    K = K+1
0048            DENK = V(K)
0049            COLF(K) = DENK
0050            IF (K.EQ.J) GO TO 20
0051            DENKM = V(K-1)
0052            DENKP = V(K+1)
0053            IF(DENK.LT.DENA) GO TO 2
0054            IF (DENKM.LT.DENA) GO TO 11
0055            IF (DENKP.LT.DENA) GO TO 11
0056            IF(DENK.LT.DENB) GO TO 2
0057            IF (DENKM.LT.DENB) GO TO 12
```

```
FORTRAN IV G LEVEL 1, MOD 4          SORT          DATE = 70153          14/50/21

0058                  IF (DENKP.LT.DENB) GO TO 12
0059                  IF (DENK.LT.DENG) GO TO 3
0060                  DENG = DENK
0061                  VPTE = ALT(K)
0062                  VPE = TIME + TDELAY(K)
0063            3     CONTINUE
0064                  IF(DENK.LT.DENC) GO TO 2
0065                  IF (DENKM.LT.DENC) GO TO 13
0066                  IF (DENKP.LT.DENC) GO TO 13
0067                  IF(DENK.LT.DEND) GO TO 2
0068                  IF (DENKM.LT.DEND) GO TO 14
0069                  IF (DENKP.LT.DEND) GO TO 14
0070                  IF (DENK.LT.DENE) GO TO 2
0071                  IF (DENKM.LT.DENE) GO TO 15
0072                  IF (DENKP.LT.DENE) GO TO 15
0073                  IF (DENK.LT.DENF) GO TO 2
0074                  IF (DENKM.LT.DENF) GO TO 16
0075                  IF (DENKP.LT.DENF) GO TO 16
0076                  GO TO 2
0077            11    MA = MA+1
0078                  PTA(MA) = ALT(K)
0079                  PA(MA) = TIME + TDELAY(K)
0080                  GO TO 2
0081            12    MB = MB+1
0082                  PTB(MB) = ALT(K)
0083                  PB(MB) = TIME + TDELAY(K)
0084                  GO TO 2
0085            13    MC = MC+1
0086                  PTC(MC) = ALT(K)
0087                  PC(MC) = TIME + TDELAY(K)
0088                  GO TO 2
0089            14    MD = MD+1
0090                  PTD(MD) = ALT(K)
0091                  PD(MD) = TIME + TDELAY(K)
0092                  GO TO 2
0093            15    ME = ME+1
0094                  PTE(ME) = ALT(K)
0095                  PE(ME) = TIME+ TDELAY(K)
0096                  GO TO 2
0097            16    MF = MF+1
0098                  PTF(MF) = ALT(K)
0099                  PF(MF) = TIME+ TDELAY(K)
0100                  GO TO 2
0101            20    CONTINUE
0102                  MG = MG+1
0103                  PTG(MG) = VPTE
0104                  PG(MG) = VPE
0105            21    RETURN
0106                  END
```

FORTRAN IV G LEVEL 1, MOD 4 PRINTA DATE = 70153 14/50/21

```
0001            SUBROUTINE PRINTA
0002            COMMON HNSTEP,QPO, HK(300),DEN(300),DENN(300),ALT(300),TEMP(300)
0003            COMMON X(300),VNXO(300),DELTIM,HCON,J,SINI,COSI,Y,  AMPL,COLF(300)
0004            COMMON WVNZR(300),WVNZI(300),WVNZTR(300),WVNZTI(300),AMPGW(300)
0005            COMMON BETALO(300),TE(300),TI(300),CHAP(300),BCO,TIME,ALPHA,ALITRN
0006            COMMON HO,CHI,TXMIN,TXMAX,TEEMIN,TEEMAX,T120,HOQ,DEN120,VNYO(300)
0007            COMMON II, GC(300),BETAO,DECLR,RLATR,AMPLG(300),AMPLH(300),IPRT
0008            COMMON VOB,VLB,FLUX,CONTV,V(300),TDELAY(300),GRADH(300),EFLUX(300)
0009            COMMON/COMA/ PN(300),PT(300),PX(300),PZ(300)
0010            COMMON/COMD/QP(300),BETA(300),A(300),B(300),C(300),D,E
0011            COMMON/COME/ U(300),S(300),P(300),Q(300),R(300)
0012            INH = 100./HNSTEP
0013            PRINT 77, TIME
0014      77    FORMAT (1HO,'  TIME  =     ',F7.2/)
0015            PRINT 1, (   ALT(K), K=IPRT,J,INH)
0016      1     FORMAT('     ALT = ',8(7X,F5.0))
0017            PRINT 2, (  TEMP(K), K=IPRT,J,INH)
0018      2     FORMAT('    TEMP = ',8(6X,F6.0))
0019            PRINT 3, (    TI(K), K=IPRT,J,INH)
0020      3     FORMAT(' ION TEM= ',8(6X,F6.0))
0021            PRINT 4, (    TE(K), K=IPRT,J,INH)
0022      4     FORMAT(' EL TEMP= ',8(6X,F6.0))
0023            PRINT 5, (    HK(K), K=IPRT,J,INH)
0024      5     FORMAT(' SCAL HT= ',8(6X,F6.0))
0025            PRINT 7, (BETALO(K), K=IPRT,J,INH)
0026      7     FORMAT(' BETALO = ',8(2X,E10.3))
0027            PRINT 8, (  DENN(K), K=IPRT,J,INH)
0028      8     FORMAT(' DENSITY= ',8(2X,E10.3))
0029            PRINT 9, (  CHAP(K), K=IPRT,J,INH)
0030      9     FORMAT(' CHAP FN= ',8(2X,E10.3))
0031            PRINT 10,(   DEN(K), K=IPRT,J,INH)
0032      10    FORMAT(' EL DEN = ',8(2X,E10.3))
0033            PRINT 12,(  BETA(K), K=IPRT,J,INH)
0034      12    FORMAT(' BETA   = ',8(2X,E10.3))
0035            PRINT 13,(     V(K), K=IPRT,J,INH)
0036      13    FORMAT(' EL DEN = ',8(2X,E10.3))
0037            PRINT 14,(    QP(K), K=IPRT,J,INH)
0038      14    FORMAT(' QP     = ',8(2X,E10.3))
0039            PRINT 15,(     A(K), K=IPRT,J,INH)
0040      15    FORMAT('  A     = ',8(2X,E10.3))
0041            PRINT 16,(     B(K), K=IPRT,J,INH)
0042      16    FORMAT('  B     = ',8(2X,E10.3))
0043            PRINT 17,(     C(K), K=IPRT,J,INH)
0044      17    FORMAT('  C     = ',8(2X,E10.3))
0045            PRINT 18,(     U(K), K=IPRT,J,INH)
0046      18    FORMAT('  U     = ',8(2X,E10.3))
0047            PRINT 19,(     S(K), K=IPRT,J,INH)
0048      19    FORMAT('  S     = ',8(2X,E10.3))
0049            PRINT 20,(     P(K), K=IPRT,J,INH)
0050      20    FORMAT('  P     = ',8(2X,E10.3))
0051            PRINT 21,(     Q(K), K=IPRT,J,INH)
0052      21    FORMAT('  Q     = ',8(2X,E10.3))
0053            PRINT 22,(     R(K), K=IPRT,J,INH)
0054      22    FORMAT('  R     = ',8(2X,E10.3))
0055            PRINT 23,(    PN(K), K=IPRT,J,INH)
0056      23    FORMAT(' PN     = ',8(2X,E10.3))
0057            PRINT 24,(    PT(K), K=IPRT,J,INH)
0058      24    FORMAT(' PT     = ',8(2X,E10.3))
```

```
0059            PRINT 25,(    PX(K), K=IPRT,J,INH)
0060       25   FORMAT(' PX      = ',8(2X,E10.3))
0061            PRINT 26,(    PZ(K), K=IPRT,J,INH)
0062       26   FORMAT(' PZ      = ',8(2X,E10.3))
0063            PRINT 30,D,E,VLB
0064       30   FORMAT('0D  = ',E10.3,' E  = ',E10.3,' FLUX =  ',E10.3//)
0065            RETURN
0066            END
```

FORTRAN IV G LEVEL 1, MOD 4 TRIDIA DATE = 70153 14/50/21

```
0001          SUBROUTINE TRIDIA
              C     CALCULATE ELEMENTS OF TRIDIAGONAL COEFFICIENT MATRIX
0002          COMMON HNSTEP,QPO, HK(300),DEN(300),DENN(300),ALT(300),TEMP(300)
0003          COMMON X(300),VNXO(300),DELTIM,HCON,J,SINI,COSI,Y, AMPL,COLF(300)
0004          COMMON WVNZR(300),WVNZI(300),WVNZTR(300),WVNZTI(300),AMPGW(300)
0005          COMMON BETALO(300),TE(300),TI(300),CHAP(300),BCO,TIME,ALPHA,ALITRN
0006          COMMON HO,CHI,TXMIN,TXMAX,TEEMIN,TEEMAX,T120,HOQ,DEN120,VNYO(300)
0007          COMMON II, GC(300),BETAO,DECLR,RLATR,AMPLG(300),AMPLH(300),IPRT
0008          COMMON VOB,VLB,FLUX,CONTV,V(300),TDELAY(300),GRADH(300),EFLUX(300)
0009          COMMON/COMD/QP(300),BETA(300),A(300),B(300),C(300),D,E
0010          COMMON/COME/ U(300),S(300),P(300),Q(300),R(300)
0011          L=J
0012          DELX = HNSTEP   /HCON
0013          DELXSQ=DELX**2
0014          TODELX=2.*DELX
0015          DO 6 I=1,L
0016          AC=A(I)/DELXSQ
0017          BC=B(I)/TODELX
0018          P(I)=AC-BC
0019          Q(I)=C(I)-BETA(I)-2.*AC
0020          R(I)=AC+BC
0021          IF (I.NE.L) GO TO 6
0022          P(I)=P(I)+R(I)
0023          Q(I)=Q(I)-(( TODELX*E*R(I))/D)
0024          R(I)=( TODELX*R(I))/D
0025    6     CONTINUE
0026          GLB=-QP(L)-R(L)*VLB
0027          GOB=-QP(1)-P(1)*VOB
              C     CALCULATION OF OFF DIAGONAL ELEMENTS OF U MATRIX AND ELEMENTS OF S
0028          DO 20 I=1,L
0029          IF(I-1)  11,10,11
0030    10    UNUM=R(I)
0031          DEM=Q(I)
0032          SNUM=GOB
0033          GO TO 130
0034    11    IF(I-L)  13,12,13
0035    12    UNUM=0.
0036          DEM=Q(I)-P(I)*U(I-1)
0037          SNUM=GLB-P(I)*S(I-1)
0038          GO TO 130
0039    13    UNUM=R(I)
0040          DEM=Q(I)-P(I)*U(I-1)
0041          SNUM=-QP(I)-P(I)*S(I-1)
0042    130   CONTINUE
0043          S(I)=SNUM/DEM
0044          U(I)=UNUM/DEM
0045    20    CONTINUE
              C     SOLUTION OF THE CANONICAL MATRIX EQUATION FOR V(N)
0046    23    V(L)=S(L)
0047          L=L-1
0048          N = L
0049          DO 24 I=1,L
0050          V(N)=S(N)-U(N)*V(N+1)
0051          N=N-1
0052    24    CONTINUE
0053          RETURN
0054          END
```

```
FORTRAN IV G LEVEL 1, MOD 4          PRODUC          DATE = 70153          14/50/21

0001                  SUBROUTINE PRODUC (PROD,DENOO,DENN2O,TNO,TNL,XRJ,XNJ,ALPHAO,
                     1ALPHAN,CHI,BC,XOM,XN2M,G,RE,HO,DELHN,N,DENO,ABO,ABN2,PHOFLU)
0002                  DIMENSION PROD(300),DENO(300)
0003                  HCON=1.0E-05
0004                  IF(CHI-1.9800) 1,2,2
0005                1 CALL CHAPMN (CHAPM1,CHAPM2,CHI,BC,XOM,G,TNO,TNL,XRJ,XNJ,ALPHAO,
                     1HNUK,ALP,ALPH)
0006                  B=DENOO*(TNL**ALPH)
0007                  DEPO1=B*CHAPM1
0008                  DEPO2=B*CHAPM2
0009                  HNUKO=HNUK
0010                  ALPO=ALP
0011                  CALL CHAPMN (CHAPM1,CHAPM2,CHI,BC,XN2M,G,TNO,TNL,XRJ,XNJ,ALPHAN,
                     1HNUK,ALP,ALPH)
0012                  C=DENN2O*(TNL**ALPH)
0013                  DEPN1=C*CHAPM1
0014                  DEPN2=C*CHAPM2
0015                  HNUKN=HNUK
0016                  ALPN=ALP
0017                  A=SIN(CHI)
0018                  ALTO=RE+HO
0019                  DO 100 I=1,N
0020                  YI=I
0021                  ALTD=YI*DELHN
0022                  P=(ALTO+ALTD)*A
0023                  IF(CHI-1.5688) 3,3,4
0024                4 CONTINUE
0025                  IF(P-ALTO) 5,5,3
0026                3 DEPTHO=(DEPO1*EXP(-ALTD/HNUKO)+DEPO2*EXP(-ALPO*ALTD/HNUKO))*P*ABO
                     1/HCON
0027                  DEPTHN=(DEPN1*EXP(-ALTD/HNUKN)+DEPN2*EXP(-ALPN*ALTD/HNUKN))
                     1*P*ABN2/HCON
0028                  SUM=DEPTHO+DEPTHN
0029                  IF(SUM-150.) 7,7,5
0030                7 PROD(I)=ABO*PHOFLU*EXP(-SUM)*DENO(I)
0031                  GO TO 6
0032                5 PROD(I)=0.0
0033                6 CONTINUE
0034              100 CONTINUE
0035                  GO TO 300
0036                2 DO 200 I=1,N
0037                  PROD(I)=0.0
0038              200 CONTINUE
0039              300 CONTINUE
0040                  RETURN
0041                  END
```

FORTRAN IV G LEVEL 1, MOD 4 CHAPMN DATE = 70153 14/50/21

```
0001          SUBROUTINE CHAPMN (CHAPM1,CHAPM2,CHI,BC,XM,G,TNO,TNL,XRJ,XNJ,
             1ALPHA,HNUK,ALP,ALPH)
0002           HCON=1.0E-05
0003           P=800.0
0004           Q=750.0
0005           R=1.722E-04
0006           TNU=TNO*(1.+XRJ*((COS(CHI/2.))**XNJ))
0007           S=TNU-P
0008           Y=S/(Q+R*(S**2))
0009           TS=0.0291*EXP(-(Y**2)/2.)
0010           HNU=(BC*TNU)/(XM*G)
0011           HNUK=HNU*HCON
0012           ALP=1.+TS*HNUK
0013           ALPH=1.+ALPHA+1./(TS*HNUK)
0014           IF(CHI-0.0870) 1,2,2
0015         1 CHAPM1=(TNU**(-ALPH))*HNU
0016           CHAPM2=(HNU/ALP)*(TNU**(-ALPH-1.))*(TNU-TNL)*ALPH
0017           GO TO 500
0018         2 A=SIN(CHI)
0019           X=0.8170
0020           IF(CHI-1.5688) 3,3,4
0021         3 CHIX=ARSIN(X*A)
0022           GO TO 400
0023         4 CHIX=0.9560
0024       400 DCHI=(CHI-CHIX)/200.0
0025           TCIFI1=0.0
0026           TGIFI2=0.0
0027           GI11=TNU**(-ALPH)/A**2
0028           GI21=ALPH*(TNU**(-ALPH-1.))*(TNU-TNL)/A**2
0029           DO 100 I=1,200
0030           YI=I
0031           CHI2=CHI-(YI-0.5)*DCHI
0032           CHI3=CHI-YI*DCHI
0033           A2=SIN(CHI2)
0034           A3=SIN(CHI3)
0035           TNU2=TNU*(1.+XRJ*((COS(CHI2/2.))**XNJ))
0036           TNU3=TNU*(1.+XRJ*((COS(CHI3/2.))**XNJ))
0037           S2=TNU2-P
0038           S3=TNU3-P
0039           Y2=S2/(Q+R*(S2**2))
0040           Y3=S3/(Q+R*(S3**2))
0041           TS2=0.0291*EXP(-(Y2**2)/2.)
0042           TS3=0.0291*EXP(-(Y3**2)/2.)
0043           HNU2=(BC*TNU2)/(XM*G)
0044           HNU3=(BC*TNU3)/(XM*G)
0045           HNUK2=HNU2*HCON
0046           HNUK3=HNU3*HCON
0047           ALP2=1.+TS2*HNUK2
0048           ALP3=1.+TS3*HNUK3
0049           ALPH2=ALPHA+1.+1./(TS2*HNUK2)
0050           ALPH3=ALPHA+1.+1./(TS3*HNUK3)
0051           D2=6730./HNUK2
0052           D3=6700./HNUK3
0053           E2=D2*(A/A2-1.)
0054           E3=D3*(A/A3-1.)
0055           CI12=(TNU2**(-ALPH2))*EXP(-E2)/A2**2
0056           GI22=ALPH2*(TNU2**(-ALPH2-1.))*(TNU2-TNL)*EXP(-ALP2*E2)/A2**2
0057           GI13=(TNU3**(-ALPH3))*EXP(-E3)/A3**2
```

```
0058                GI23=ALPH3*(TNU3**(-ALPH3-1.))*(TNU3-TNU1*EXP(-ALP3*E3)/A3**2
0059                CIFI1=(GI11+4.*GI12+GI13)*DCHI/6.0
0060                GIFI2=(GI21+4.*GI22+GI23)*DCHI/6.0
0061                TCIFI1=TGIFI1+GIFI1
0062                TGIFI2=TGIFI2+GIFI2
0063                GI11=GI13
0064                GI21=GI23
0065            100 CONTINUE
0066                CHAPM1=TGIFI1
0067                CHAPM2=TGIFI2
0068            500 CONTINUE
0069                RETURN
0070                END
```

VITA

Robert Morris Clark was born at Black Rock, Arkansas, on January 8, 1938. He attended elementary and high school at Walnut Ridge, Arkansas, graduating in 1955. He received the Bachelor of Science degree in Humanities and Engineering from Massachusetts Institute of Technology in 1959, and the Master of Science degree in Electrical Engineering from the University of North Dakota in 1965. From 1959 to 1967 he served as an Electronics Warfare Officer and as a staff intelligence officer with the United States Air Force, leaving active duty with the rank of Captain. He is a member of Eta Kappa Nu and a Registered Professional Engineer.